PHDG

Professor Heinemanns
Doktorandengruppe
Verein zur Förderung
von wissenschaftlichen Arbeiten
in Reservoircharakterisierung und -simulation

TEXTBOOK SERIES

VOLUME 4

INTRODUCTION TO RESERVOIR SIMULATION

by

Zoltán E. HEINEMANN
Professor for Reservoir Engineering
Leoben, October 2005

actualized
by
Dr. Georg Mittermeir
Tehran, February 2013

For kind Attention

The Textbook series of the PHDG is an aid for PhD students accepted by the Association or those applying for support from it. These scripts have the objective to stabilize and homogenize the knowledge of the candidates, not necessarily studied petroleum engineering and originating from different countries and universities.

The textbooks are subject to continuous update and improvement. PHDG suggests to download them in yearly sequence. In some cases they are provided on different levels of knowledge making it easier to enter the subjects. Therefore there is also some overlapping between the volumes. It is expected that the users will suggest improvements for both, the contents and the formulations.

PHDG's Textbooks available at 1.1.2015:

1. Fluid Flow in Porous Medium
2. Well Testing
3. Systematic of the Reservoir Flow Equations
4. Introduction to Reservoir Simulation
5. Natural Fractured Reservoir Engineering

***PHDG Textbooks in preparation, intended to be issued during 2015*:**

1. Discretization and Gridding in Reservoir Simulation
2. Advanced Reservoir Simulation
3. Reservoir Fluid Characterisation

Supplementary scripts *used at the Montanuniversität up to the retirement of Professor Zoltán E. Heinemann in July 2006.*

1. Reservoir Fluids
2. Petroleum Recovery

Table of Contents

List of Figures

1 Introduction

This volume is the fourth within the series of the reservoir engineering textbooks provided by the Association of Professor Heinemann Doctorate Group.

The accompanying lecture presumes that the reader possesses profound knowledge of reservoir engineering. A moderate level in applied mathematics and computer application will also be expected. However, this text book is written for petroleum engineers and not for scientists. Wherever if it is possible, application of higher mathematics will be avoided. On the other hand no relation will be made to any given commercial simulator and no special methods will be discussed. The task is to achieve profound understanding rather than to write a manual or a guide line for the simulation work.

This textbook is only one of the tools to teach the reservoir simulation techniques at the university and in post graduate courses efficiently. It is important to learn by doing. The readers have to work with a sophisticated reservoir simulator to deepen their theoretical knowledge too. A collection of exercises with growing complexity was worked out and will be used. The exercises are based on the simulator ***PRS***, but they can easily be adapted to any other similar system.

1.1. What does Simulation mean

For developing an engine, a prototype of it will be built after some preliminary computation and examinations on different modules. The prototype will be tested and improved step by step. Knowledge about the already used product can be gathered and serves as basis for further improvements. This approach is not applicable to every real system, due to one of the following circumstances:

- the system is unique,
- it is inaccessible,
- its dimensions are too large or too small,
- its life cycle is long.

For hydrocarbon reservoirs all four limitations are valid. For such cases three principle possibilities for modeling are given: physical, analogous and numerical. The criteria for all of them is to be able to formulate every or a least the most important physical and chemical processes in a mathematical model. This makes it possible to deduce the similarity conditions for a physical model or to replace the real processes with analogous, but easy realizable

processes. When dealing with a hydrocarbon reservoir the possibilities for modeling would be a three dimensional sand pack laboratory model or an electrical model consisting of a network of resistivity and electrical capacities. Both were tried but without or with very limited success. The only remaining possibility is numerical modeling.

No mathematical model can be complete. The mathematical formulae are more or less approximations of the physical phenomena Furthermore, to be able to calculate with the formulae they have to be simplified. In most cases they reflect only the most important aspects of reality. With a particular mathematical model, only those processes formulated in this model can be examined.

The same mathematical model can be used in two modes:

- as modeling tool (analytical mode),
- as simulation tool.

Figure 1.1 shows this classification. The correctness of a computation in analytical mode is guaranteed when the basic equations are based on experimental evidence and when the calculations are mathematically correct. In the simulation mode the above is proved by matching the calculated results with the system behavior. The tuning of the model, even if it has no physical explanation, is allowed.

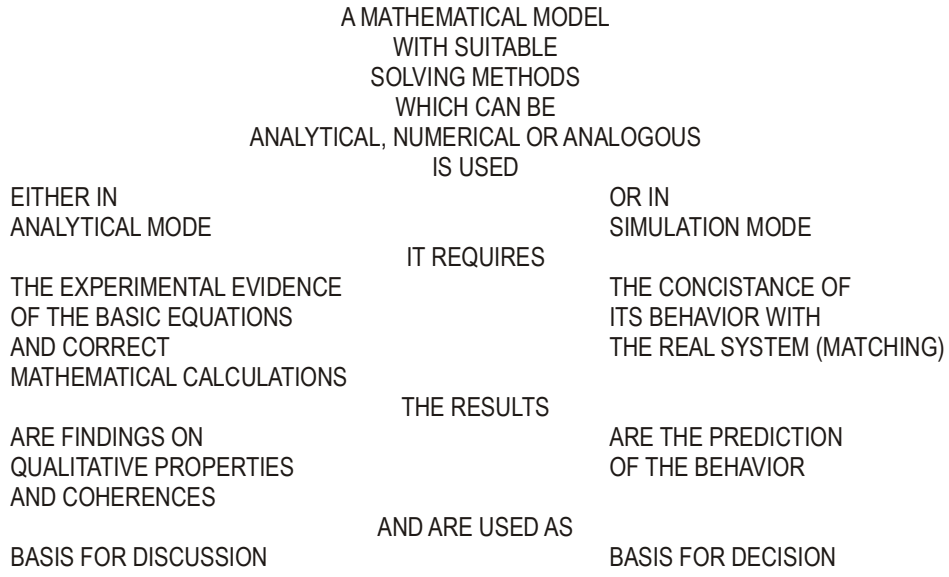

Figure 1.1: Use mathematical models in analytical and simulation mode

This classification is independent of the solving method which can be analytical or numerical. In this term a material balance calculation based on the production history to determine the water influx and OOIP is a simulation, the calculation of a steam flooding with a three dimensional non-isotherm numerical model before starting this process is a numerical modeling (in analytical mode). Nevertheless, the mathematical models used as simulation tools are so complex that only numerical solutions are possible.

The numerical models, which are mainly used in simulation techniques will be discussed in this volume. Commonly these models (and computer programs) will be called simulation models, eve if they are used for analytical purposes too.

The nature of numerical simulation is demonstrated in Figure 1.2. It has two sides, a real and an imaginary one. The computer program, based on the mathematical model needs input. These data are measured on the object (e.g. reservoir), the parameters are matched so that one part of the output coincides with the observations on the object. A greater part of the output cannot be compared with observations, but gives valuable information about the object and can be regarded as serious in case the matching is successful. Without reliable data and serious comparison the model cannot solve real problems. No simulator can replace reliable data or the brain of the user.

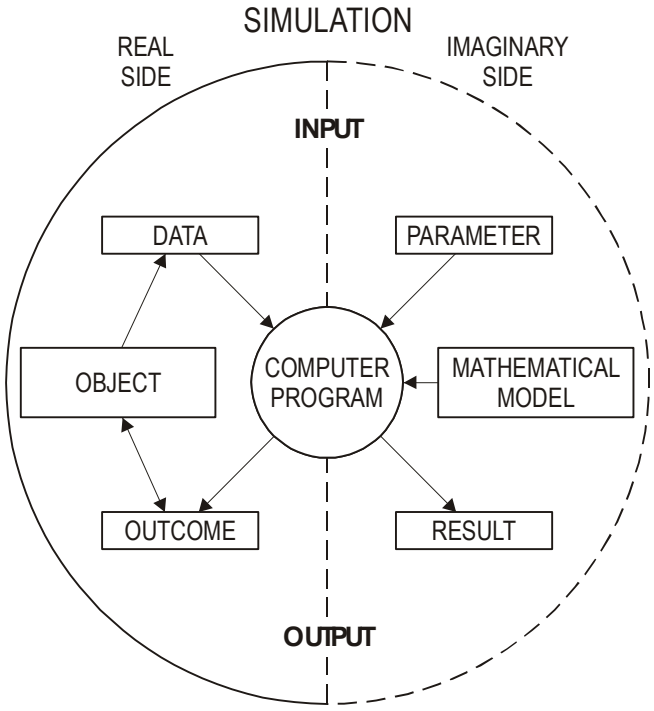

Figure 1.2: The nature of numerical simulation

1.2. What does Reservoir Simulation mean

The reservoir simulation technique makes it possible to gain insight into the recovery processes of a reservoir. To understand fluid flow and, by this, to evaluate the performance of oil and gas recovery methods, the petroleum engineer models the relevant physical and chemical processes by systems of partial differential equations. These equations account for mass and heat transfer. They include terms for gravity, capillary and viscous forces. Thermodynamic equilibrium conditions determine the number of existing phases, their composition and properties. Reservoir simulation involves the numerical solution of such systems with a computer, together with

appropriate boundary conditions as supplementary relationships.

A reservoir is a three-dimensional, heterogeneous, anisotropic rock body, filled up inhomogenously with fluids of different composition. It is evident that a reservoir model can only be constructed mathematically. As already mentioned, a reliable physical or analogous model is not possible.

The workflow when building a simulation model is shown in Figure 1.3.

Formulation of the Physical Model

Modeling

Partial Differential Equations

Discretization

Non-linear Algebraic Equations

Linearization

Linear Matrix Equation

Figure 1.3: Workflow for building a simulation model

In the physical model all relevant processes and properties must be considered. The mathematical model consists of constitutive equations (e.g.: Darcy equation), balance equations, property functions and constraints.

The discretization method can be based

- on Taylor series, leading to finite difference method (FDM),
- on integral formulation, leading to control volume difference method (CVDE) or
- on variational formulation resulting in finite element method (FEM). A special variant of FEM is the control volume finite element method (CVFE).

The discretization involves two main steps:

- Construction of an appropriate grid.
- Setup of proper algebraic equations.

The major requirements are:

- The discrete solution has to be a good approximation to the exact solution.
- The number of grid points has to be as small as possible.
- The structure of the matrix equation must ensure to be able to solve it economically.

The discretization scheme will be called convergent if the numerical solution approaches the exact solution of the mathematical model (i.e.: those of the partial differential equations) as the grid size and time step length tend to zero. All discretization methods, if applied correctly, will

lead to the same algebraic equation system. If this is not the case then one of them is erroneous. Therefore the question to use CVFD or to use CVFE method is practically irrelevant.

The balance equations combined with Darcy's law yield highly non-linear, partial differential equations of mixed hyperbolic-parabolic type. In general, those equations cannot be solved analytically, but can be solved numerically by replacing the differential equations with difference equations. This process is called *discretization*.

Basically, there are two methods available for discretization: the *finite difference* and the *finite element* method. When dealing with mass transfer both methods need a definition of a control volume around a grid point. Consequently, they are called the *Control Volume Finite Difference* (CVFD) and the *Control Volume Finite Element* (CVFE) method. Both methods reduce the differential equations to a finite-dimensional system of algebraic equations.

1.3. About the Contents

This volume gives a first theoretical insight into numerical reservoir simulation. All necessary concepts are addressed. The goal is to help the reader to achieve a fundamental understanding.

Chapter 2 deals with the conventional black oil formulation of the flow equations. At first a two-component, two-phase and two-dimensional black oil model will be formulated and the concept of ***I**mplicit-**P**ressure-**E**xplicit-**S**aturation* (**IMPES**) will be introduced. This model will be extended to three components, three phases and three dimensions. In this Chapter a simple Cartesian grid is used, explaining the difference between 2½ -dimensional and fully 3-dimensional grids. The equations will be written in implicit form and the difference between IMPES and fully implicit solution will be explained. It will be shown that IMPES and fully-implicit solution can be combined within one model and time step, leading to the concept of a*daptive implicitness*.

Chapter 3 mainly discusses the 2½D grid, usable for full-field simulation. Both isotropic and anisotropic cases will be considered. This Chapter introduces the *Local Grid Refinement* (LGR) and deals with the layering techniques. As special case the radial grid, applicable for single vertical wells, will be presented. Short discussions about corner-point and curvilinear grids complete this Chapter.

Chapter 4 deals with the initialization of a grid model and which requirements and conditions have to be satisfied when calculating the initial vertical pressure and saturation distributions for a reservoir model. Benefits and limitations of different initialization methods will be elucidated. The chapter is closed by some practical remarks.

Chapter 5 introduces the classical well models. Wells are handled as source/sink terms within the blocks in which they are perforated. The productivity indices are calculated for every perforation, which gives a linear relationship between the bottom-hole pressure, the rate and the average block pressure.

2 Basic Concept of a Reservoir Simulator (IMPES Models)

2.1. Derivation of a Two-Dimensional Two-Phase Black Oil Model

A rectangular Cartesian mesh is laid over the structure map of the reservoir. Each block represents one part of the reservoir. The top depth, thickness, porosity, pressure, water and oil saturation of the blocks are chosen so that its position, the bulk and pore volumes and the oil-, gas- and water contents coincides with the values of the represented piece of the reservoir. In this way a block model is generated, which imitates, at least volumetrically, the real reservoir. Figure 2.1 shows a two dimensional block model. It becomes three dimensional if the blocks are vertically divided.

Each grid block has a point of gravity. In this case, we presume the geometric center as this point. Furthermore, we presume that the block contains only one phase (e.g.: oil). The phase potential for block I is:

$$\Phi_{oI} = p_{oI} - g\rho_{oI} z_I, \tag{2.1}$$

where p is the pressure, ρ is the density and z_I is the vertical distance of the grid point to a reference depth.

Figure 2.2 shows a block, divided by a plane through the block center M_I, perpendicular to the coordinate I_2. The side $\overline{abcd}$ through M_I has the potential Φ_{oI} and the side $\overline{efgh}$ has the potential Φ_o. Both sides have the same surface A and the distance between these two is H_2^+. According to DARCY`S law, the oil flow rate in the coordinate direction I_2 can be calculated by the following formula:

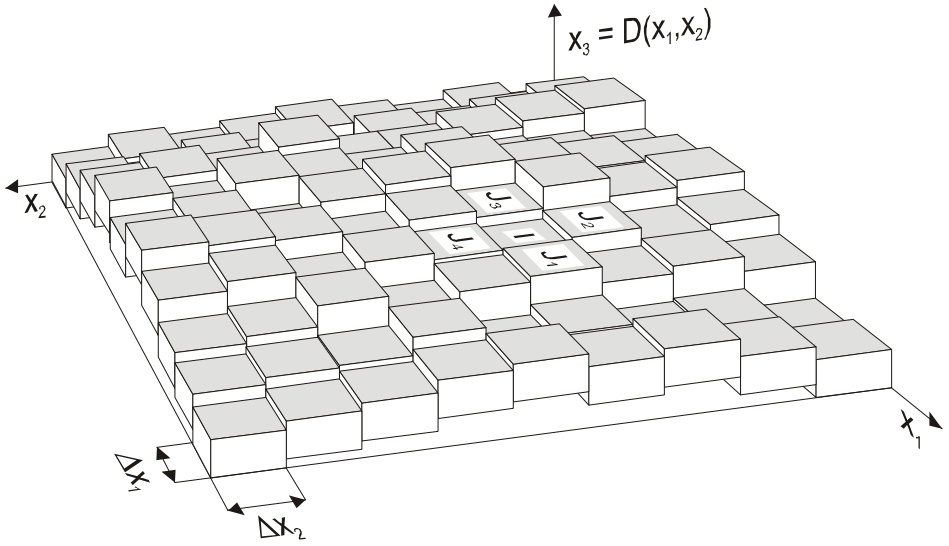

Figure 2.1: Two dimensional block model of a reservoir

$$Q_{o2} = \left(\frac{A\,\mathrm{k}}{H^{+}}\right)_2 \frac{\Phi_o - \Phi_{oI}}{\mu_o}, \tag{2.2}$$

where k is the permeability in the coordinate direction I_2 and μ_o is the oil viscosity. The quantities are gathered in such a manner that the first group contains only constant properties of the block. This group gets the symbol τ_2^+ and it is called *block half-transmissibility* for the positive I_2 direction. Equation 2.2 can be also written in a form:

$$Q_{o2} = \frac{\tau_{2I}^{+}}{\mu_o}(\Phi_o - \Phi_{oI}). \tag{2.3}$$

Six *block half-transmissibilities* can be defined for each block in the same manner:

$\tau_{1I}^{-}, \tau_{1I}^{+}, \tau_{2I}^{-}, \tau_{2I}^{+}, \tau_{3I}^{-}, \tau_{3I}^{+}$.

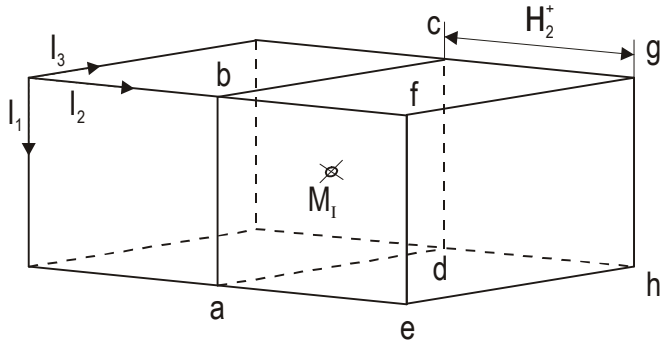

Figure 2.2: Block I is divided by a side through the block center

A block pair with serial number *I* and *J* shall now be considered, Figure 2.3. As the fluid flows from block *I* into block *J*, the following relations can be applied:

$$Q_{o2} = \frac{\tau_{2I}^{+}}{\mu_o}(\Phi_o - \Phi_{oI}) = \frac{\tau_{2J}^{-}}{\mu_o}(\Phi_{oJ} - \Phi_o) = \frac{\tau_{IJ}}{\mu_o}(\Phi_{oJ} - \Phi_{oI}) . \tag{2.4}$$

Φ_{oI} and Φ_{oJ} are the potentials in M_I and M_J.τ_{IJ} is the *block pair transmissibility.* From Equation 2.4 follows:

$$\tau_{IJ} = \frac{\tau_{2I}^{+}\tau_{2J}^{-}}{\tau_{2I}^{+} + \tau_{2I}^{-}} . \tag{2.5}$$

Two immiscible and compressible fluids (oil and water) shall be considered now. The following quantity of oil flows between block *I* and block *J* at multiphase saturation conditions:

$$Q_{oIJ} = \tau_{IJ}\frac{k_{ro}}{\mu_o B_o}(\Phi_{oJ} - \Phi_{oI}) . \tag{2.6}$$

Q_{oIJ} is positive, if oil flows into block *I* and negative, if it flows out of it. The oil mobility

$$\frac{k_{ro}}{\mu_o B_o} = \lambda^*(p, S) \tag{2.7}$$

is a function of saturation and pressure. The values λ^*_{oI} and λ^*_{oJ} can be calculated from the saturations and pressure of block *I* and block *J.* The reason why one and not the average value of these functions has to be included in Equation 2.6 for calculating the rate can be easily explained.

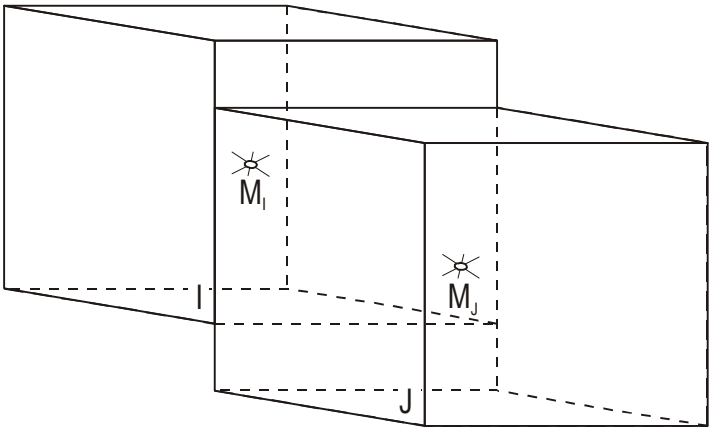

Figure 2.3: The neighboring blocks *I* and *J*

If, for example, block *I* is saturated with oil and block *J* is saturated with water, the following applies:

$$\lambda^*_{oI} > 0, \lambda^*_{oJ} = 0 . \tag{2.8}$$

If the potential in block *I* is greater then in block *J* then oil will flow between both blocks, otherwise water will flow. Therefore:

$$\lambda^*_{oIJ} = \begin{cases} \lambda^*_{oI}, & \text{if } \Phi_{oI} > \Phi_{oJ} \\ \lambda^*_{oJ}, & \text{if } \Phi_{oI} \le \Phi_{oJ} \end{cases} \tag{2.9}$$

Taking the mobility from the upstream block is called *upstream weighting*. The term

$$K_{oIJ} = \tau_{IJ}\lambda^*_{oIJ} \tag{2.10}$$

is called *phase transmissibility*. Now Equation 2.6 can be written in the following form:

$$Q_{oIJ} = K_{oIJ}(\Phi_{oJ} - \Phi_{oI}) \tag{2.11}$$

or after substitution of Equation 2.1:

$$Q_{oIJ} = K_{oIJ}(p_{oJ} - p_{oI}) + r^*_{oIJ}, \tag{2.12}$$

where

$$r^*_{oIJ} = -K_{oIJ}g(\rho_{oJ}z_J - \rho_{oI}z_I) \approx -K_{oIJ}g\rho_{oIJ}(z_J - z_I) . \tag{2.13}$$

The individual oil densities were replaced with the average value:

$$\rho_{oIJ} = \frac{\rho_{oJ} + \rho_{oI}}{2} \approx \rho_o\left(\frac{p_{oJ} + p_{oI}}{2}\right) \tag{2.14}$$

Both approximations can be used in Equation 2.13.

In a two dimensional system, the block *I* has four neighbors, see Figure 2.4.

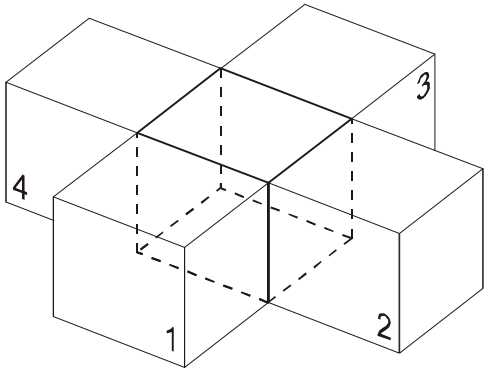

Figure 2.4: Block with its neighbors in a two dimensional system

From a well situated in block *I* oil can be produced with the rate q_{oI}. The sum

$$[Q_{oIJ1} + Q_{oIJ2} + Q_{oIJ3} + Q_{oIJ4} + q_{oI}]\Delta^{n+1}t \tag{2.15}$$

is the difference of the oil quantities flowing in or out of the block during the time interval:

$$\Delta^{n+1}t = t^{n+1} - t^n \tag{2.16}$$

J_1 to J_4 are the serial numbers of the neighboring blocks. Index *n* designates the serial number of the time point. The initial time is t^o. The amount of oil in block *I* at the time t^n is (in standard volume, sm^3):

$$V_{pI} \cdot (S_o b_o)_I^n, \qquad b_o = \frac{1}{B_o}, \tag{2.17}$$

where V_p is the block pore volume (at reservoir conditions), S_o is the oil saturation, B_o is the formation volume factor of oil and its reciprocal b_o is called *shrinkage factor*. The change during the time intervals $\Delta^{n+1}t$ is:

$$V_{pI}\left[(S_o b_o)^{n+1} - (S_o b_o)^n\right]_I. \tag{2.18}$$

If

$$S_o^{n+1} = S_o^n + \delta S_o$$

$$b_o^{n+1} = b_o^n + \delta b_o,$$

then Equation 2.18 can be written in the following way:

$$V_{pI}[(S_o^n + \delta S_o)(b_o^n + \delta b_o) - S_o^n b_o^n]_I \\ = V_{pI}[S_o^n \delta b_o + b_o^n \delta S_o + \delta S_o \delta b_o]_I \tag{2.19}$$

If the changes are small, then the last term is very small compared with the first two terms, and can be neglected. Furthermore, b_o is a function of pressure. It follows that

$$\delta b_o = \frac{b_o^{n+1} - b_o^n}{p_o^{n+1} - p_o^n}(p_o^{n+1} - p_o^n) = \left(\frac{db_o}{dp_o}\right)^n \delta p_o, \tag{2.20}$$

Equation 2.19 can be written also in the following form:

$$V_{pI}\left[S_o^n\left(\frac{db_o}{dp_o}\right)^n \delta p_o + b_o^n \delta S_o\right]_I = C_{oI}\delta p_{oI} + E_{oI}\delta S_{oI}, \tag{2.21}$$

where

$$C_{oI} = \left[V_p S_o^n \left(\frac{db_o}{dp_o}\right)^n\right]_I$$

and

$$E_{oI} = [V_p b_o^n]_I.$$

Based on the law of mass conservation, the terms Equation 2.15 and Equation 2.21 must be equal:

$$[Q_{oIJ1} + Q_{oIJ2} + Q_{oIJ3} + Q_{oIJ4} + q_{oI}]\Delta t = C_{oI}\delta p_{oI} + \mathrm{E}_{oI}\delta S_{oI} \tag{2.22}$$

Equation 2.22 is a volume balance. Both sides of the equation are written in standard m^3 and due to the fact that the standard density is a constant, it is equivalent with a mass balance. This equation is valid for the time interval Δt. Therefore Q_{oIJ} is the rate which is valid during the time interval Δt. It is possible to calculate this rate explicitly, using the block pressures at time

point t^n. In this case the unknowns δp_{oI} and δS_{oI} are only on the right hand side of the equation. It is easy to understand that in this case Δt may become very small. In other words, the numerical method becomes instable.

To demonstrate this stability problem we consider an isolated model consisting of two blocks only, containing one mobile phase (e.g.: oil). The initial pressure in block *I* should be higher than in block *J*. This fact causes a pressure adjustment with time. The pressure difference induces a flow between the two blocks. The pressure in block *I* will continuously diminish and it will rise in block *J*. After some time the block pressures becomes equal, as shown by the continuous line in Figure 2.5.

Using our numerical formulation, the flow rate can be calculated explicitly at the beginning of every time step Δt or implicitly at the end of Δt´s. This rate will be valid for the actual time step. If the flow rate is calculated explicitly and Δt is greater then a critical value then at the end of the time step the pressure becomes greater in block J as in block I. For the next time step the flow direction changes, leading to quick divergence of the calculated pressures. The calculation becomes instable.

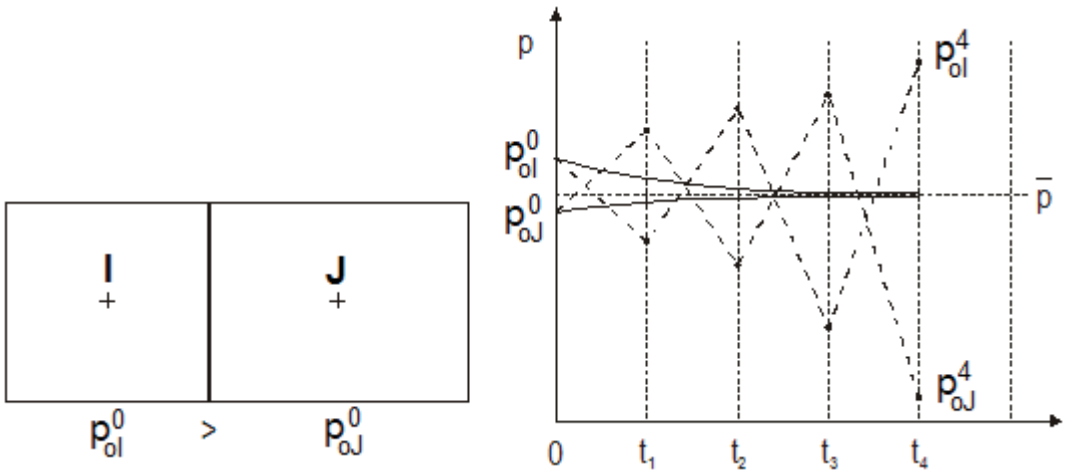

Figure 2.5: Demonstration of the instability in explicit methods

It is better to calculate the Q_o-values with the transmissibility of time point t^n, and the pressure difference at the time point t^{n+1}. By that Equation 2.12 gets the form:

$$Q_{oIJ} = K_{oIJ}{}^{n}(p^n_{oJ} + \delta p_{oJ} - p^n_{oI} - \delta p_{oI}) + r^*_{oIJ}, \tag{2.23}$$

or with gathering of known values:

$$Q_{oIJ} = K_{oIJ}(\delta_{poJ} - \delta_{poI}) + r_{oIJ}. \tag{2.24}$$

Inserting Equation 2.24 into Equation 2.22 it becomes:

$$
\begin{aligned}
&[K_{oIJ1}(\delta_{poJ1}-\delta_{poI})+r_{oIJ1}\\
&+K_{oIJ2}(\delta_{poJ2}-\delta_{poI})+r_{oIJ2}\\
&+K_{oIJ3}(\delta_{poJ3}-\delta_{poI})+r_{oIJ3}\\
&+K_{oIJ4}(\delta_{poJ4}-\delta_{poI})+r_{oIJ4}+q_{oI}]\Delta t\\
&=[C_{oI}\delta p_{oI}+E_{oI}\delta S_{oI}]
\end{aligned}
\tag{2.25}
$$

Dividing both sides by E_{oI} and writing the equation in a shorter form:

$$
-\frac{\Delta t}{E_{oI}}\left[\sum_{k=1}^{4}K_{oIJk}+\frac{C_{oI}}{\Delta t}\right]\delta p_{oI}+\frac{\Delta t}{E_{oI}}\sum_{k=1}^{4}K_{oIJk}\delta p_{oJk}=\delta S_{oI}+d_{oI} \tag{2.26}
$$

where

$$
d_{oI}=-\frac{\Delta t}{E_{oI}}\left[\sum_{k=1}^{4}r_{oIJk}+q_{oI}\right]
$$

Equation 2.26 contains six unknowns, five pressure changes and δS_o.

The equation for water is written analogously to Equation 2.26:

$$
-\frac{\Delta t}{E_{wI}}\left[\sum_{k=1}^{4}K_{wIJk}+\frac{C_{wI}}{\Delta t}\right]\delta p_{wI}+\frac{\Delta t}{E_{wI}}\sum_{k=1}^{4}K_{wIJk}\delta p_{wJk}=\delta S_{wI}+d_{wI} \tag{2.27}
$$

Equation 2.27 also contains six unknowns.

Confined to two phases, there is

$$
S_w+S_o=1\,, \tag{2.28}
$$

and

$$
\delta S_w+\delta S_o=0 \tag{2.29}
$$

The capillary pressure is

$$
p_o-p_w=P_{cow}(S_w) \tag{2.30}
$$

and

$$
\delta p_o-\delta p_w=\delta P_{cow}(S_w) \tag{2.31}
$$

In practical cases often

$$\delta P_{cow} \ll \delta p_o \tag{2.32}$$

and can be neglected. But herewith

$$\delta p_o = \delta p_w = \delta p\,. \tag{2.33}$$

Adding Equation 2.26 and Equation 2.27

$$a_I \delta p_I + \sum_{k=1}^{4} b_{IJk} \delta p_{Jk} = e_I \tag{2.34}$$

where

$$a_I = -\Delta t \left(\frac{1}{E_{oI}} \left(\sum_{k=1}^{4} K_{oIJk} + \frac{C_{oI}}{\Delta t} \right) + \frac{1}{E_{wI}} \left(\sum_{k=1}^{4} K_{wIJk} + \frac{C_{wI}}{\Delta t} \right) \right) \tag{2.35}$$

$$b_{IJk} = \Delta t \left[\frac{K_{oIJk}}{E_{oI}} + \frac{K_{wIJk}}{E_{wI}} \right]$$

$$e_I = (d_{oI} + d_{wI})$$

Equation 2.34 contains five unknowns.

Taking boundary conditions into account the following applies: The boundary of a reservoir (i.e.: the block model) may either be closed, that means no mass transfer across this boundary is possible, or the pressure is constant at this boundary. Figure 2.6 shows a simple model, in which both boundary conditions occur.

For blocks 12-14, the following applies:

$$\delta p_{12} = \delta p_{13} = \delta p_{14} = 0 \tag{2.36}$$

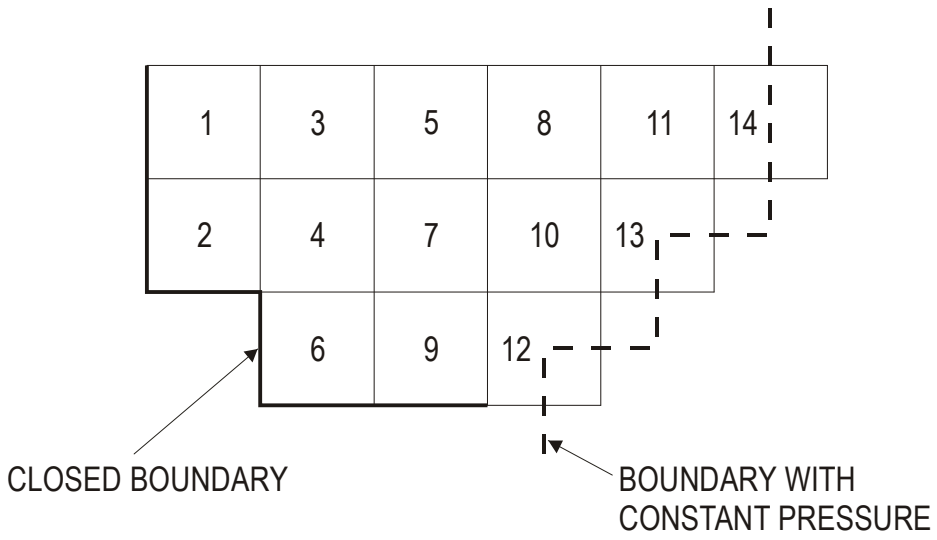

Figure 2.6: Block model with closed and constant pressure boundaries

With that, the system of Equation 2.34 contains 11 equations with 11 unknowns. The system of equations is written in detail to visualize it better:

$$
\begin{array}{ll}
1 & a_1\ \delta_{p1}+b_{1,2}\delta_{p2}+b_{1,3}\delta_{p3} = e_1 \\
2 & b_{2,1}\delta_{p1}+a_2\ \delta_{p2}+b_{2,4}\delta_{p4} = e_2 \\
3 & b_{3,1}\delta_{p1}+a_3\ \delta_{p3}+b_{3,4}\delta_{p4}+b_{3,5}\delta_{p5} = e_3 \\
4 & b_{4,2}\delta_{p2}+b_{4,3}\delta_{p3}+a_4\ \delta_{p4}+b_{4,6}\delta_{p6}+b_{4,7}\delta_{p7} = e_4 \\
5 & b_{5,3}\delta_{p3}+a_5\ \delta_{p5}+b_{5,7}\delta_{p7}+b_{5,8}\delta_{p8} = e_5 \\
6 & b_{6,4}\delta_{p4}+a_6\ \delta_{p6}+b_{6,9}\delta_{p9} = e_6 \\
7 & b_{7,4}\delta_{p4}+b_{7,5}\delta_{p5}+a_7\ \delta_{p7}+b_{7,9}\delta_{p9}+b_{7,10}\delta_{p10} = e_7 \\
8 & b_{8,5}\delta_{p5}+a_8\ \delta_{p8}+b_{8,10}\delta_{p10}+b_{8,11}\delta_{p11} = e_8 \\
9 & b_{9,6}\delta_{p6}+b_{9,7}\delta_{p7}+a_9\ \delta_{p9} = e_9 \\
10 & b_{10,7}\delta_{p7}+b_{10,8}\delta_{p8}+a_{10}\ \delta_{p10} = e_{10} \\
11 & b_{11,8}\delta_{p8}+a_{11}\ \delta_{p11} = e_{11}
\end{array}
$$

Figure 2.7: Equation system corresponding to Figure 2.6

It is simpler to write the system of equations system in Figure 2.7 in matrix form:

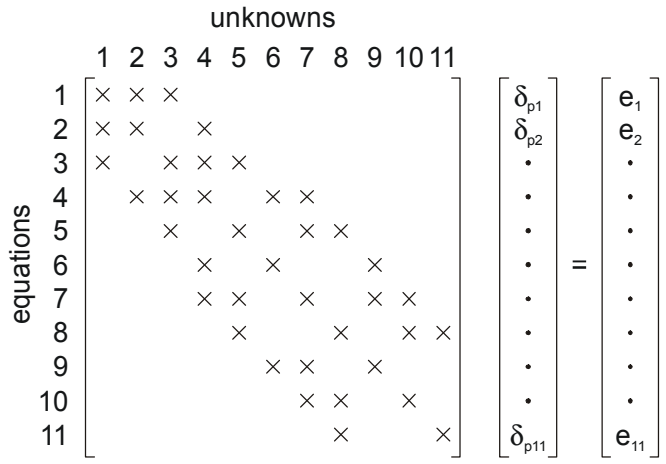

(2.37)

or even shorter as

$$\bar{\bar{A}}\delta\bar{p} = \bar{e} \tag{2.38}$$

where $\bar{\bar{A}}$ is the sparse matrix shown above in Figure 2.7.

The calculation is described as follows:

1. Pressure and saturations for the blocks are known for the time point $t^{n=0}$. This is the initial situation and $n = 0$.
2. We choose a time interval Δt and designate the production rates q_o and q_w describing the average values for the time interval Δt.
3. We designate the terms *K, r, C, E* and *d* of Equation 2.26, Equation 2.27 for block *I*.
4. We calculate the coefficients *a, b* and *e* of Equation 2.34.
5. We solve the linear equation system Equation 2.37 by a suitable method. The results are the pressure changes δp during the time interval Δt. Therefore the pressures at the end of the time interval are:

$$p^{n+1} = p^n + \delta p \tag{2.39}$$

6. We calculate the saturation changes δS_w and δS_o from Equation 2.26 and Equation 2.27:

$$S_o^{n+1} = S_o^n + \delta S_o \tag{2.40}$$

$$S_w^{n+1} = S_w^n + \delta S_w \tag{2.41}$$

7. We check the accuracy by a material balance calculation.

Steps 2 to 7 are repeated until the entire production time is calculated.

2.2. The Gas Equation

Gas can be contained in a reservoir either as free gas or as dissolved gas. The pressure p_{oI} in block I can be higher or equal to the bubble point pressure p_b. If the oil is saturated, the dissolved gas in oil ration R_{sI} is a function of pressure for pressures $p < p_b$:

$$R_{sI} = R_s(p_{oI}) \tag{2.42}$$

The general case also taking into account the undersaturated state $p > p_b$, will be considered in Chapter 2.7.. The change of the gas quantity in block I during the time interval Δt can be written analogously to Equation 2.18

$$V_{pI}\left[(S_g b_g + R_s S_o b_o)^{n+1} - (S_g b_g + R_s S_o b_o)^{n}\right]_I. \tag{2.43}$$

where b_g is the gas shrinkage factor. Like in Equation 2.21 the following applies:

$$V_{pI}\left[\left(S_g \frac{db_g}{dp}\right)^n \delta p_g + b_g^n \delta S_g + \left(S_o \frac{d(R_s b_o)}{dp}\right)^n \delta p_o + (R_s b_o)^n \delta S_o\right]_I \tag{2.44}$$

The difference between oil- and gas phase pressure is the gas-oil capillary pressure:

$$p_g - p_o = P_{cgo}(S_g) \tag{2.45}$$

From experience, the change of P_{cgo} with time is small. Analogously to Equation 2.31 it follows that:

$$\delta p_g - \delta p_o = \delta P_{cgo}(S_g) = 0, \tag{2.46}$$

and therefore with Equation 2.33 the following applies:

$$\delta p_o = \delta p_w = \delta p_g = \delta p. \tag{2.47}$$

Including Equation 2.46 into Equation 2.43:

$$V_{pI}\left\{\left[S_g \frac{db_g}{dp} + S_o \frac{d(R_s b_o)}{dp}\right]^n \delta p + (R_s b_o)^n \delta S_o + b_g^n \delta S_g\right\}_I \tag{2.48}$$

$$= C_{gI}\delta p_I + E_{gI}\delta S_{gI} + D_{gI}\delta S_{oI}$$

Gas will be transported between two blocks in two phases, in the gas phase and in the oil phase. According to Equation 2.12 the gas rate is

$$Q_{gIJ} = K^*_{gIJ}(p_{gJ} - p_{gI}) + (R_s K_o)_{IJ}(p_{oJ} - p_{oI}) + r^*_{gIJ}, \tag{2.49}$$

where

$$r^*_{gIJ} = -[K_{gIJ}\rho_{gIJ} + (R_s K_o)_{IJ}\rho_{oIJ}]g(z_J - z_I). \tag{2.50}$$

R_{sIJ} is the dissolved GOR of the oil flowing from one block to the other, and must be set equal to R_s of the upstream block, from the same reason as the phase mobility λ (Equation 2.9):

$$R_{sIJ} = \begin{cases} R_{sI}, & \text{if } \Phi_{oI} > \Phi_{oJ}, \\ R_{sJ}, & \text{if } \Phi_{oI} \le \Phi_{oJ}. \end{cases} \tag{2.51}$$

Inserting

$$\begin{aligned} p^{n+1}_{gI} &= p^n_{gI} + \delta p_I \\ p^{n+1}_{oI} &= p^n_{oI} + \delta p_I \end{aligned} \tag{2.52}$$

into Equation 2.48 while taking Equation 2.46 into consideration, the following applies

$$\begin{aligned} Q_{gIJ} = {} & K^*_{gIJ}(p_{gJ} - p_{gI})^n + (R_s K_o)_{IJ}(p_{oJ} - p_{oI})^n \\ & + (K^*_g + R_s K_o)_{IJ}(\delta p_J - \delta p_I) + r^*_{gIJ} \\ = {} & K_{gIJ}(\delta p_J - \delta p_I) + r_{gIJ} \end{aligned} \tag{2.53}$$

where

$$K_{gIJ} = (K^*_g + R_s K_o)_{IJ},$$

and

$$r_{gIJ} = r^*_{gIJ} + K^*_{gIJ}(p_{gJ} - p_{gI})^n + (R_s K_o)_{IJ}(p_{oJ} - p_{oI})^n. \tag{2.54}$$

Equation 2.24 and Equation 2.53 are formally equal, caused by the notation applied. Analogously to Equation 2.22, Equation 2.25 and Equation 2.26, the balance equation for gas follows as:

$$\left[\sum_{k=1}^{4} Q_{gIJk} + q_{gIJk}\right]\Delta t = C_{gI}\delta p_I + E_{gI}\delta S_{gI} + D_{gI}\delta S_{oI} \tag{2.55}$$

After including Equation 2.53 into Equation 2.55

$$-\frac{\Delta t}{E_{wI}}\left[\sum_k K_{gIJk} + \frac{C_{gI}}{\Delta t}\right]\delta p_I + \frac{\Delta t}{E_{gI}}\sum_{k=1} K_{gIJk}\delta p_{IJk} \tag{2.56}$$
$$= \delta S_{gI} + \frac{D_{gI}}{E_{gI}}\delta S_{oI} + d_{gI}.$$

with

$$d_{gI} = -\frac{\Delta t}{E_{gI}}\left[\sum_k r_{gIJk} + q_{gI}\right]$$

2.3. Cartesian Coordinate System

Although the rigid Cartesian coordinate system does not seem very suitable for the geometry and flow pattern of a real reservoir, this technique is widely applied for reservoir simulation. At first a two-dimensional Cartesian system - having the coordinates aligned to the *I2* and *I3* axes - is selected to assemble the block system for reservoir simulation.

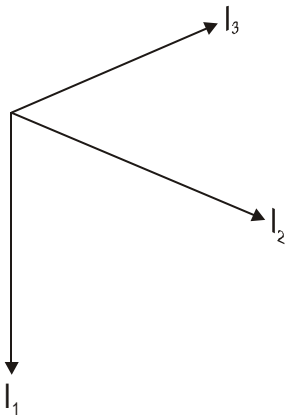

Figure 2.8: Cartesian coordinate system

The *I1-axis* is perpendicular to the *I2-I3-plane* and points downwards. The block system can be defined one-dimensionally, two-dimensionally or three-dimensionally. This orientation, as

depicted in Figure 2.8, is not the usual one, but it has the advantage that the depth is measured and the layers are numbered in the same manner as in the geological representation. Then, a basic grid is constructed based on the geological structure. The grid can be defined in two ways:

- ***Block centered scheme***: For the block centered grid the block sizes are selected at first and then the nodal points are centered between the boundaries. *M* is the geometrical center point of the block (Figure 2.9).
- ***Point distributed scheme***: A basic grid is constructed by determining the nodal points, taking into consideration the concepts of geological structures. The block boundaries divide the distance between the nodes in halves. The margin boundary is determined by reflecting the last block boundary at the outmost nodal point (Figure 2.10).

The *block centered approach* is very common in reservoir simulation.

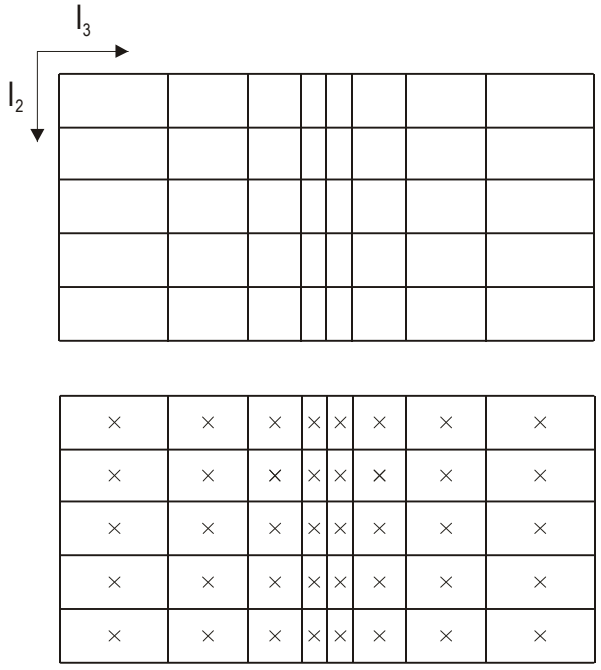

Figure 2.9: Construction of a block centered Cartesian grid

However from a practical point of view, there is not any additional difference when using one or the other type of grid. That means, the application of the point distributed grid is not more complicated than the using the block centered one. The only difference seems to be that a better consistency is provided for the point distributed grid by the mathematical error analysis. This is sufficient for us to give a recommendation for that type of grid, without refusing the applicability of the other one.

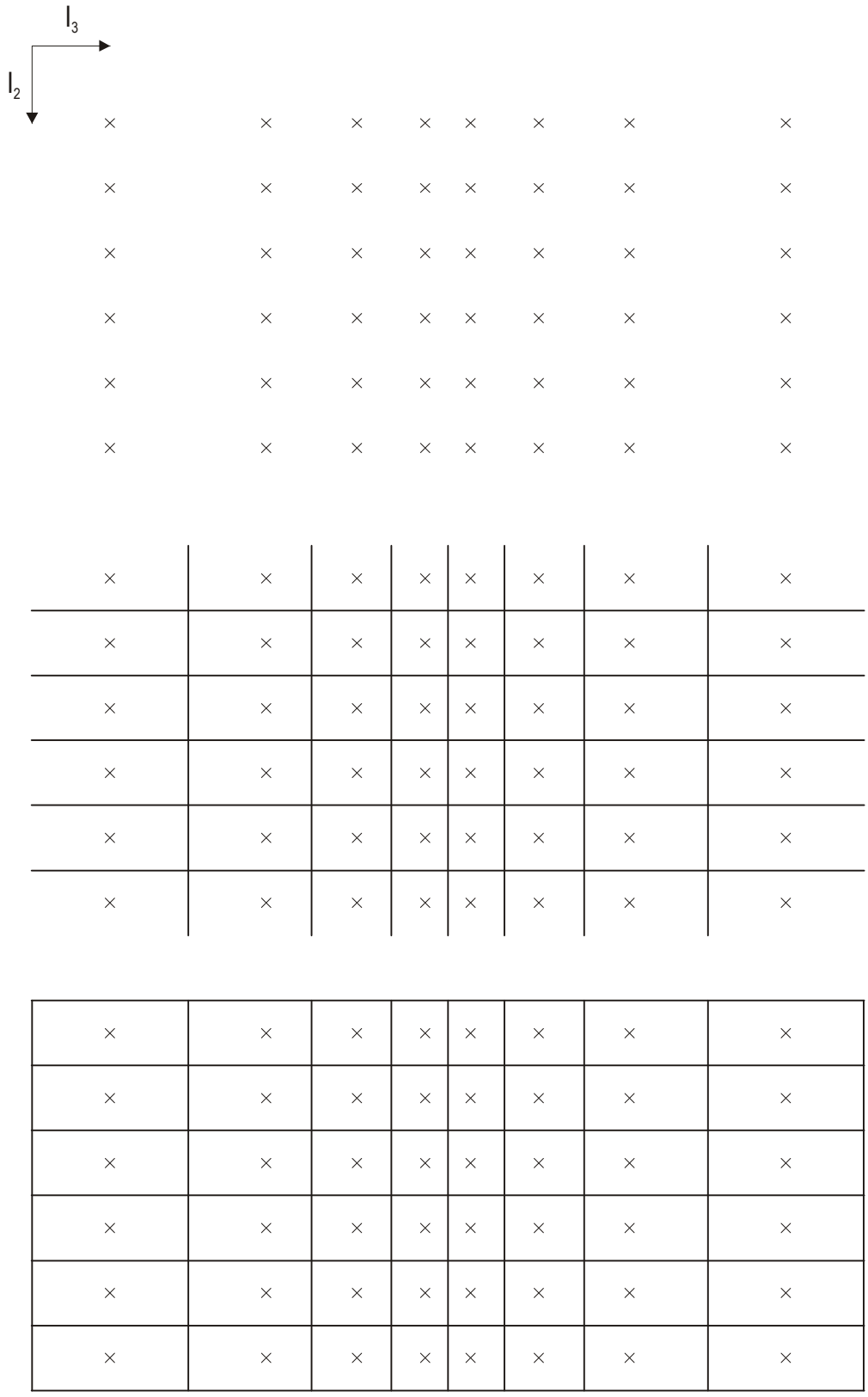

Figure 2.10: Construction of a point distributed Cartesian grid

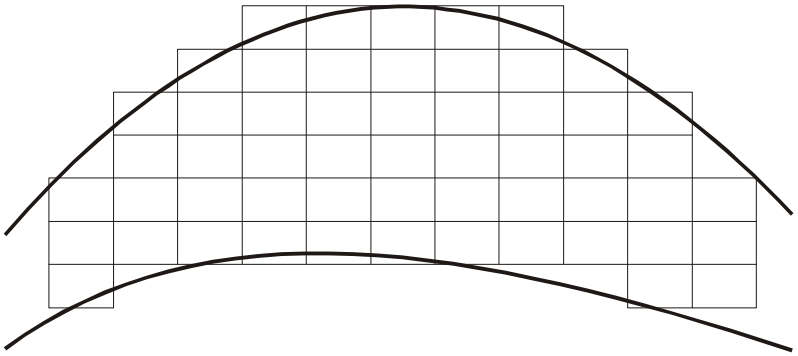

Figure 2.11: Three-dimensional Cartesian grid

The same procedure of block construction can be applied in the vertical direction if the extension of the reservoir is comparable with the horizontal one (Figure 2.11). Most frequently however, the vertical extension is smaller in order of magnitude than the horizontal one and it is also layered, so that such a discretization cannot be used or requires very small grid spacing. Instead of doing so it is better to use a stream tube approach in the cross section, as shown in (Figure 2.12). We assume that the vertical component of the flow velocity as well as its components parallel to the layering can be calculated independently.

A 3D block system is shown in (Figure 2.13). It is evident that this grid is only Cartesian and orthogonal in the horizontal plane but not in the cross section.

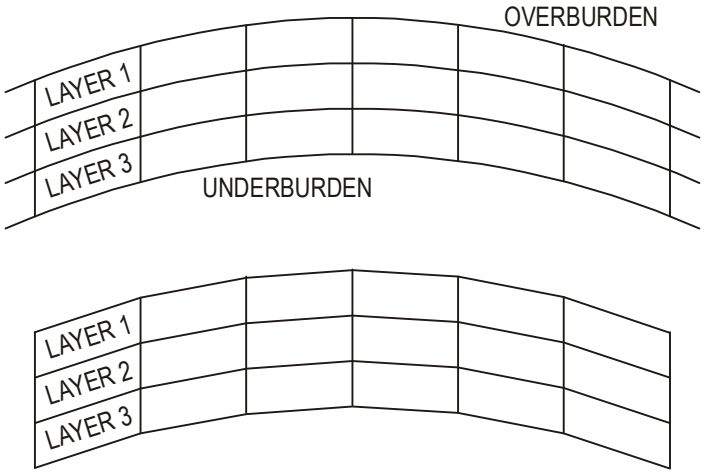

Figure 2.12: Steam tube approach in cross section

In practical application the geometrical torsions in the cross section are sometimes neglected and the block system will display as a system of rectangular horizontal blocks as shown in (Figure 2.14). The blocks are shifted vertically from each other, their surfaces are not the same for the neighbors and the overlapping is only partly. This is only a question of the graphical illustration and has no influence on the calculation of the transmissibilities.

2.3.1 Transmissibilities

In Chapter 2.1. we already introduced the concept of block transmissibilities. A fundamental Cartesian grid has six of them, oriented from the grid point toward the six block sides. Those six transmissibilities are indicated with τ^{+}_{Ii} or τ^{-}_{Ii} (i= 1,2,3). They are calculated in a simple way, supposing a linear incompressible one-phase DARCY-flow, orthogonal on the block surface. From the DARCY law:

$$Q^{+}_{Ii} = \left(\frac{AK}{L}\right)^{+}_{Ii} \frac{\Phi - \Phi_I}{\mu} = \frac{\tau^{+}_{Ii}}{\mu}(\Phi - \Phi_I) \tag{2.57}$$

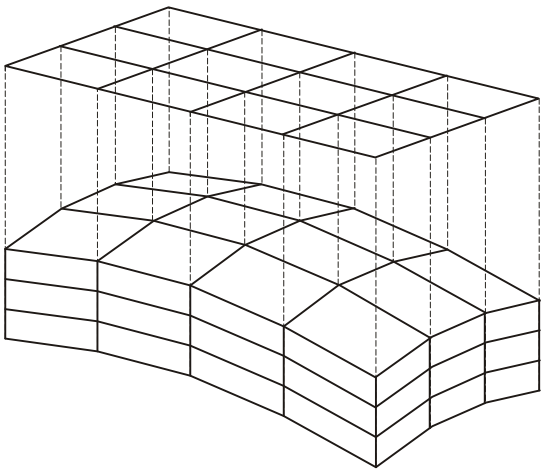

Figure 2.13: Three dimensional Cartesian grid

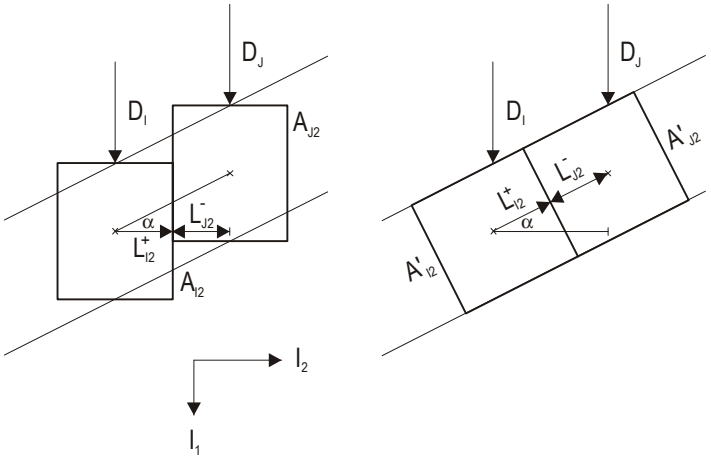

Figure 2.14: Dip correction of the transmissibilities

where Φ is the phase potential on the block surface. The transmissibility between two grid points will be calculated - based on the KIRCHOFF law - as the harmonic average of two block

transmissibilities

$$\tau_{IJ} = \frac{\tau_{Ii}^{+}\tau_{Ji}^{-}}{\tau_{Ii}^{+} + \tau_{Ji}^{-}} \tag{2.58}$$

In this way, not only the permeabilities of the neighboring blocks but also the block surfaces are averaged. If the layer is not horizontal, then this approximation will not be correct, because the direction of the flow is parallel to the layer and not to the block edge. The true distance from the grid point to the communication surface and the true surface can be calculated easily, as shown in Figure 2.14:

$$\begin{aligned} \tilde{L}_I^{+} &= \frac{L_I^{+}}{\cos\alpha}, \\ \tilde{A}_I &= A_I \cos\alpha, \end{aligned} \tag{2.59}$$

where α is the dip of the layer. Applying the definition after Equation 2.57

$$Q_{Ii}^{+} = \left(\frac{\tilde{A}K}{\tilde{L}}\right)_{Ii}^{+} \frac{\Phi - \Phi_I}{\mu} \tag{2.60}$$

we get

$$\tau_{Ii}^{+} = \left(\frac{\tilde{A}K}{\tilde{L}}\right)_{Ii}^{+} = \left(\frac{AK}{L}\right)_{Ii}^{+} \cos^2\alpha\,. \tag{2.61}$$

2.4. Three-Dimensional Three-Phase IMPES-Equation

The balance equation for oil (according Equation 2.26):

$$-\frac{\Delta t}{E_{oI}}\left[\sum_k K_{oIJk} + \frac{C_{oI}}{\Delta t}\right]\delta_{pI} + \frac{\Delta t}{E_{oI}}\sum_k K_{oIJk}\delta p_{Jk} = \delta S_o + d_{oI}, \tag{2.62}$$

The balance equation for water (according Equation 2.27):

$$-\frac{\Delta t}{E_{wI}}\left[\sum_k K_{wIJk} + \frac{C_{wI}}{\Delta t}\right]\delta p_I + \frac{\Delta t}{E_{wI}}\sum_k K_{wIJk}\delta p_{Jk} = \delta S_w + d_{wI}, \tag{2.63}$$

The balance equation for gas (according Equation 2.56):

$$-\frac{\Delta t}{E_{gI}}\left[\sum_k K_{gIJk} + \frac{C_{gI}}{\Delta t}\right]\delta_{pI} + \frac{\Delta t}{E_{gI}}\sum_k K_{gIJk}\delta p_{IJk} \tag{2.64}$$
$$= \delta S_{gI} + \frac{D_{gI}}{E_{gI}}\delta S_{oI} + d_{gI}$$

$\sum_k$ is the summation over all neighboring blocks of block I. The summation from 1 to 4, done in Chapter 2.1., was not exactly correct. Inevitable, there are blocks with only 2 or 3 neighbors in a two dimensional model. The extension to the third dimension is simply made by taking the neighboring blocks of the third coordinate direction into account too. There are no differences between one-, two- and three dimensional models when applying this formalism. After multiplying Equation 2.62 by

$$1 - \frac{D_{gI}}{E_{gI}}$$

Equation 2.62, Equation 2.63 and Equation 2.64 will be added. For the saturations is valid:

$$S_w + S_o + S_g = 1, \tag{2.65}$$

Consequently:

$$\delta S_w + \delta S_o + \delta S_g = 0. \tag{2.66}$$

Therefore the resulting equation contains no saturation changes. The obtained equation has the same form as Equation 2.34:

$$a_1\delta p_I + \sum_k b_{IJk}\delta p_{Jk} = e_I \tag{2.67}$$

where

$$a_1 = -\Delta t\left[\frac{E_{gI}-D_{gI}}{E_{oI}E_{gI}}\left(\sum_k K_{oIJk}+\frac{C_{oI}}{\Delta t}\right)+\frac{1}{E_{wI}}\left(\sum_k K_{wIJk}+\frac{C_{wI}}{\Delta t}\right)+\frac{1}{E_{gI}}\left(\sum K_{gIJk}+\frac{C_{gI}}{\Delta t}\right)\right] \tag{2.68}$$

$$b_{IJk} = \Delta t\left[\frac{E_{gI}-D_{gI}}{E_{oI}E_{gI}}K_{oIJk}+\frac{K_{wIJk}}{E_{wI}}+\frac{K_{gIJk}}{Eg_I}\right]$$

$$e_I = \frac{E_{gI}-D_{gI}}{E_{gI}}d_{oI}+d_{wI}+d_{gI}$$

2.5. Formulation of a Fully Implicit Black Oil Model

2.5.1 The Balance Equations

The balance equations for the three components are:

Water:

$$\sum_{J=1}^{N(I)} \tau_{IJ}\lambda^{*n+1}_{wIJ}(\Phi_{wJ}-\Phi_{wI})^{n+1}+q^{n+1}_{wI}=\frac{V_I}{\Delta t}\Delta_t(\phi S_w b_w)_I; \tag{2.69}$$

Oil:

$$\sum_{J=1}^{N(I)} \tau_{IJ}\lambda^{*n+1}_{oIJ}(\Phi_{oJ}-\Phi_{oI})^{n+1}+q^{n+1}_{oI}=\frac{V_I}{\Delta t}\Delta_t(\phi S_o b_o)_I \tag{2.70}$$

Gas:

$$\sum_{J=1}^{N(I)} \tau_{IJ}[\lambda^{*n+1}_{g}(\Phi_{gJ}-\Phi_{gI})^{n+1}+\lambda^{*n+1}_{RIJ}(\Phi_{oJ}-\Phi_{oI})^{n+1}] \tag{2.71}$$

$$+q^{n+1}_{GI}=\frac{V_I}{\Delta t}\Delta_t(\phi S_g b_g+\phi S_o b_o R_s)_I$$

Differences between these equations and those in Chapter 2.1. exist, because not only the

potentials but also the λ^* and the production rate q are described for the time point t^{n+1}. Furthermore, the porosity is pressure dependent, that means changeable in time.

N(I) is the number of neighbors of block *I*. V_I is the block bulk volume, therefore the pore volume is:

$$V_{pI} = V_I \phi_I. \tag{2.72}$$

The potentials Φ are given through:

$$\Phi_w = p_w - \rho_w g z, \tag{2.73}$$

$$\Phi_o = p_o - \rho_o g z, \tag{2.74}$$

$$\Phi_g = p_g - \rho_g g z, \tag{2.75}$$

where z is the depth of the grid point. The differences between the phase pressures are the capillary pressures:

$$p_o - p_w = P_{cow}, \tag{2.76}$$

$$p_g - p_o = P_{cgo}. \tag{2.77}$$

The component mobility λ^* is defined by:

$$\lambda^*_{mIJ} = \frac{k_{rm} b_m}{\mu_m} \qquad (m = w, o, g) \tag{2.78}$$

with $b_m = 1/B_m$, which is the shrinkage factor. The mobility related to the gas dissolved in oil is:

$$\lambda^*_{RIJ} = \frac{k_{ro} b_o R_s}{\mu_o}. \tag{2.79}$$

For the PVT - and rock properties the following applies, if $p \le p_b$:

$$\begin{aligned} &B_w = B_w(p) && \mu_w = const \\ &B_o = B_o\ (p, R_s), && \mu_o = \mu_o(p, R_s) \\ &B_g = B_g\ (p), && \mu_g = \mu_g(p) \\ &R_s = R_s\ (p) \end{aligned} \tag{2.80}$$

$$\begin{aligned} &\phi = \phi(p), \\ &k_{rw} = k_{rw}(S_w), && k_{ro} = k_{ro}(S_w, S_g), && k_{rg} = k_{rg}(S_g) \\ &P_{cow} = P_{cow}(S_w), && P_{cgo} = P_{cgo}(S_g) \end{aligned} \tag{2.81}$$

Furthermore, the depth z, the thickness h and the porosity ϕ have to be functions of place. The production rate of phase m in block I at time point t^{n+1} is given through the well equation:

$$q_{mI}^{n+1} = -WI_{Ik}\lambda_{mI}^{*n+1}[p_{mI}^{n+1} - p_{wfk}^{n+1} - \rho_{tk}g(z_I - z_{ref})] \tag{2.82}$$

with k being the serial number of the well. p_{wfk} is the bottom hole flowing pressure of the k^{th} well in reference depth z_{ref}. ρ_{tk} is the average density of the fluid, residing in the well between the top and the bottom of the perforation, corrected towards the reference depth.

WI_{Ik} is a productivity index for the perforation of the k^{th} well in block I.

The total gas production rate is calculated with

$$q_{GI}^{n+1} = (q_g + q_o R_s)_I^{n+1} \tag{2.83}$$

The well production rates result from the summation of Equation 2.82 and Equation 2.83 respectively, over the blocks I in which the well k is perforated.

The equations Equation 2.69 - Equation 2.71 and Equation 2.82 are not linear. An iterative solution method must be applied for these equations.

2.6. Generation and Linearization of the Equations

2.6.1 Notations

Let x be an unknown. The sequence of the iterated will be named with

$$x^{n,0}, x^{n,1}, ..., x^{n,\nu}, x^{n,\nu+1} ... \tag{2.84}$$

Furthermore

$$x^{n,0} = x^n \tag{2.85}$$

and

$$x^{n+1} = x^{n,\nu^*(n)+1} \tag{2.86}$$

ν^* depends on the break-off criteria for the iteration. For abbreviation, the following applies:

$$\delta^{n,\nu+1}x = x^{n,\nu+1} - x^{n,\nu} \tag{2.87}$$

or for sake of simplicity:

$$\delta x = x^{n,\nu+1} - x^{n,\nu} \tag{2.88}$$

2.6.2 Linearization

Lets regard the following non-linear expression:

$$\varphi(x^{n+1})\psi(x^{n+1}, y^{n+1}) \tag{2.89}$$

where the functions φ and ψ can be unlimited derived and therefore they can be expanded in Taylor series. For φ:

$$\varphi(x^{n+1}) = \tag{2.90}$$

$$\varphi(x^n) + \left(\frac{d\varphi}{dx}\right)^n \delta x + \frac{1}{2!}\left(\frac{d^2\varphi}{dx^2}\right)^n \delta x^2 + \frac{1}{3!}\left(\frac{d^3\varphi}{dx^3}\right)^n \delta x^3 + \ldots \frac{1}{m!}\left(\frac{d^m\varphi}{dx^m}\right)^n \delta x^m$$

If δx is small, than the higher terms can be neglected and

$$\varphi(x^{v+1}) \cong \varphi(x^v) + \left(\frac{d\varphi}{dx}\right)^v \delta x\,,\ \nu = 0, 1, \ldots, \nu_m \tag{2.91}$$

Similarly for ψ:

$$\psi(x^{v+1}, y^{v+1}) \cong \psi(x^v, y^v) + \left(\frac{\partial\psi}{\partial x}\right)^v \delta x + \left(\frac{\partial\psi}{\partial y}\right)^v \delta y\,. \tag{2.92}$$

For the expression the linearized approximation is then:

$$\varphi(x^{v+1})\psi(x^{v+1}, y^{v+1}) \cong \tag{2.93}$$

$$\varphi(x^v)\psi(x^v, y^v) + \left[\psi\frac{d\varphi}{dx} + \varphi\frac{\partial\psi}{\partial x}\right]^v \delta x + \left[\varphi\frac{\partial\psi}{\partial y}\right]^v \delta y$$

where the higher order terms with δx^2 and $\delta x \delta y$ are already neglected.

The non-linear equation

$$\varphi(x) = 0 \tag{2.94}$$

can be solved by Newton-Raphson iteration. Let $x^{v=0}$ be the first approximation for the root, then we solve the linear equation

$$\varphi(x^v) + \varphi'(x^v)\delta^{v+1}x = 0 \tag{2.95}$$

for $\delta^{v+1}x$ and the next approximation for the unknown is

$$x^{v+1} = x^v + \delta^{v+1}x \tag{2.96}$$

This value will be applied in Equation 2.95 again and again. The iteration converged if

$$\delta^{v+1}x < \varepsilon\,. \tag{2.97}$$

The Newton-Raphson iteration converges if φ is monotone and

$$|\varphi''(x)| < 1\,. \tag{2.98}$$

The Newton-Raphson iteration is widely used for solving non-linear equation systems too, but there is no theoretical prove for convergence.

For the sake of simplicity the difference operator δ^{v+1} will be replaced by δ for further notations.

2.6.3 Production Rate

The oil production rate emerges from equation Equation 2.82 with the TAYLOR series method:

$$q_{oI}^{\nu+1} = q_{oI}^{\nu} + \delta q_{oI} \tag{2.99}$$

$$= q_{oI}^{\nu} + WI_{Ik}\lambda_{oI}^{*\nu}\delta p_{wfk} - WI_{Ik}\lambda_{oI}^{*\nu}\delta p_{oI}$$

$$+ q_{oI}^{\nu}\left[\frac{\mu}{b}\frac{\partial}{\partial p_o}\left(\frac{b}{\mu}\right)\right]_{oI}^{\nu}\delta p_I + q_{oI}^{\nu}\left[\frac{\mu}{b}\frac{\partial}{\partial R_s}\left(\frac{b}{\mu}\right)\right]_{oI}^{\nu}\delta R_{sI}$$

$$+ q_{oI}^{\nu}\left[\frac{1}{k_{ro}}\frac{\partial k_{ro}}{\partial S_w}\right]_{oI}^{\nu}\delta S_{wI} + q_{oI}^{\nu}\left[\frac{1}{k_{ro}}\frac{\partial k_{ro}}{\partial S_g}\right]_{oI}^{\nu}\delta S_{gI}$$

respectively with the particular abbreviations:

$$q_{oI}^{\nu+1} = q_{oI}^{\nu} + \alpha_{oI1}\delta p_{wfk} + \alpha_{oI2}\delta p_{oI} + \alpha_{oI3}\delta S_{wI} + \alpha_{oI4}\delta S_{gI} + \alpha_{oI5}\delta R_{sI}. \tag{2.100}$$

The calculation of the flow terms is made with the component transmissibilities of the upstream blocks. That means that the k_r-values are calculated with the saturations and the pressure of the dominant block. The *dominance operator* is introduced to describe this in a formalism:

$$dom_{IJ}(x) = \begin{cases} x_I & \text{if} \quad \Phi_{mI} > \Phi_{mJ} \\ x_J & \text{if} \quad \Phi_{mI} \le \Phi_{mJ} \end{cases}; \quad m = w, o, g \tag{2.101}$$

For the oil phase the upstream weighting can be symbolized as follows:

$$\tau_{IJ}\lambda^*_{oIJ} = \tau_{IJ} dom^o_{IJ}\left(\frac{k_{ro} b_o}{\mu_o}\right) \tag{2.102}$$

The TAYLOR series method provides:

$$dom^o_{IJ}\left(\frac{k_r b}{\mu}\right)_o^{\nu+1} = dom^o_{IJ}\left(\frac{k_r b}{\mu}\right)_o^{\nu} \tag{2.103}$$

$$+ dom^o_{IJ}\left[k_r \frac{\partial}{\partial p_o}\left(\frac{b}{\mu}\right)\right]_o^{\nu} dom^o_{IJ}\delta p_o + dom^o_{IJ}\left[k_r \frac{\partial}{\partial R_s}\left(\frac{b}{\mu}\right)\right]_o^{\nu} dom^o_{IJ}\delta R_s$$

$$+ dom^o_{IJ}\left[\left(\frac{b}{\mu}\right)\frac{\partial k_r}{\partial S_w}\right]_o^{\nu} dom^o_{IJ}\delta S_w + dom^o_{IJ}\left[\left(\frac{b}{\mu}\right)\frac{\partial k_r}{\partial S_g}\right]_o^{\nu} dom^o_{IJ}\delta S_g$$

The following applies for generating the potential difference:

$$(\Phi_{oJ} - \Phi_{oI})^{\nu+1} = (p_{oJ} - \rho_{oJ} g z_J - p_{oI} + \rho_{oI} g z_I)^{\nu+1} \tag{2.104}$$

$$= \left[p_{oJ} - p_{oI} - \frac{1}{2}(\rho_{oJ} + \rho_{oI}) g (z_J - z_I)\right]^{\nu+1}$$

$$= \left[p_{oJ} - p_{oI} - \frac{1}{2}(\rho_{oJ} + \rho_{oI}) g (z_J - z_I)\right]^{\nu}$$

$$+ \left[1 - \frac{1}{2} g (z_J - z_I)\left(\frac{\partial \rho_o}{\partial p_o}\right)_J^{\nu}\right]\delta p_J$$

$$- \left[1 + \frac{1}{2} g (z_J - z_I)\left(\frac{\partial \rho_o}{\partial p_o}\right)_I^{\nu}\right]\delta p_I$$

$$- \frac{1}{2} g (z_J - z_I)\left(\frac{\partial \rho_o}{\partial R_s}\right)_J^{\nu} \delta R_{sJ}$$

$$+ \frac{1}{2} g (z_J - z_I)\left(\frac{\partial \rho_o}{\partial R_s}\right)_J^{\nu} \delta R_{sI}$$

The generation of the potential difference for the water phase and the gas phase differ from that for the oil phase caused by the capillary pressure.

For water:

$$(\Phi_{wJ}-\Phi_{wI})^{\nu+1} = \left[p_{oJ}-p_{oI}-\frac{1}{2}(\rho_{wJ}+\rho_{wI})g(z_J-z_I)-P_{cowJ}+P_{cowI}\right]^{\nu+1} \tag{2.105}$$

$$= \left[p_{oJ}-p_{oI}-\frac{1}{2}(\rho_{wJ}+\rho_{wI})gz_{IJ}-P_{cowJ}+P_{cowI}\right]^{\nu}$$

$$+\left[1-\frac{1}{2}gz_{JI}\left(\frac{d\rho_w}{dp_w}\right)_J^{\nu}\right]\delta p_{oJ}-\left[1+\frac{1}{2}gz_{JI}\left(\frac{d\rho_w}{dp_w}\right)_I^{\nu}\right]\delta p_{oI}$$

$$+\left(\frac{dP_{cow}}{dS_w}\right)_J^{\nu}\delta S_{wJ}-\left(\frac{dP_{cow}}{dS_w}\right)_I^{\nu}\delta S_{wI},$$

with

$$z_{JI}= z_J-z_I. \tag{2.106}$$

The expression for the gas potential difference can be written analogously. The first term of Equation 2.70 can be generated in the following form, after having inserted Equation 2.103 and Equation 2.104, neglecting very small terms of second order:

$$\sum_{J=1}^{N(I)} \tau_{IJ}\lambda^{*n+1}_{oIJ}(\Phi_{oJ}-\Phi_{oI})^{n+1} = \sum_{J=1}^{N(I)} \tau_{IJ} dom^{o}_{IJ}\left(\frac{k_r b}{\mu}\right)_o^{\nu+1}(\Phi_{oJ}-\Phi_{oI})^{\nu+1} \qquad (2.107)$$

$$= \sum_{J=1}^{N(I)} \tau_{IJ} dom^{o}_{IJ}\left(\frac{k_r b}{\mu}\right)_o^{\nu+1}(\Phi_{oJ}-\Phi_{oI})^{\nu}$$

$$+ dom^{o}_{IJ}\left(\frac{k_r b}{\mu}\right)_o^{\nu}\Bigg(\quad + \left[1-\frac{1}{2}g(z_J-z_I)\left(\frac{\partial \rho_o}{\partial p_o}\right)_J^{\nu}\right]\delta p_J$$

$$-\left[1+\frac{1}{2}g(z_J-z_I)\left(\frac{\partial \rho_o}{\partial p_o}\right)_I^{\nu}\right]\delta p_I$$

$$-\frac{1}{2}g(z_J-z_I)\left(\frac{\partial \rho_o}{\partial R_s}\right)_J^{\nu}\delta R_{sJ}$$

$$+\frac{1}{2}g(z_J-z_I)\left(\frac{\partial \rho_o}{\partial R_s}\right)_J^{\nu}\delta R_{sI}\Bigg)$$

$$+ (\Phi_{oJ}-\Phi_{oI})^{\nu}\Bigg(dom^{o}_{IJ}\left[k_r\frac{\partial}{\partial p_o}\left(\frac{b}{\mu}\right)\right]_o^{\nu} dom^{o}_{IJ}\delta p_o$$

$$+ dom^{o}_{IJ}\left[k_r\frac{\partial}{\partial R_s}\left(\frac{b}{\mu}\right)\right]_o^{\nu} dom^{o}_{IJ}\delta R_s$$

$$+ dom^{o}_{IJ}\left[\left(\frac{b}{\mu}\right)\frac{\partial k_r}{\partial S_w}\right]_o^{\nu} dom^{o}_{IJ}\delta S_w + dom^{o}_{IJ}\left[\left(\frac{b}{\mu}\right)\frac{\partial k_r}{\partial S_g}\right]_o^{\nu} dom^{o}_{IJ}\delta S_g\Bigg)$$

If *I* is the dominant block, the particular dom-term can added to the previous $\delta^{v+1}p_{oI}$ term. With the abbreviations already used before, Equation 2.107 can be written in a shorter form. The expressions for *ß's* can be written by the comparison of the two equations. The short symbolic forms are:

$$\sum_{J=1}^{N(I)} \tau_{IJ}\lambda^{*\nu+1}_{oIJ}(\Phi_{oJ}-\Phi_{oI})^{\nu+1} \tag{2.108}$$

$$= \beta^{\nu}_{oI0} + \beta^{\nu}_{oI2}\delta^{\nu+1}p_{oI} + \sum^{*}\beta^{\nu}_{oJ6}\delta^{\nu+1}p_{oJ}$$

$$+ \beta^{\nu}_{oI3}\delta^{\nu+1}S_{wI} + \sum^{*}\beta^{\nu}_{oJ7}\delta^{\nu+1}S_{wJ}$$

$$+ \beta^{\nu}_{oI4}\delta^{\nu+1}S_{gI} + \sum^{*}\beta^{\nu}_{oJ8}\delta^{\nu+1}S_{gJ}$$

$$+ \beta^{\nu}_{oI2}\delta^{\nu+1}R_{sI} + \sum^{*}\beta^{\nu}_{oJ9}\delta^{\nu+1}R_{sJ}$$

$\sum^{*}$ means, that the summation is only made with these neighbors which are dominant in regard to block J.

2.6.4 Accumulation Term

For the right hand side of Equation 2.70 - paying attention to

$$\delta^{\nu+1}S_o = -\delta^{\nu+1}S_w - \delta^{\nu+1}S_g \tag{2.109}$$

follows this description:

$$\frac{V_I}{\Delta t}\Delta t[\phi S_o b_o]_I = \frac{V_I}{\Delta t}\left[(\phi S_o b_o)_I^{\nu+1} - (\phi S_o b_o)^{o}\right] \tag{2.110}$$

$$+ \frac{V_I}{\Delta t}[(\phi S_o b_o)^{\nu} - (\phi S_o b_o)^{o} + \delta^{\nu+1}(\phi S_o b_o)]_I$$

$$= \frac{V_I}{\Delta t}(\phi S_o b_{oI})^{\nu} - (\phi S_o b_o)_I^{o} + \left(S_o\phi\frac{\partial b_o}{\partial b p_o} + S_o b_o\frac{\partial\phi}{\partial p_o}\right)_I \delta^{\nu+1}p_{oI}$$

$$-(\phi b_o)_I^{\nu}\delta^{\nu+1}S_{wI} - (\phi b_o)_I^{\nu}\delta^{\nu+1}(S_{gI})$$

$$+ \left(S_o\phi\frac{\partial b_o}{\partial R_s}\right)_I^{\nu}\delta^{\nu+1}R_{sI}\Bigg]$$

By using symbolic writing, Equation 2.110 can be written as follows:

$$\frac{V_I}{\Delta t}\Delta_t[\phi S_o b_o]_I = \gamma_{oI0} + \gamma_{oI2}\delta^{\nu+1}p_{oI} + \gamma_{oI3}\delta^{\nu+1}S_{wI} + \gamma_{oI4}\delta^{\nu+1}S_{gI} + \gamma_{oI5}\delta^{\nu+1}R_{sI} \tag{2.111}$$

Finally, the linearized oil equation results from inserting Equation 2.100, Equation 2.108 and Equation 2.110 into Equation 2.70, taking Equation 2.88 into account and summarizing the coefficients.

$$\begin{aligned}\eta^{\nu}_{oI1}\delta^{\nu+1}p_{wfk} + \eta^{\nu}_{oI2}\delta^{\nu+1}p_I + \sum\eta^{\nu}_{oJ6}\delta^{\nu+1}p_J \\ + \eta^{\nu}_{oI3}\delta^{\nu+1}S_{wI} + \sum\eta^{\nu}_{oJ7}\delta^{\nu+1}S_{wJ} \\ + \eta^{\nu}_{oI4}\delta^{\nu+1}S_{gI} + \sum\eta^{\nu}_{oJ8}\delta^{\nu+1}S_{gJ} \\ + \eta^{\nu}_{oI5}\delta^{\nu+1}R_{sI} + \sum\eta^{\nu}_{oJ9}\delta^{\nu+1}R_{sJ} = d^{\nu}_{oI}\end{aligned} \tag{2.112}$$

The water equation follows analogously taking Equation 2.105 into account:

$$\begin{aligned}\eta_{wI1}\delta^{\nu+1}p_{wfk} + \eta^{\nu}_{wI2}\delta^{\nu+1}p_I + \sum\eta^{\nu}_{wJ6}\delta^{\nu+1}p_{oJ} \\ + \eta^{\nu}_{wI3}\delta^{\nu+1}S_{wI} + \sum\eta^{\nu}_{wJ7}\delta^{\nu+1}S_{wJ} = d^{\nu}_{wI}\end{aligned} \tag{2.113}$$

And also the gas equation:

$$\begin{aligned}\eta^{\nu}_{gI1}\delta^{\nu+1}p_{wfk} + \eta^{\nu}_{gI2}\delta^{\nu+1}p_I + \sum\eta^{\nu}_{gJ6}\delta^{\nu+1}p_{oJ} \\ + \eta^{\nu}_{gI3}\delta^{\nu+1}S_{wI} + \sum\eta^{\nu}_{gJ7}\delta^{\nu+1}S_{wJ} \\ + \eta^{\nu}_{gI4}\delta^{\nu+1}S_{gI} + \sum\eta^{\nu}_{gJ8}\delta^{\nu+1}S_{gJ} \\ + \eta^{\nu}_{gI5}\delta^{\nu+1}R_{sI} + \sum\eta^{\nu}_{gJ9}\delta^{\nu+1}R_{sJ} = d^{\nu}_{gJ}\end{aligned} \tag{2.114}$$

The right sides of Equation 2.112 - Equation 2.114 allows estimation of the magnitude of the unknowns $\delta^{\nu+1}S_w$ and $\delta^{\nu+1}S_g$ as an example the left side of Equation 2.113 will be written in a more detailed form:

$$d_{wI}^{\nu} = \gamma_{wI0}^{\nu} - \beta_{wI0}^{\nu} - q_{wI}^{\nu} \tag{2.115}$$

$$= \frac{V_I}{\Delta t}[(\phi S_w b_w)^{\nu} - (\phi S_w b_w)^{o}]$$

$$- \sum_{J=1}^{N(I)} \tau_{IJ}\left[dom_{IJ}^{w}\left(\frac{k_r b}{\mu}\right)_w (\Phi_{wJ} - \Phi_{wI})^{\nu}\right] - q_{wI}^{\nu}.$$

The first term is the accumulation rate, the second one the influx or outflux rate and the third one the production rate of water. The dimension is standard m^3/s. If $d_{wI}^{\nu} = 0$, then the $\delta^{\nu+1} S_{wI}$ will be a smaller value because this is a proper function of other variables, mainly of $\delta^{\nu+1} p's$. If d_{wI}^{ν} is greater then zero there is a strong uncompensated water in - or outflux from the block and greater changes of the water saturation must be expected. The quantity

$$e_w = \frac{d_{wI}^{\nu} \Delta t}{V_I \phi_I}, \tag{2.116}$$

shows how much is this water compared to the pore volume and can be used to estimate the magnitude of saturation changes for the next iteration step. In the same manner e_o and e_g can be determined.

The total production rate of well k is the sum of the partial rates q_{mI}. The summation of Equation 2.99 - for those blocks I in which well k is perforated - provides:

$$\delta^{\nu+1} p_{wfk} \sum_{I=1}^{M(k)} \alpha_{oI1}^{\nu} + \sum_{I=1}^{M(k)} [\alpha_{oI2}^{\nu} \delta^{\nu+1} p_I + \alpha_{oI3}^{\nu} \delta^{\nu+1} S_{wI} \tag{2.117}$$

$$+ \alpha_{oI4}^{\nu} \delta^{\nu+1} S_{gI} + \alpha_{oI5}^{\nu} \delta^{\nu+1} R_{sI}] = d_{ok}^{\nu}$$

A similar equation follows if the gross production rate is given. For gas wells the gas production rate, for water injection wells the injection rate is given.

It is also possible to fix the bottom hole flowing pressure instead of the production rate. The following applies:

$$\delta^{\nu+1} p_{wfk} = 0 \tag{2.118}$$

and Equation 2.112 and Equation 2.114 can be reduced by this term.

2.7. Variable Bubble Point

The oil in block *I* is undersaturated, if the following applies:

$$R_{sI} < R_s(p_{oI}). \tag{2.119}$$

In that case

$$S_{gI} = 0 \quad \text{and} \quad \delta^{\nu+1} S_{gI} = 0, \tag{2.120}$$

so $\delta^{\nu+1} S_{gI}$ does not appear in Equation 2.112 - Equation 2.117 anymore.

If the gas saturation is larger than zero, R_s is a function of pressure:

$$R_{sI} = R_{s(pI)}, \qquad \delta^{\nu+1} R_{sI} = \left(\frac{dR_s}{dp_o}\right)_I^{\nu} \delta^{\nu+1} p_{oI} \tag{2.121}$$

and block *I* will be considered as saturated or undersaturated in Equation 2.112 and Equation 2.114 at time point t^n. After inserting either Equation 2.120 for undersaturated or Equation 2.121 for saturated case, the equation system Equation 2.112 - Equation 2.117 can be reduced to one unknown.

A possible passover from one to the other state within one time step will not be considered yet. Therefore, an initial undersaturated block may become oversaturated:

$$R_{sI}^{n+1} > R_s(p_{oI}^{n+1}), \qquad S_{gI}^{n+1} = 0 \tag{2.122}$$

In that case, the correction is made in the next time step:

$$R_{sI}^{n+1} = R_s(p_{oI}^{n+1}). \tag{2.123}$$

In the opposite case, more gas than available dissolves in oil,

$$R_{sI}^{n+1} = R_s(p_{oI}^{n+1}), \qquad S_{gI}^{n+1} < 0 \tag{2.124}$$

the following correction is made:

$$S_{gI}^{n+1} = 0. \tag{2.125}$$

This corrected saturation and solution gas ratio gives the initial state for the next time step. The corrections Equation 2.123 and Equation 2.124 may cause significant material balance errors. These can be eliminated by mass correction.

Let block *I* be oversaturated at the timepoint t^n before time $n + 1$. The oil- and gas content

follows as:

$$G_o = V_I(\phi S_o b_o)_I^n, \tag{2.126}$$

$$G_g = V_I(\phi S_o b_o R_{sI})_I^n, \tag{2.127}$$

If this block is transferred into the saturated state, the following changes occur:

$$G_o^* = V_I(\phi S_o)_I^n b_o(p_I^n), \tag{2.128}$$

$$G_o^* = V_I(\phi S_o)_I^n b_o(p_I^n) R_s(p_I^n), \tag{2.129}$$

where

$$b^n{}_{oI} < b_o(p_{oI}^n) \text{ and } (R_{sI} > R_s(p_{oI}^n)) \tag{2.130}$$

The differences

$$\Delta G_o = G_o - G_o^* = V_I(\phi S_o)_I^n [b_{oI}^n - b_o(p_I^n)], \tag{2.131}$$

$$\Delta G_o = G_o - G_o^* = V_I(\phi S_o)_I^n [b_{oI}^n R_{sI} - b_o(p_{oI}^n) R_s(p_{oI})], \tag{2.132}$$

will be reinjected into this block if ΔG is positive, or produced out of this block if ΔG is negative during the time step $n + 1$.

If the oil is saturated (the bubble point is equal with the block pressure) but the gas saturation becomes negative, then the gas saturation will be set zero and the oil saturation will be adequately increased at the timepoint t^n. In the next time step the oil quantity of

$$\Delta G_o = -V_I(\phi S_g b_o)_I^n \tag{2.133}$$

must be produced out of this block and the gas quantity of

$$\Delta G_o = -V_I(\phi S_g b_g)_I^n \tag{2.134}$$

must be injected into this block.

2.8. Solution Methods

There are three possibilities to solve the Equation 2.112 - Equation 2.117:

- **Fully implicit method**. The iteration method given by Equation 2.112 - Equation

2.117 will be applied until the changes $\delta^{\nu+1}p_I$, $\delta^{\nu+1}S_{wI}$, $\delta^{\nu+1}S_{gI}$ or $\delta^{\nu+1}R_{SI}$ are smaller than the given limits.

- **Semi-implicit method**. The equation system will be solved only once ($\nu = 0$) per time step.
- **IMPES-method**. IMPES stands for **I**mplicit **P**ressure **E**xplicit **S**aturation.

The combination of these three methods is the adaptive implicitness. In a proper IMPES formulation the phase transmissibilities, the capillary pressures and the production rates at time point t^n are taken. Therefore Equation 2.116 does not belong anymore to those equations being solved simultaneously. Because all coefficients in Equation 2.70, Equation 2.72 refer to the time point t^n, the terms following the summation $\Sigma*$ disappear from Equation 2.112 - Equation 2.114 which can be written as follows:

$$\eta^n_{oI2}\delta^{n+1}p_I + \sum \eta^n_{oJ6}\delta^{n+1}p_J + \eta^n_{oI3}\delta^{n+1}S_{wI} + \sum \eta^n_{oI4}\delta^{n+1}S_{gJ} + \eta^n_{oI5}\delta^{n+1}R_{sI} = d^n_{oI} \tag{2.135}$$

$$\eta^n_{wI2}\delta^{n+1}p_I + \sum \eta^n_{wJ6}\delta^{n+1}p_J + \eta^n_{wI3}\delta^{n+1}S_{wI} = d^n_{wI} \tag{2.136}$$

$$\eta^n_{gI2}\delta^{n+1}p_I + \sum \eta^n_{gI6}\delta^{n+1}p_J + \eta^n_{gI3}\delta^{n+1}S_{wI} + \eta^n_{gI4}\delta^{n+1}S_{gI} + \eta^n_{gI5}\delta^{n+1}R_{sI} = d^n_{gI} \tag{2.137}$$

At first one of the unknown $\delta^{\nu+1}S_{gI}$ and $\delta^{\nu+1}R_{sI}$ should be eliminated on the basis of Equation 2.118 or Equation 2.119. Afterwards these three equations are multiplied with the following factors and added:

for saturated case	for undersaturated case
$-\eta^n_{gI4}$	$-\eta^n_{gI4}$
$\dfrac{\eta^n_{oI3}\eta^n_{gI4} - \eta^n_{gI3}\eta^n_{oI4}}{\eta^n_{wI3}}$	$\dfrac{\eta^n_{oI3}\eta^n_{gI5} - \eta^n_{gI3}\eta^n_{oI5}}{\eta^n_{wI3}}$
η_{oI4}	η^n_{oI5}

The unknowns $\delta^{\nu+1}S_{wI}$, $\delta^{\nu+1}S_{gI}$ and $\delta^{\nu+1}R_{sI}$ are eliminated by this procedure because the resulting equations only contains the pressure change $\delta^{\nu+1}p$ as unknown:

$$\varepsilon_I^n \delta^{\nu+1} p_I + \sum_{J=1}^{N(I)} \varepsilon_I^n \delta^{\nu+1} p_J = C_I^n. \tag{2.138}$$

$\delta^{\nu+1}S_{wI}$ and $\delta^{\nu+1}S_{gI}$ or $\delta^{\nu+1}R_{sI}$ can be calculated explicitly from Equation 2.35 and Equation 2.36, after having solved the linear equation system Equation 2.138.

Applying adaptive implicitness first at the residuals d_ν , i.e. the norm *e*, given by Equation 2.116 have to be examined. If for a given block all of them are smaller than a given value (e.g.: 0.01, that means 1% of the pore volume) then this block will be taken as an IMPES block. All coefficients originating from the derivatives regarding the saturations or R_s will drop out. From the equations written for the neighboring blocks the terms containing the saturation changes (or$\delta^{\nu+1}R_{sI}$) will be cancelled. After that the three equations for the IMPES block can be reduced to one equation, similar to Equation 2.138. If this block has neighbors, which remained implicit then also saturation changes ($\delta^{n+1}S_{wJ}\,\delta^{n+1}S_{wJ}$) exist in the IMPES equation for those neighbors.

The average degree of implicitness IGA is defined as the average number of implicitly calculated variables per block and time step:

$$IGA = \frac{1}{N \times NLL}\left[\sum_{i=1}^{N}\sum_{\nu=1}^{\nu^*}\sum_{I=1}^{LL} n_I + K\right] \tag{2.139}$$

where

N - number of time steps

LL - number of blocks

ν^* - number of iteration steps for the time step

n_I - number of implicit unknown for block I in an iteration step

K - number of wells

For a proper IMPES calculation IGA = 1 for the semi-implicit method slightly above 3 and for fully implicit 5 to 10. For field scale simulation the adaptive implicitness usually has a value between 1.2 and 1.6, without loosing stability performance compared to the fully implicit computation.

Although the IMPES method requires solving a fewer number of unknowns simultaneously, it

has lower performance than the semi- or fully-implicit solution methods because due to poor stability only smaller time steps can applied. The superiority of the adaptive implicitness is that larger time steps can applied. The superiority of the adaptive implicitness is unambiguous. (At least by scalar computing. On vector computers this advantage can be lost because the irregularity of the matrix equation impedes the vectorization).

3 2½-Dimensional Grid Models

3.1. Cartesian Coordinate System

It should be noted, that Section 3.1. is to some part a repetition of Section 2.3., however some in-depth discussion is added.

Although the rigid Cartesian coordinate system does not seem very suitable for the geometry and flow pattern of a real reservoir, this technique has been widely applied for reservoir simulation. Other coordinate systems and grid construction methods were used only for special purposes. An exception is the radial cylindrical coordinate system for solving single well problems.

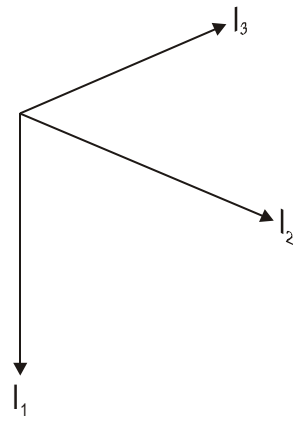

Figure 3.1: Cartesian coordinate system

At first a two-dimensional Cartesian system - having the coordinates aligned to the *I2* and *I3* axes - is selected to assemble the block system for reservoir simulation. The *I1-axis* is perpendicular to the I_2-I_3-*plane* and points downwards. This orientation (as shown in Figure 3.1) is not the usual one, but it has the advantage that the depth is measured and the layers are numbered in the same manner as in the geological representation. Then, a basic grid is constructed. The grid can be defined in two ways:

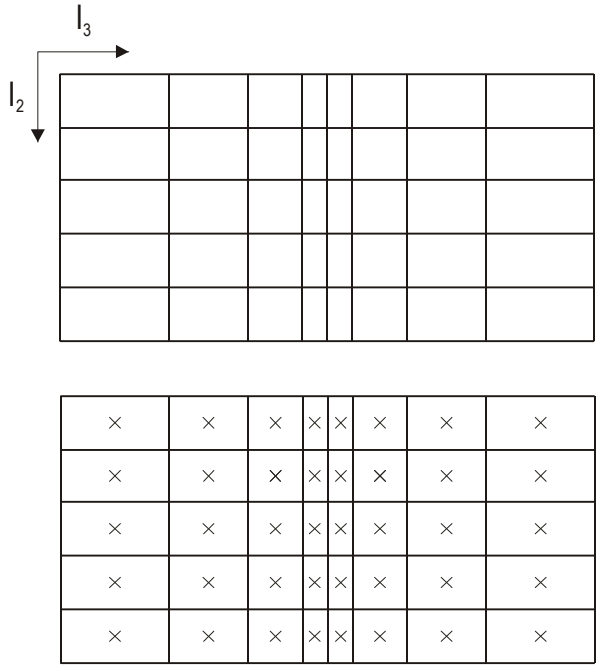

Figure 3.2: Construction of a block centered Cartesian grid

- ***Block centered scheme**:* For the block centered grid the block sizes are selected at first and then the nodal points are centered between the boundaries (Figure 3.2).

- ***Point distributed scheme**:* The grid points are set at first and the block boundaries halve the distance between the nodes. The boundaries at the model margins are determined by reflecting the last block boundary at the outmost grid point, as shown in Figure 3.3.

The Cartesian grid is orthogonal per definition. Therefore the flow rate between two blocks can be approximated by two-point approximation. The point distributed scheme is a special kind of the perpendicular bisection (PEBI) grid while the block centered grid is not.

Aziz and Settari[13] discussed the properties of the two grid types using differential formulation of the flow equation. Aziz and Settari calculated the potential gradient for the grid point and not at the block boundaries. For this case there is no difference between the two grids if the mobility λ is a constant. When using integral formulation it becomes evident that the order of approximation of the potential gradient term remains different. The significance of the discretization error analysis is that the point-distributed approximation is consistent and therefore for any stable finite difference method it will be convergent. However, there is no *a priori* guarantee for convergence for the block centered grid.

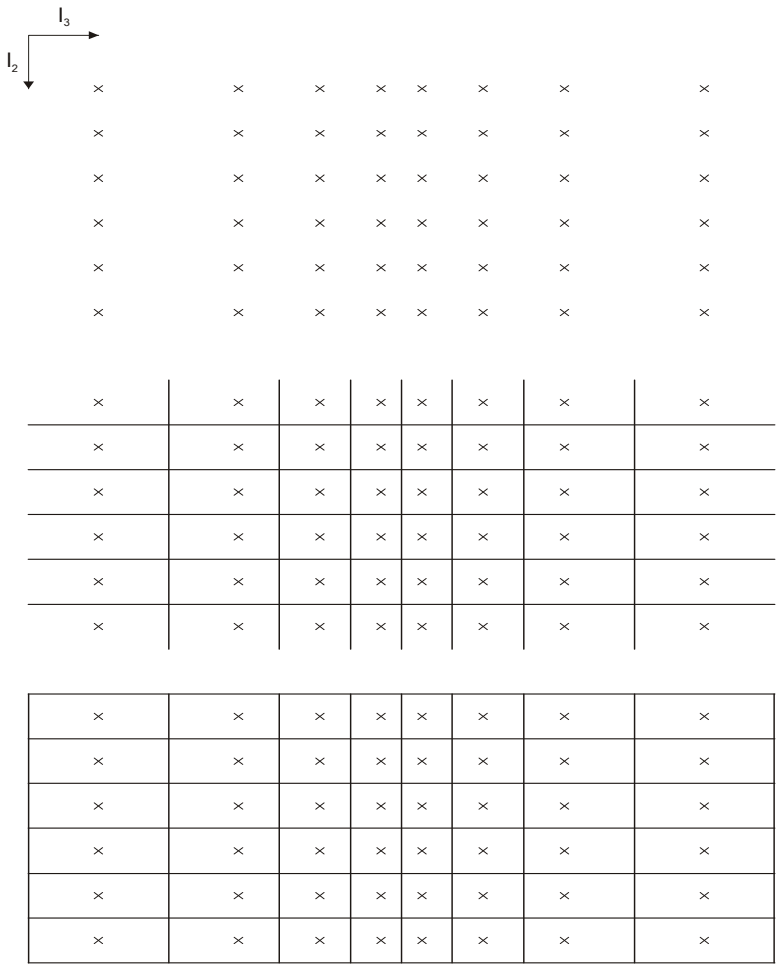

Figure 3.3: Construction of a point distributed Cartesian grid

It should be emphasized that inconsistency does not necessarily imply divergence as the block size goes to zero ($\|h\| \to 0$).The actual order of convergence depends on the manner or the irregularity of the grid spacing. Because the discretization errors act as error sources for the solution of the equations, their effects are smoothed out. Based on numerical experiments, we conclude that for any reasonably smooth variation of grid spacing the block centered difference scheme will also be convergent in the limit. However from a practical point of view, there is no additional difference when using one or the other type of Cartesian grid. That means, the application of the point distributed grid is not more complicated than the block centered one. The only difference seems to be that a better consistency is provided for the point distributed grid by the numerical error analysis. This is sufficient for us to give a recommendation for that type of grid, without refusing the applicability of the other one. From mathematical point of view the regular Cartesian grid provides the minimum time and spatial discretization errors therefore this grid should be used if no other reason exists for irregular grid spacing.

The same procedure for block construction can be applied in the vertical direction if the extension of the reservoir is comparable with the horizontal one (see Figure 3.4). Most frequently however, the vertical extension is smaller in order of magnitude than the horizontal

one and it is also layered, so that such a discretization cannot be used or requires very small grid spacing. Instead of doing so it is better to construct the grid in the horizontal plane and project it through the layers as shown in Figure 3.5. This is the 2½-dimensional grid.

In 3D and 2½D Cartesian block system a block has maximum six neighbors. It is evident that this grid is only Cartesian and orthogonal in the horizontal plane but not in the cross section. The basic idea is to use a stream tube approach in the cross section. We assume that the vertical component of flow velocity as well as its components parallel to layer can be de-coupled.

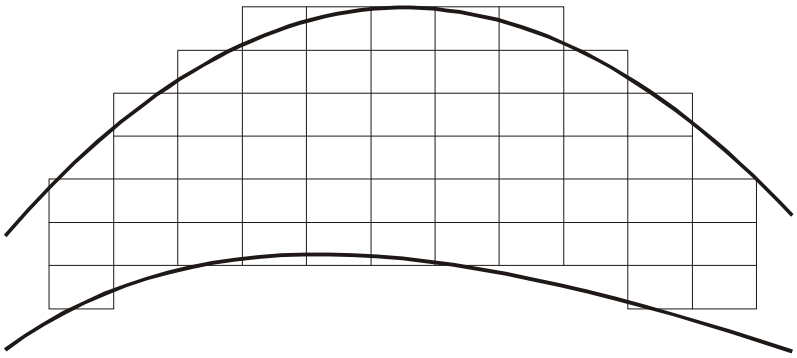

Figure 3.4: 3D Cartesian grid in cross section

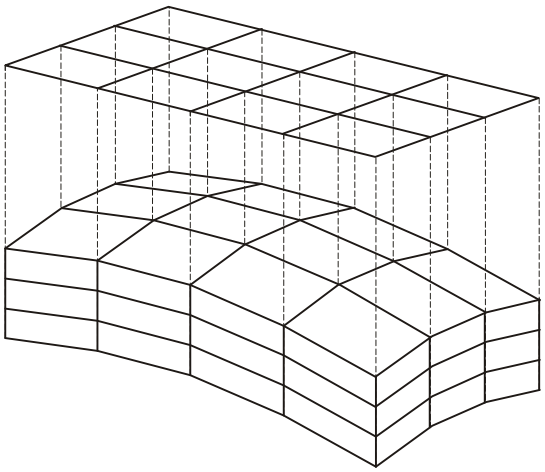

Figure 3.5: 2½-dimensional Cartesian grid

In Chapter 2.1. we already introduced the concept of block transmissibilities. A fundamental Cartesian grid has six of them, oriented from the grid point toward the six block sides. Those six transmissibilities are indicated with τ_{Ii}^{+} or τ_{Ii}^{-} (i= 1,2,3). They are calculated in a simple way, supposing a linear incompressible one-phase DARCY-flow, orthogonal on the block surface. From the DARCY law:

$$Q_{Ii}^{+} = \left(\frac{AK}{L}\right)_{Ii}^{+} \frac{\Phi - \Phi_I}{\mu} = \frac{\tau_{Ii}^{+}}{\mu}(\Phi - \Phi_I) \tag{3.1}$$

Therefore the *block half-transmissibility* has the form of

$$\tau_{Ii}^{+} = \left(\frac{Ak}{L}\right)_{Ii}^{+}. \tag{3.2}$$

where A is the block surface, L the half-length of the block and k the permeability.

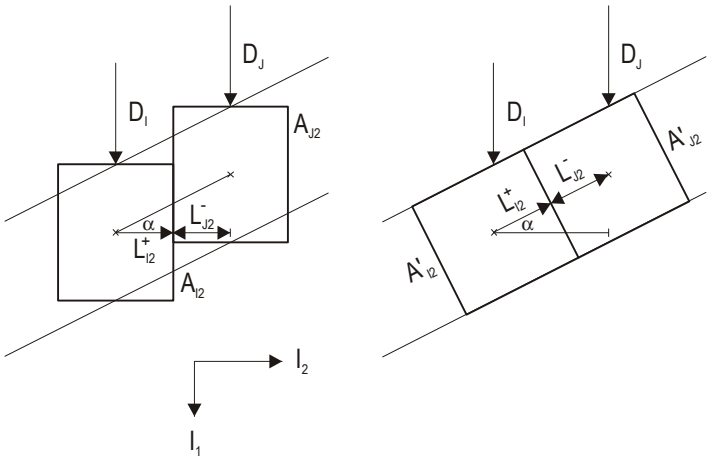

Figure 3.6: Dip correction of the transmissibilities (must be corrected, D should point to the middle of the block)

The transmissibility between two grid points, called *block-pair transmissibility*, will be calculated - based on the KIRCHOFF law - as the harmonical average of two half-block transmissibilities

$$\tau_{IJ} = \frac{\tau_{Ii}^{+}\tau_{Ji}^{-}}{\tau_{Ii}^{+} + \tau_{Ji}^{-}} \tag{3.3}$$

In this way, not only the permeabilities of the neighboring blocks but also the block surfaces are averaged. If the layer is not horizontal, then this approximation will not be correct, because the direction of the flow is parallel to the layer and not to the block edge. The true distance from the grid point to the communication surface and the true surface can be calculated easily, as shown in Figure 3.6:

$$\begin{aligned} \tilde{L}_I^{+} &= \frac{L_I^{+}}{\cos\alpha}, \\ \tilde{A}_I &= A_I \cos\alpha, \end{aligned} \tag{3.4}$$

where α is the dip of the layer. Applying Equation 3.4 to Equation 3.2 and considering Equation 3.3 the right block-pair transmissibility is:

$$\tau_{IJ} = \frac{\tau_{Ii}^{+}\tau_{Ji}^{-}}{\tau_{Ii}^{+} + \tau_{Ji}^{-}}(\cos\alpha)^2 . \qquad (3.5)$$

In practical application the geometrical torsions in the cross section are sometimes neglected and the block system will be displayed as a system of rectangular horizontal blocks as shown in Figure 3.7. The blocks are shifted vertically from each other, their surfaces are not the same for the neighbors and the overlapping is only partly. This is only a question of the graphical illustration and has no influence on the calculation of the transmissibilities.

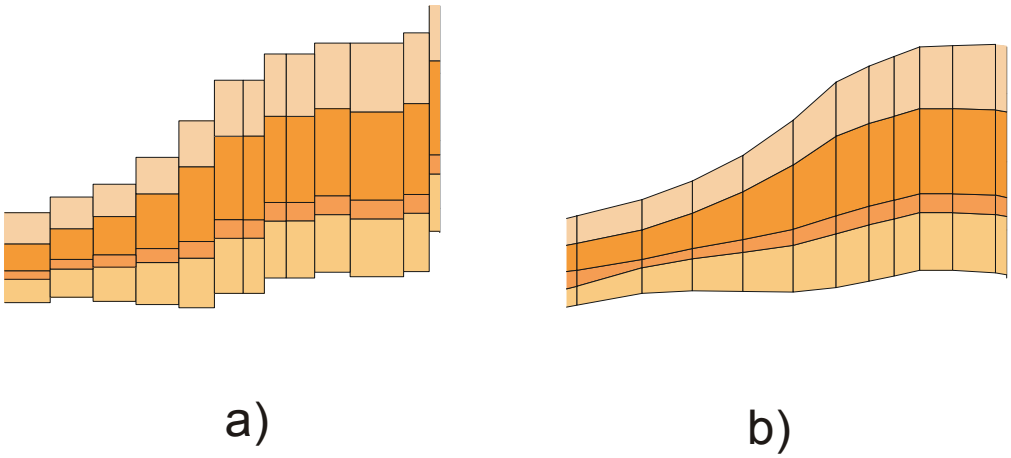

Figure 3.7: Cross section of a Cartesian layered model
a) discretization grid, b) visualized grid

3.2. Local Grid Refinement

In most of the cases the Cartesian grid is not sufficient to provide the necessary resolution for particularly interesting areas, e.g. at the vicinity of wells. To achieve a high resolution in relevant areas, and at the same time to keep the overall number of blocks as small as possible, selected blocks can be subdivided. This subdivision is called *local grid refinement (LGR)*. LGR was introduced by *Heinemann et al.*[58] in 1983 and it was discussed in many papers since then.

To distinguish between the original (coarse) and the resulting (fine) blocks the expressions *"fundamental"* and *"refined"* blocks will be used. Three divisor numbers (K_{I1}, K_{I2}, K_{I3}) can be assigned to every fundamental block. They indicate the number of partial blocks into which the fundamental block is to be subdivided in the corresponding direction. In this way, sub-coordinates (I_{1T}, I_{2T}, I_{3T}) are defined in every fundamental block, with the same orientation as the main coordinates (Figure 3.8).

In this way, each partial block can be addressed by specifying the coordinates (I_1, I_2, I_3) of the fundamental block and the sub-coordinates (I_{1T}, I_{2T}, I_{3T}). (For brevity, we refer fundamental blocks as *F*-blocks and the refinded blocks as *R*-blocks in the following).

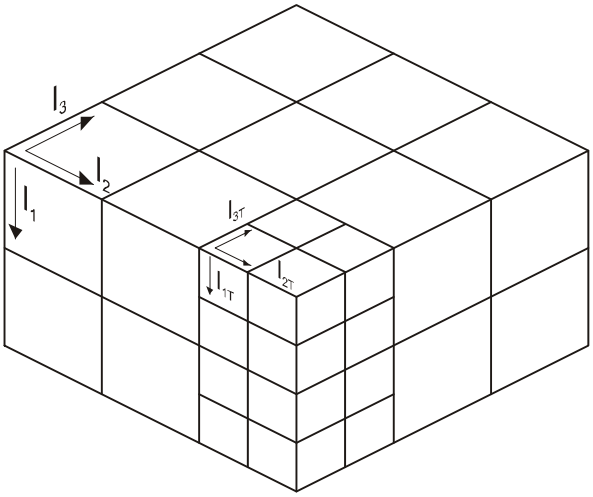

Figure 3.8: Determination of the sub-coordinates

The subdivision can be done on more levels, uniformly or irregularly. Possibilities which are not recommended are shown in Figure 3.9. All these types of LGR were discussed in the literature with contradicting results. Even if the advantage of a certain kind of LGR was demonstrated for a couple of problems, it was always possible to find a case in which the deviations from the equivalent, fully refined grid was unacceptable, or the coarse grid gives even more reliable results. To avoid these pitfalls the following requirements must be satisfied:

- The grid must be point distributed and not block centered.
- The coarse blocks must be equally and uniformly divided in x- and y- directions.
- The coarse-fine grid transition must be smooth; the transition ratio between finer and coarser grid should be 1:2 or 1:3.
- The orthogonality at the transition zone must be assured.

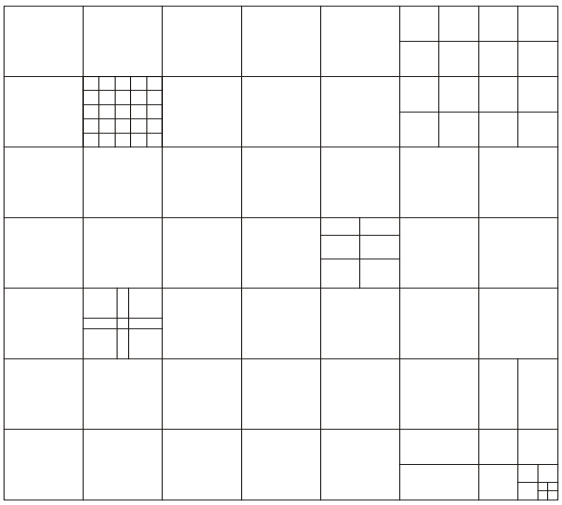

Figure 3.9: Not recommended Cartesian grid refinements.

The necessity of the first requirement was demonstrated by *Nacul et al.*[98]. Most of the commercial simulators use block-centered grids. In such a case the LGR can be used for the area with square Cartesian blocks which are block-centered and point-distributed at the same time. No LGR can be recommended for corner point geometry.

If the second requirement is not satisfied, thus a supplementary artificial orientation effect will be introduced if the main flow direction changes, leading to wrong conclusions. The third requirement is necessary to assure an acceptable accuracy in calculating the flow between refined and coarse regions as it was proved by *Nacul et al.*[98]. By disregarding the fourth requirement the two-point flux approximation is not applicable. When the refined block system is determined, the divided region should have as few corners as possible (Figure 3.10).

It is suggested to use 2x2, 4x4, 8x8 or 3x3 and 6x6 areal refinement only. The transition ratios 1:2 or 1:3 between coarse and fine grids can be satisfied by extending the refined zone as shown in Figure 3.10b. There is no argument against a multilevel LGR in which the individual refined blocks are further refined, satisfying the same requirements. However, there is no practical need for such an option. It is better to exploit the possibilities offered by the windowing technique[32],[33].

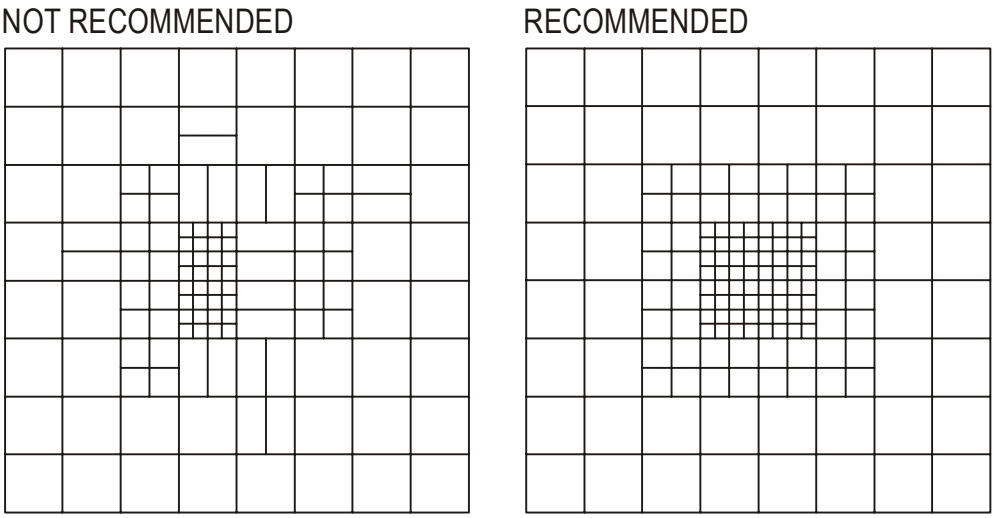

Figure 3.10: Definition of the subdivided area. a) not recommended, b) recommended

The shortcoming of the classical LGR, as shown in Figure 3.10b, is that the transition between coarse and refined grid is not orthogonal, therefore the two point approximation cannot be used, or if it is used it leads to considerable discretization errors. To overcome this problem different approaches exist. One possibility is to make use of multi-point flux approximation. Alternatively *Quandal et al.* introduced pseudo-points along the transition boundaries. Both solutions are limited applicable and complicated. The right solution is to construct the grid by the PEBI method assuring orthogonal transition between the coarse and refined blocks as shown in Figure 3.11. It is easy to understand that this solution has also some limitations. It can be used only if the Cartesian grid is point-distributed and the grid spacing of the F-blocks does not change very much. For blocks with stretched shape it is not possible to construct such a geometry (Figure 3.12).

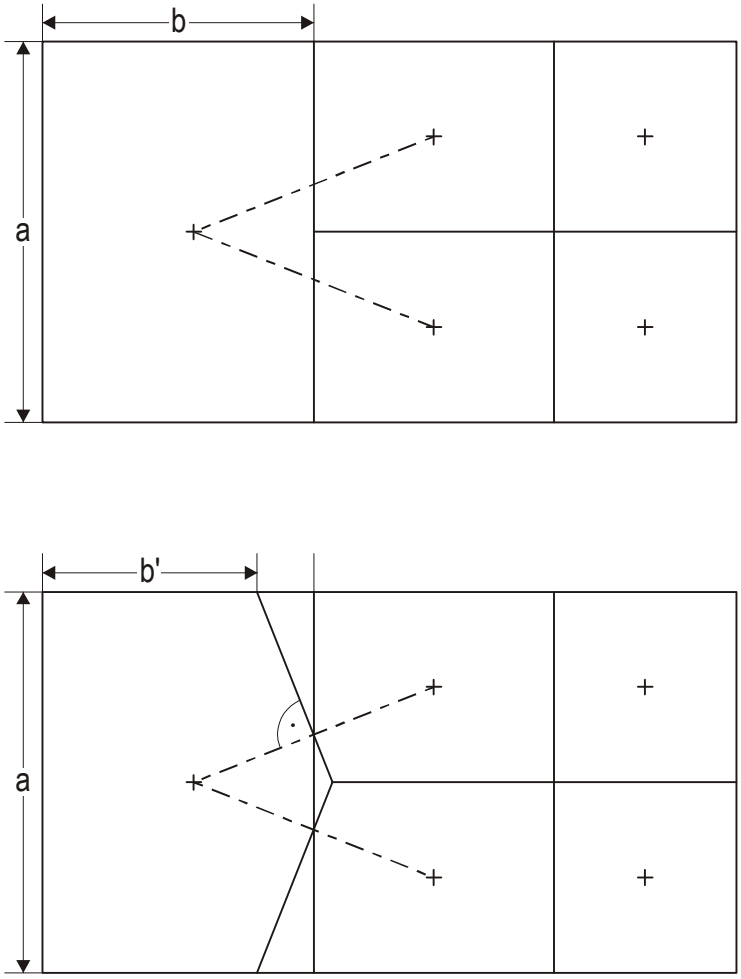

Figure 3.11: Incorrect and correct block interfaces for refined grid

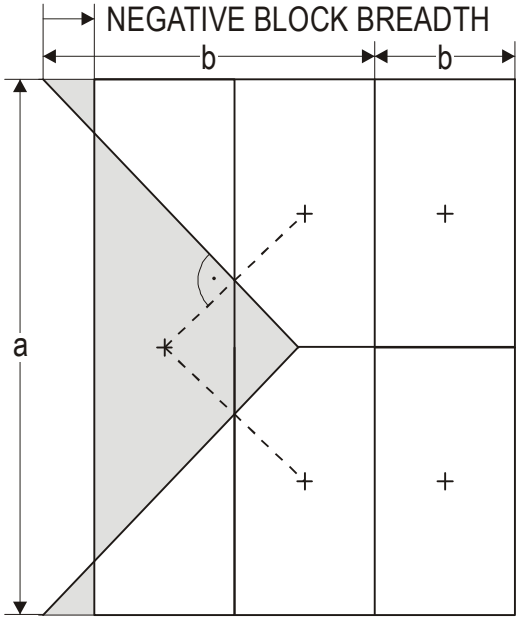

Figure 3.12: No orthogonal refinement possible by stretched blocks

3.3. 2½ -Dimensional Full-Scale Grid Construction

We combine three kinds of independently constructed grids in one full field project: Productive Area grid (PA), Aquifer grid and Window grid. The PA and Aquifer grids are always (without exceptions) a 2½ dimensional (layered) grid. A window grid can be a 2½D or a fully 3D grid.

A 2½ D grid will be constructed in the horizontal plane. Laterally the grid points are set in the mid-surfaces of the layers and in the third dimension they are located on vertical lines.

3.3.1 The Aquifer Grid

While the geological and petrophysical properties of the productive areas are known at the beginning of a simulation project, the aquifer is usually unknown. The size, the porosity, the permeability and their distributions around the productive area will be determined by matching reservoir pressure. The permeability is in areal extension isotropic, i.e.: does not depend on the direction. The History Match is a step-by-step procedure in which the aquifer model becomes more and more complex by re-sizing and re-parametrizing the aquifer without changing the productive area.

The aquifer grid is constructed from the global mesh outside the PA. At the boundary of the productive area the PEBI method is applied to obtain a correct transition between the different grids. Figure 3.14 shows the two-dimensional block model constructed from the global mesh in

Figure 3.13. Please note, that two productive areas are modelled within one common aquifer.

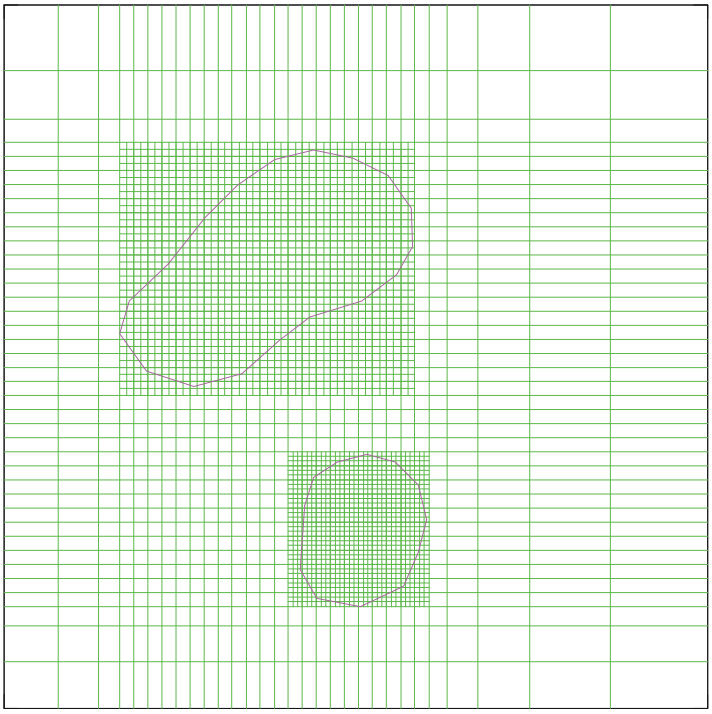

Figure 3.13: Global mesh with two PA's and different spacing in the aquifer

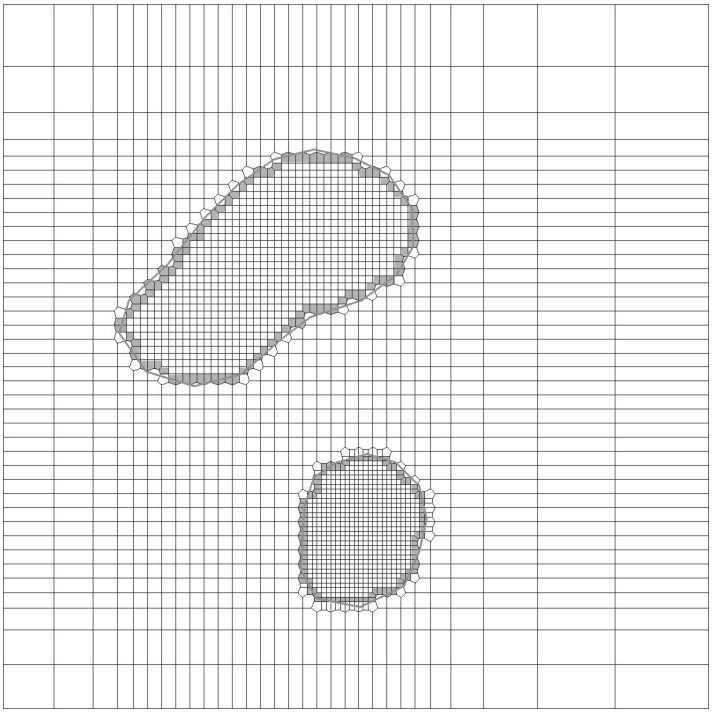

Figure 3.14: Block model constructed from the global mesh

3.3.2 Productive Area Grid

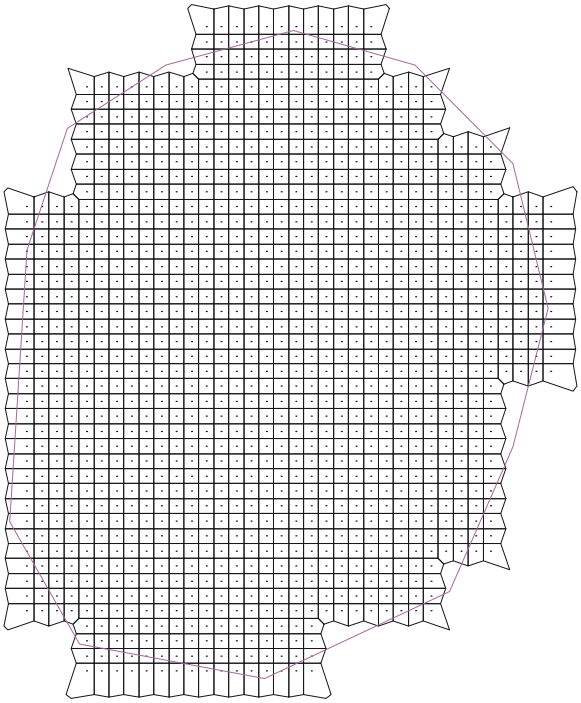

Figure 3.15: Productive Area grid

The grid in the productive areas will be constructed independently from the aquifer. Figure 3.15 shows one of the PA's from the previous example. The grid is always a simple regular Cartesian mesh. It is assumed that the principal directions of the permeability tensor coincide with the lateral direction of the grid lines or that they are diagonal to it. This is a simplification but practical. The areal anisotropy is not or only poorly known. In the global view it is satisfactory to offer four possibilities for the highest permeability direction as shown in Figure 3.16 and Figure 3.17. The direction can be different for all quadrangles formed by four grid points.

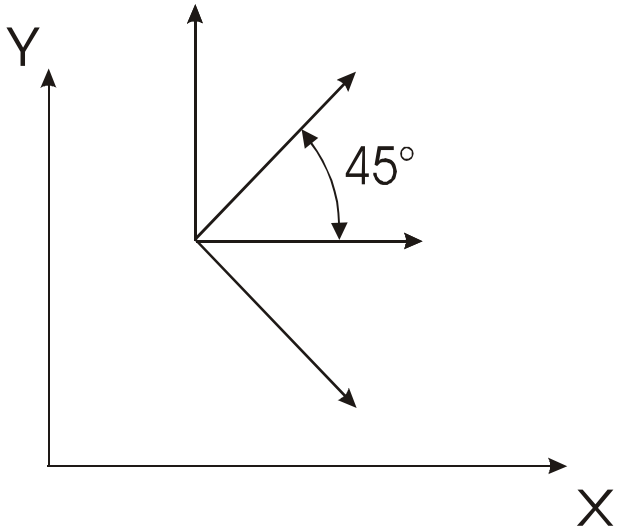

Figure 3.16: Possibilities offered for the highest permeability directions

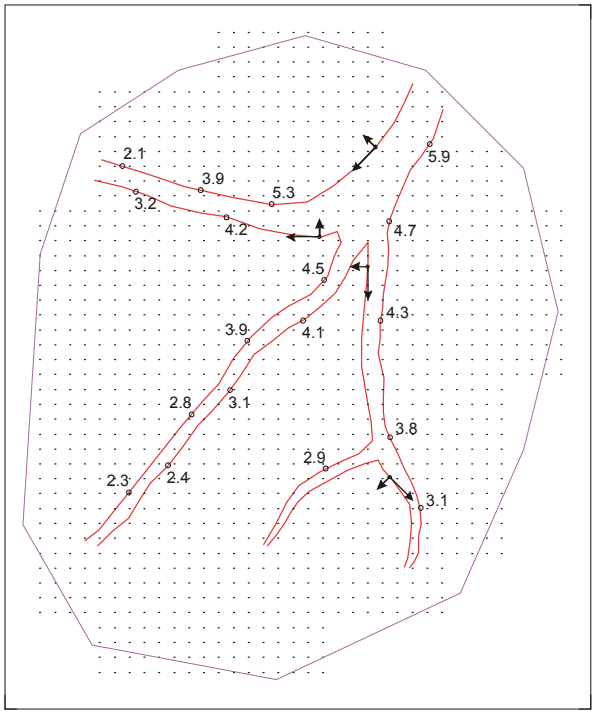

Figure 3.17: Definition of the areal anisotropy

Lets assume an anisotropic reservoir, where the permeability values $k_x \neq k_y$ are known. If the principal directions coincide with the coordinate directions, then the grid remains as shown in Figure 3.15. Figure 3.18 is a productive area grid for the case of partially diagonal permeability direction.

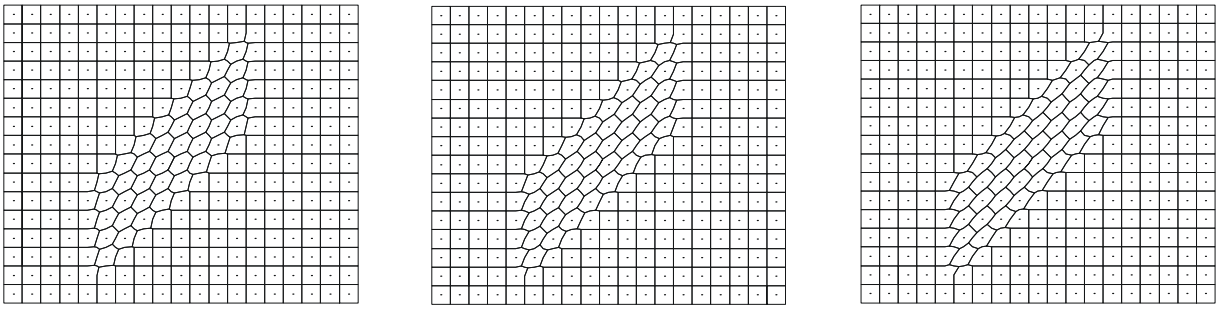

Figure 3.18: Cartesian grid with partially diagonal main permeability direction and increasing anisotropy ratio (from left to right)

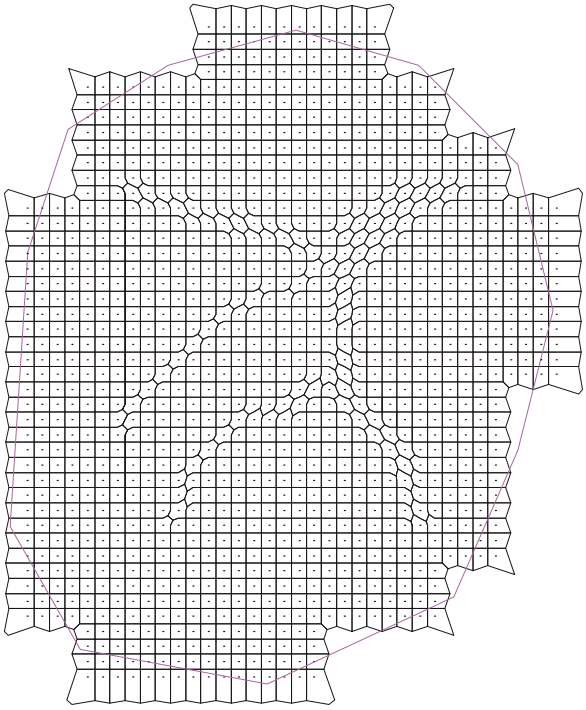

Figure 3.19: Productive area with channels

Channel structures can be characterized by the polygons built by segments in x, y and diagonal direction, approximating the principal axis of permeability. The corresponding PA grid is depicted in Figure 3.19. Note that the position of the grid points remained unchanged.

Figure 3.20 shows a PA with two refined zones for the isotropic case. In anisotropic cases the principal permeability directions (horizontal, vertical or diagonal) will not be parallel with the edges of the triangular grid elements in the transition zone, therefore the permeability ratio applicable for the kPEBI grid construction is limited. From a practical point of view this restrictions do not hamper the application of LGR. The refined area should be extended so that the conditions are satisfied in the transition zones.

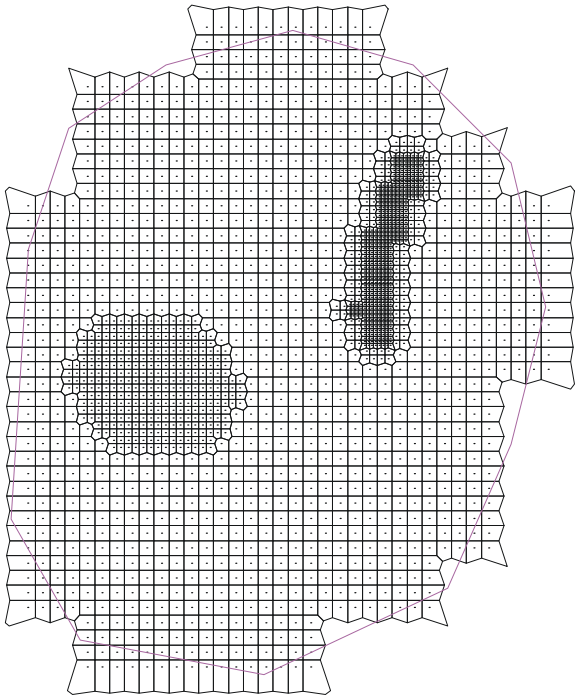

Figure 3.20: PA with two refined zones

3.4. Vertical Extension

In the isotropic case the vertical extension of the grid model can be done easily. The grid constructed for the top will be projected through all layers and sublayers. The same is valid for the anisotropic case, if the principal permeability directions are parallel to the x- and y-axis. The anisotropy ratio can be different in all vertically connected blocks. All features of the conventional layering such as vertical refinement, pinch-outs, discountinuities, etc. can be applied.

If the principal permeability direction is diagonal the shape of the blocks changes with the anisotropy ratio and the surfaces of the stacked blocks will not be identical and they will produce an apparent discrepancy in the overlapping as shown in Figure 3.21. In such a case a 2D grid must be constructed for all layers individually. Note that the grid lines are always vertical. From the point of view of flow calculation this is not a serious problem. The vertical transmissibilities will be calculated as harmonic average of the block half-transmissibilities depending on the two block surfaces.

We consider a quadrangle formed by 4 grid points on top of the reservoir (1st layer). If the principal permeability directions do not coincide with the coordinate axis then the block shape will be different to the Cartesian one as it was shown in Figure 3.18. The block shape depends on the direction and the permeability ratio as well. The 2D grid must be constructed now for all layers individually, producing an apparent discrepancy in the overlapping of the stacked blocks

as shown in Figure 3.21. One could conclude that the construction of a 2½D model is no longer possible. This is understandable from geometrical point of view, but the conclusion, based on the Control Volume Finite Discretization (CVFD) theory, is wrong. Theoretically it is not required that the communication surfaces must be identical from both sides. It is solely required that both blocks have one surface which is the unique communication surface with the neighboring grid block. As given by Equation 3.6, the block pair transmissibility τ_{ij} will be calculated as harmonic average from the so call half-block transmissibilities Υ_{ij} and Υ_{ji} using properties of a single block only. As explained previously, the permeability and thickness of neighboring blocks can be different. Therefore, why it should be required that the surfaces must be equal?

$$\tau_{ij} = \left[\frac{1}{\Upsilon_{ij}} + \frac{1}{\Upsilon_{ji}}\right]^{-1} \tag{3.6}$$

In fact, such an apparent "discrepancy" is not new. The cross section of a simple layered grid looks as shown in Figure 3.7a. One grid block is apparently connected to more than one block in the neighboring column which is naturally not the case. Therefore it is usual to visualize the cross sections and also the 3D plots in a smoothed form as it is shown in Figure 3.7b.

As shown in Figure 3.21, the vertical coordinate line I_1 remains vertical, which is a fundamental requirement for all kinds of 2½D grid models.

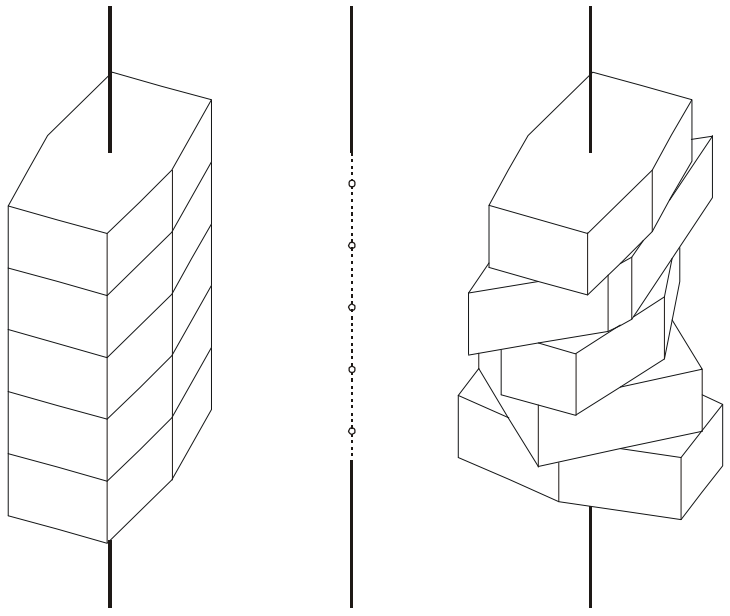

Figure 3.21: Vertical column of blocks if (a) anisotropy is uniform and (c) changes over the layers

A fully three dimensional grid construction is not applicable for this kind of stretched blocks. The thickness of a layer is by magnitudes smaller than the horizontal extensions of the blocks

which can be easily over 1000 feet. Theoretically an alternative solution would be using Multi-Point Flux Approximation (MPFA) instead of a kPEBI grid, keeping the block shapes unchanged through the layers.

Until now no theoretical investigation or numerical experiences were made for comparing the two methods, namely the kPEBI layered model versus a Cartesian or general quadrilateral grid using MPFA. Based on sound engineering judgment the kPEBI solution may be applicable to most of the practical problems.

3.5. Cylindrical Coordinate System

For dealing with rotational-symmetric problems a cylindrical (r, z) coordinate system should be used. Such a grid is illustrated in Figure 3.22 and Figure 3.23.

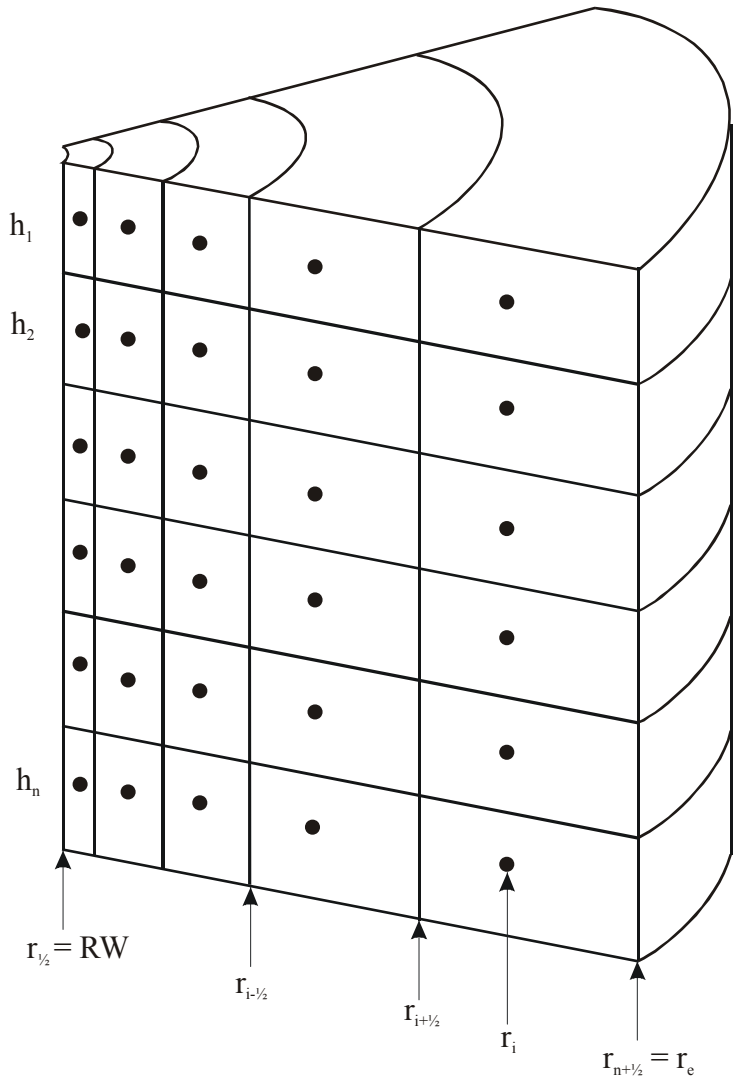

Figure 3.22: Block-centered cylindrical block model

3.5.1 Block Construction

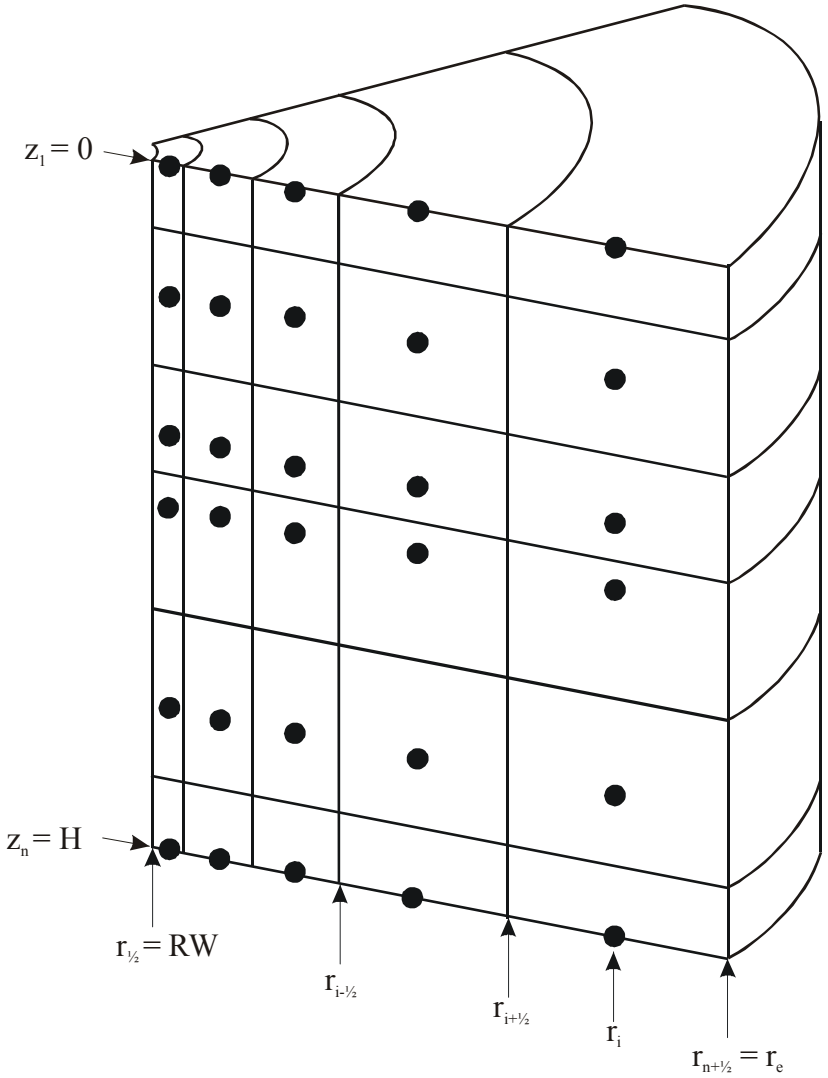

Figure 3.23: Point-distributed cylindrical block model

In Figure 3.22 the grid is block-centered in the vertical direction, which means that the grid points are the midpoints of the layers. Figure 3.23 shows the point-distributed case. In radial direction the block boundaries ($r_{i+1/2}$, $r_{i-1/2}$) are specified by the user. The first ring is the well radius ($r_{1/2}$ = RW) and the last one the outer boundary ($r_{n+1/2} = r_e$). It is recommended to distribute the rings in such a way, that assuming steady-state radial flow, the pressure drop between two neighboring blocks is equal.

This is the case, if

$$\ln\frac{r_{i+1/2}}{r_{i-1/2}} = c = const \tag{3.7}$$

and

$$c = \left(\frac{r_e}{r_w}\right)^{\frac{1}{n-1}} \tag{3.8}$$

n is the number of blocks in radial direction. The pressure distribution within the block boundaries $r_{i-1/2}, r_{i+1/2}$ is different for steady-state or pseudo-steady state flow. For steady-state flow the dimensionless pressure may be expressed as

$$P_D = \ln r_D \tag{3.9}$$

and for pseudo-steady state flow

$$P_D = \frac{r_{i+1/2}^2}{r_{i+1/2}^2 - r_{i-1/2}^2}\left[\ln r_D - \frac{1}{2}\cdot\frac{(r^2 - r_{i-1/2}^2)}{r_{i+1/2}^2}\right] \tag{3.10}$$

The dimensionless variables are

$$P_D = \frac{2\pi hk}{\mu q}[p(r) - p(r_{i-1/2})] \tag{3.11}$$

$$t_D \cdot \frac{kt}{\mu\phi c_t, r_{1/2}^2} \tag{3.12}$$

$$r_D = \frac{r}{r_{i-1/2}} \tag{3.13}$$

The average dimensionless pressure for a block is:

$$\bar{P}_D = \frac{\int_{r_{D=1}}^{r_{De}} P_D \cdot 2\pi r_D dr_D}{\int_{r_{D=1}}^{r_{De}} 2\pi r_D dr_D} \tag{3.14}$$

The correct position of the grid points (r_i) is where the pressure calculated from the steady-state (or pseudo-steady state, resp.) pressure distribution is equivalent with the volumetrically averaged pressure of the radial block. This radius can be calculated for the steady-state case by setting the right sides of Equation 3.9 and Equation 3.14 equal. The correct position of the grid point now is

$$r_i = \exp\left[\frac{r_{i+1/2}^2 \ln r_{i+1/2} - r_{i-1/2}^2 \ln r_{i+1/2}}{r_{i+1/2}^2 - r_{i-1/2}^2} - \frac{1}{2}\right] \tag{3.15}$$

For the pseudo-steady state case Equation 3.10 and Equation 3.14 are set equal. The result is the following equation which must be solved iteratively for r_i:

$$\ln\left(\frac{r_i}{r_{i-1/2}}\right) - \frac{1}{2\alpha^2} \cdot \left(\frac{r_i}{r_{i-1/2}}\right)^2 = \frac{\alpha^2}{\alpha^2 - 1} \cdot \ln\alpha - \frac{1}{4\alpha^2} - \frac{3}{4} \tag{3.16}$$

with

$$\alpha = \frac{r_{i+1/2}}{r_{i-1/2}} \tag{3.17}$$

The correct grid point location is then calculated with

$$r_i = r_D \cdot r_{i-1/2} \tag{3.18}$$

3.5.2 Transmissibilities

After the determination of the grid point radii, r_i, the pore volumes and the transmissibilities can be calculated (j denotes the vertical direction, i the radial direction)

$$V_{IJ} = \pi\phi_{ij} \cdot [(r_{i+1/2}^2 - r_{i-1/2}^2) \cdot h_j] \tag{3.19}$$

$$\tau_{i+1/2,j}^r = k_{i+1/2,j}^r \cdot \frac{2\pi h_j}{\ln\frac{r_{i+1}}{r_i}} \cdot \mathrm{DIS3}_{i,j} \tag{3.20}$$

and

$$\tau_{i,j+1/2}^z = k_{i,j+1/2}^z \cdot \frac{2\pi(r_{i+1/2}^2 - r_{i-1/2}^2)}{h_{j+1} + h_j} \cdot \mathrm{DIS1}_{i,j} \tag{3.21}$$

$k_{i,j+1/2}^r$ is the permeability in the radial direction and $k_{i,j+1/2}^z$ is the permeability in the axial direction. Both values are averaged from the permeability values of the two involved blocks.

$$k_{i+1/2,j}^r = \frac{2k_{i,j} \cdot \mathrm{FKTX3}_{i,j} \cdot k_{i+1,j} \cdot \mathrm{FKTX3}_{i+1,j}}{k_{i,j} \cdot \mathrm{FKTX3}_{i,j} + k_{i+1,j} \cdot \mathrm{FKTX3}_{i+1,j}} \tag{3.22}$$

$$k^z_{i,j+1/2} = \frac{2k_{i,j} \cdot \mathrm{FKTX1}_{i,j} \cdot k_{i,j+1} \cdot \mathrm{FKTX1}_{i,j+1}}{k_{i,j} \cdot \mathrm{FKTX1}_{i,j} + k_{i+1,j} \cdot \mathrm{FKTX1}_{i,j+1}} \tag{3.23}$$

The z-direction corresponds to direction I_1, and the radial direction to direction I_3. A subdivision of the blocks is not possible.

The two gridding methods (for steady-state and pseudo-steady state flow respectively) give similar results in most of the cases. Calculating transient flow behaviors (well testing), the pseudo-steady state grid is more suitable.

For a generalized case the third dimension is the rotation angle Θ, as shown in Figure 3.24.

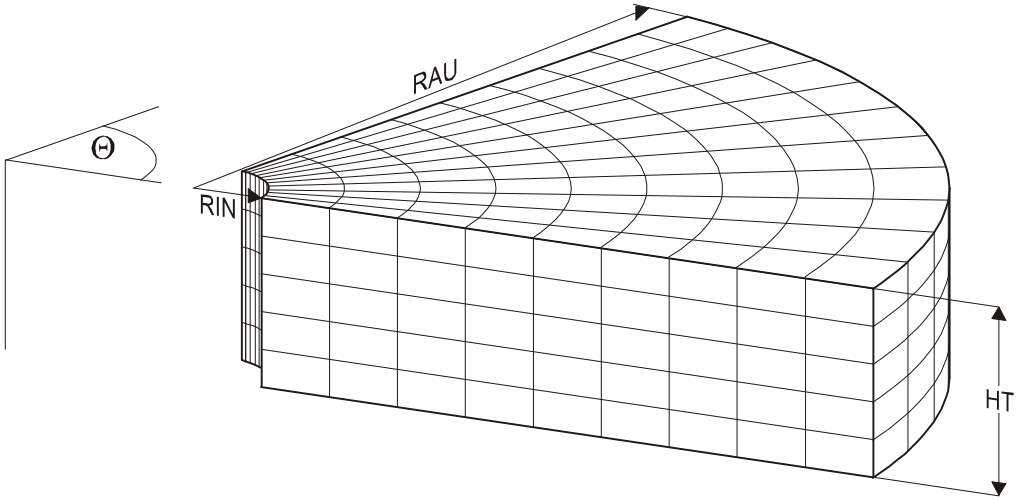

Figure 3.24: Three-dimensional radial coordinate system

3.6. Curvilinear Grid

3.6.1 Orthogonal Curvilinear Grid

A coordinate system is orthogonal if the coordinate lines are mutually orthogonal everywhere. In this case the inter-block flow term for one block surface can be calculated from two grid points and there are no cross derivative terms in the transformed flow equations. For any orthogonal block system, the inter-block transmissibilities can be calculated from intuitive geometrical concepts. This means in general:

$$\tau_{IJ} = \frac{A_{IJ}}{h_{IJ}} k_{IJ} \cos\gamma \tag{3.24}$$

where

- k_{IJ} - is the average permeability between block I and J,
- A_{IJ} - is the cross-sectional area and,
- h_{IJ} - is the distance between grid points,
- γ - is the angle h_{IJ} on the surface A_{IJ}.

The only reason to use an orthogonal curvilinear grid system is to reduce grid orientation effects. From this reason the curvilinear grid system should be based upon a stream tube model, without neglecting the cross tube flow terms. The stream tube model coincides with physical reservoir stream lines. However they will change with time. Therefore such a grid is valid only for a prefixed situation.

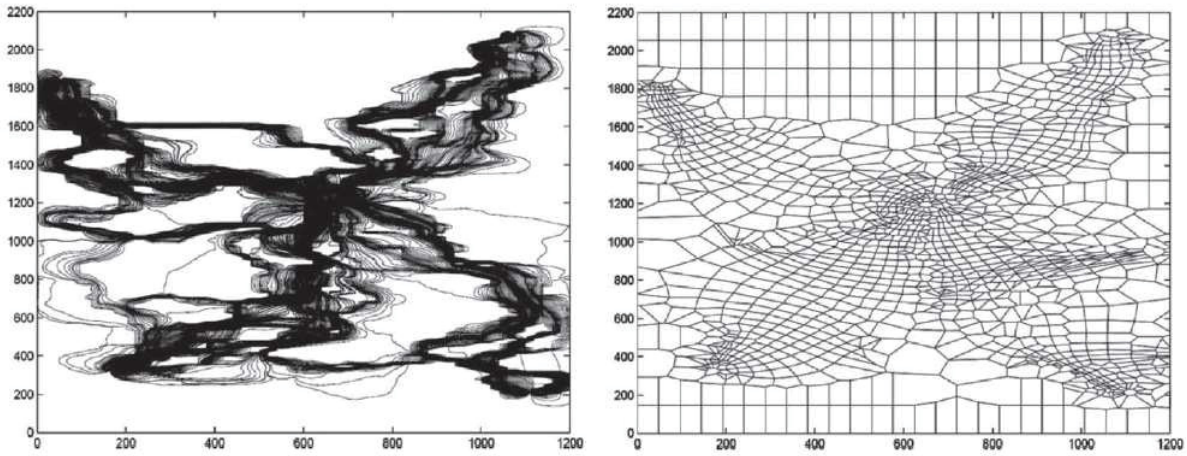

Figure 3.25: Streamlines and orthogonal streamtube grid after Mlacnik *et al*.

3.6.2 Stream Tube Grid

The stream-tube approximation was introduced by Higgins and Leighton[72]. They presented convincing evidence that the performance of a five-spot pattern waterflood can be calculated by holding the streamlines constant as the flood progresses. They calculated the fluid displacement along streamlines using the Buckley-Leverett[22] theory.

If the stream lines are known, the grid points can be distributed arbitrarily along them. The block boundaries are in one direction stream lines, forming the so called stream tubes, in the other direction they are arbitrary surfaces cutting the stream tubes into blocks.

Figure 3.26 shows a five-spot pattern grid. On one side the stream tubes are irregularly cut into grid blocks. On the other side an equivalent orthogonal grid was constructed via stream lines and equipotential surfaces. The two grids are equivalent so far in the sense that the stream lines

remain unchanged. The interblock transmissibilities have to be calculated with Equation 3.24 for both cases, only the angle γ is 90 degree for the orthogonal case and variable for the other one.

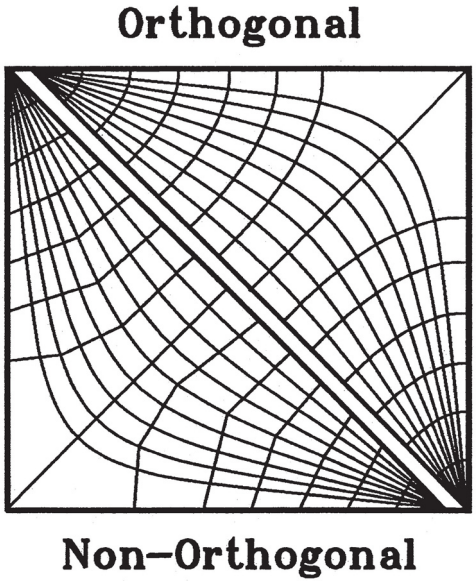

Figure 3.26: Orthogonal and non-orthogonal stream tube grid for five-spot pattern

The applicability of the stream tube model is limited to simple patterns and favorable mobility ratio.

If the mobility ratio is adverse, the stream tubes will change significantly during displacement. Martin and Wegner[90] proposed a method to change the stream tubes over time. Such a way seems to be too complicated for general purpose applications.

The orthogonal stream tube grid has curved block boundaries and so it is a little bit complicated to calculate block volumes, surfaces etc. To overcome these difficulties Wadsley[136] suggested using non rectangular coordinate lines. The curvilinear edges of the blocks are approximated with straight lines. Such a grid is shown in Figure 3.27. The approximation of the flow problem is as good as the approximation of the geometry.

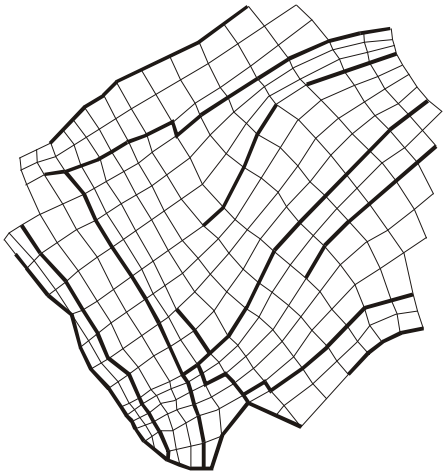

Figure 3.27: Use of non-rectangular grid to approximate stream tube grid (after WADSLEY[136])

3.6.3 Corner Point Geometry

The way to this type of grid is a straight one: Beginning with the non-orthogonal stream tube grid which is correct, through the non-rectangular grid which is an approximation of the stream tube grid, to the free choosing of the corner points of the grid blocks. The latter is devoid of any theoretical background.

Figure 3.28 shows such a grid, taken from the advertising material of a commercial simulator. Such a freedom is naturally tempting but the outcome completely uncertain.

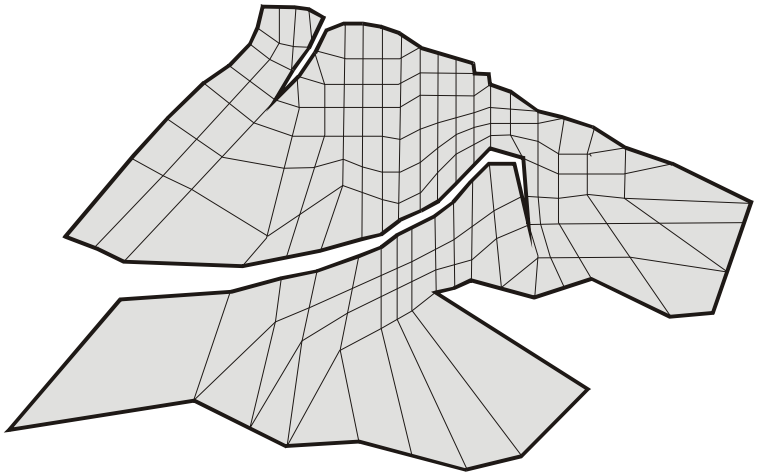

Figure 3.28: Grid construction with corner point geometry

4 Initialization of a Grid Model

4.1. Initial Pressure and Saturation Distribution in a Reservoir

In a reservoir containing hydrocarbons and non-hydrocarbons, the initial phase distribution is determined by the equilibrium between capillary and gravitational forces. Capillary pressure is the pressure difference between two phases showing different properties, like oil and water or gas and liquids. For example, the capillary pressure for the oil-water system is given by:

$$p_o - p_w = P_{cow}(S_w), \tag{4.1}$$

where p_o and p_w are the oil and water phase pressures. Due to the phenomenon of capillary pressure the vertical saturation distribution is continuous, building a more or less extended transition zone between the phases. In equilibrium, the capillary pressure gradient must be equal with the gravitational one. Therefore, the following equation must be satisfied:

$$\frac{dP_{cow}(S_w)}{dS_w} \cdot \frac{dS_w}{dz} = g(\rho_w - \rho_o). \tag{4.2}$$

The coordinate axes z represents the vertical direction and is oriented downwards. The phase densities are a function of the pressure, temperature and additionally of the composition.

The capillary pressure is not only a function of the saturation, it depends on the direction of the saturation change, too (hysteresis effect). Therefore, the concept of initialization must be based on the assumed process of hydrocarbon accumulation and needs some further considerations.

4.1.1 Fluid Properties at Initial State

The compositions of the reservoir fluids at the initial state are not uniform. On one hand side the reservoir can be divided by sealing faults and interbeddings into more parts, called compartments, that communicate through a common aquifer only. Due to this communication they build one hydrodynamic unit, that must be integrated into one single block model. The reasons for different fluid compositions across a reservoir are manifold. The hydrocarbon accumulation could have happened at different time. Also geochemical processes, taking place after the accumulation, can lead to different compositions. This kind of differences are handled

by introducing PVT regions. The fluid properties are defined for each PVT region independently. A PVT region is, per definition, the part of the reservoir, for which the same fluid characterization is valid.

On the other hand side the hydrocarbon phases are mixtures of many chemical compounds, and if they are in equilibrium, than their spatial distribution is determined mainly by the equilibrium of the chemical potential and the gravitational force. Due to the geothermal temperature gradient, also hydrodynamic convection can manifest in a reservoir, which tends to homogenize the composition of the phases. The vertical variation of fluid compositions is generally non-linear.

How a PVT region must be handled at the initial state depends on the fluid system, the size and the complexity of the reservoir. We discuss here black oil type fluid description only. The usual approaches are the following:

4.1.1.1 The most simple case

It will be assumed that the temperature and the composition of the phases are uniform in the PVT region. That means, that the water salinity and the bubble point pressure of the oil phase are uniform. Consequently initially all densities depend on the pressure, which means on depth only:

$$\rho_w = \rho_w(p_w);\ \rho_o = \rho_o(p_o);\ \rho_g = \rho_g(p_g) \tag{4.3}$$

In an oil reservoirs with gas cap, the oil must be saturated at the gas-oil-contact (GOC). Because the bubble-point-pressure (p_b) is constant, the oil becomes bellow the GOC undersaturated. Due to the, with depth increasing phase pressures, all phase densities are increasing too. This is an important fact. If the densities would decrease with the depth then the fluid column becomes gravitational instable, inducing uncontrolled fluid movement in the model.

4.1.1.2 Variation of Bubble Point Pressure with Depth

It will be assumed that the temperature is uniform but the bubble point pressure changes monotonic with the depth:

$$R_s = R_s(z);\quad \rho_o = \rho_o(p_o, R_s) \tag{4.4}$$

The vertical changes can be defined by the bubble-point pressure or directly by the solution GOR. The condition that the oil density cannot decrease with the depth must be satisfied. Therefore the assumption that the oil is saturated at every depth is not applicable.

4.1.1.3 Variation of Salinity with Depth

The water salinity can increase with the depth. The stability requirement is satisfied because the water density increases with the salinity:

$$\rho_w = \rho_w(p_w, C_{NA}) \tag{4.5}$$

where C_{NA} is the salt concentration in kg/kg brine.

4.1.1.4 Variation of Temperature with Depth

If the vertical extension of the reservoir is considerable, than it is recommended to account for the geothermic temperature gradient. The PVT properties must be defined for two reference temperatures and will be interpolated for a given depth. The combination with variable bubble point pressure (Case B) and variable salinity (Case C) is naturally possible. For this case:

$$\rho_w = \rho_w(p_w, T, C_{NA}); \quad \rho_o = \rho_o(p_o, T, R_s); \quad \rho_g = \rho_g(p_g, T) \tag{4.6}$$

where T is the temperature.

4.1.1.5 Variation of Oil Density with Depth

In many reservoirs the oil gravity increases with the depth. In such a case a special model formulation must be used, called API Tracking. After the gravity of oil in a block is determined, the appropriate fluid properties for this particular oil gravity, saturation pressure and reservoir pressure, may be interpolated on both pressure and oil gravity. For the oil density:

$$\rho_o = \rho_o(p_o, API, R_s) \tag{4.7}$$

The combination with variable bubble-point-pressure (p_b) and salinity is possible but not with variable temperature. Assuming variable temperature it would be necessary to interpolate for both the API grade and for T, which could not be done practically.

4.1.2 Formation of Hydrocarbon Reservoirs

The porous rock of a hydrocarbon reservoir is assumed to be originally saturated with water (brine). During the migration of hydrocarbons (oil and gas) into the trap, the water phase, which is in most of the cases the wetting phase (w), is displaced by the non-wetting (nw) hydrocarbon phases. In the most simple case, the hydrocarbon mixture forms one single phase resulting in an

undersaturated oil or in a gas reservoir, as it is shown in Figure 4.1

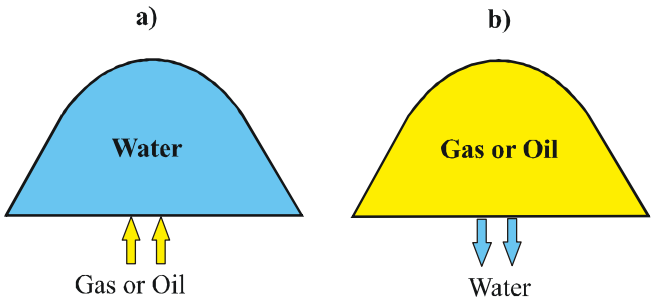

Figure 4.1: Formation of two phase reservoirs
a) Water saturated formation; b) Accumulation of gas or oil

When talking about a reservoir containing oil and free gas (a saturated oil reservoir with a gas cap), the hydrocarbon accumulation may have occurred in different ways:

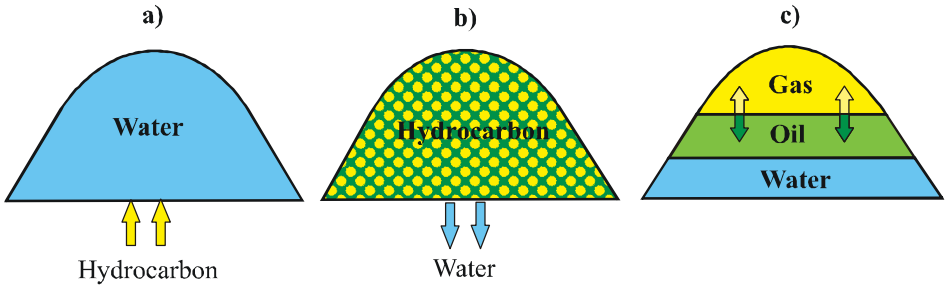

Figure 4.2: Formation of oil reservoirs
a) Water saturated formation; b) Migration of hydrocarbons into the trap; c) Separation of oil and gas

1. Contemporary migration of the light and heavy HC components into the trap and separation of the phases within the trap (Figure 4.2).
2. The heavy components accumulated first and the gas formed during the later phase of the genesis and migrated through the oil body.
3. The gas accumulated at first and the oil became trapped later on.

For the cases 1 and 2 the non-wetting gas phase displaced the oil from the gas cap volume (drainage process) which is a similar process as the oil/water and gas/water drainage process. In the third case the oil entered into the gas cap through imbibition. Nevertheless, it is very difficult, maybe impossible to get evidence how the accumulation took place. Therefore, it is assumed that both for the oil/water and gas/oil phases the accumulation was a drainage process and the primary drainage capillary curves determine the initial phase distributions.

Figure 4.4 shows the water/oil and oil/gas capillary pressure functions for a primary drainage process. The saturation changes are ranging between 100% and residual wetting phase saturation. The drainage capillary pressure shows normally a threshold pressure. It must be exceeded so that the non-wetting phase can enter the pores of the rock.

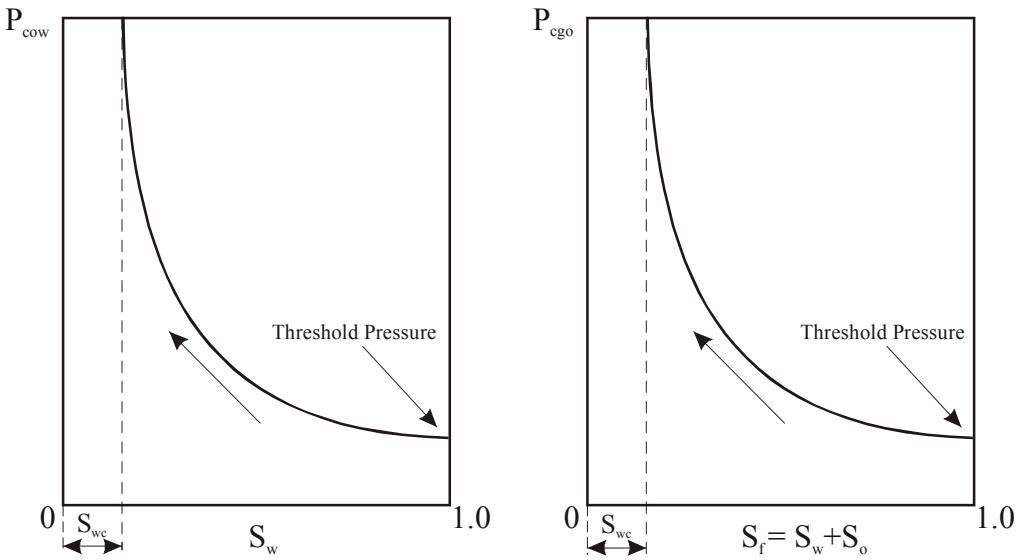

Figure 4.3: Primary drainage capillary pressure curves for oil/water and gas/oil

4.1.3 Oil-Water and Gas-Oil Contacts

The Water-Oil-Contact (WOC) and analogous the Gas-Oil-Contact (GOC) can be defined in different ways. The possible interpretations are the following:

1. At the WOC the water-oil capillary pressure is equal to zero ($P_{cow} = 0$).
2. The oil saturation below the WOC is zero ($S_o = 0$).
3. When opening a well above the WOC oil will be produced, below the WOC only water will be produced.

The definitions for the GOC are analogous. The contacts based on these three interpretations are shown in Figure 4.4. From the physical point of view the first definition is the only correct one. The surface where $P_{cow} = 0$ is a horizontal plane. It is assumed that no water movement takes place in the bottom aquifer. The $S_o = 0$ surface is normally not a horizontal plane due to the different threshold pressure in different areas. The third kind of 'phase contact' is influenced by the relative permeabilities too. It can be useful from the practical point of view (especially for petroleum production engineers) but it is not applicable for reservoir modeling.

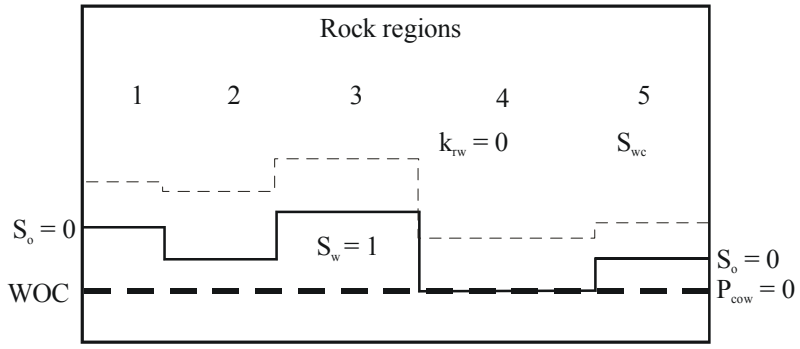

Figure 4.4: Different interpretations of the phase contact
(1) $P_{cow} = 0$; (2) $S_o = 0$; (3) $q_o = 0$

In the simulation technique always the first definition of the phase contacts must be used. It must be emphasized that even above the WOC the water saturation and above the GOC the oil saturation can be 1.0, due to the capillary threshold pressure.

4.1.4 Initial Vertical Pressure Distribution

Figure 4.5 shows the vertical distribution of the phase pressures in a reservoir. The vertical pressure distribution can be calculated as follows: The pressure of the water phase at a reference depth $z_{ref} > z_{WOC}$ is called p_{wref}. The pressure at the level z is determined by:

$$p_w(z) = p_{wref} + g \int_{z_{ref}}^{z} \rho_w(z)dz \tag{4.8}$$

Equation 4.8 is valid below and above the WOC until S_w becomes equal S_{wc} at the depth z_B.

The oil-water capillary pressure becomes zero $P_{cow} = 0$ at the WOC therefore, the oil-phase pressure above the WOC can be calculated as:

$$p_o(z) = p_w^{WOC} + \int_{z_{WOC}}^{z} \rho_o(p_o)dz \tag{4.9}$$

At the level z_A the difference between the oil and water phase pressures exceeds the threshold pressure therefore, the oil saturation becomes greater than zero. At a level z_B the water saturation becomes S_{wc} and than the water phase pressure follows the oil phase pressure parallel.

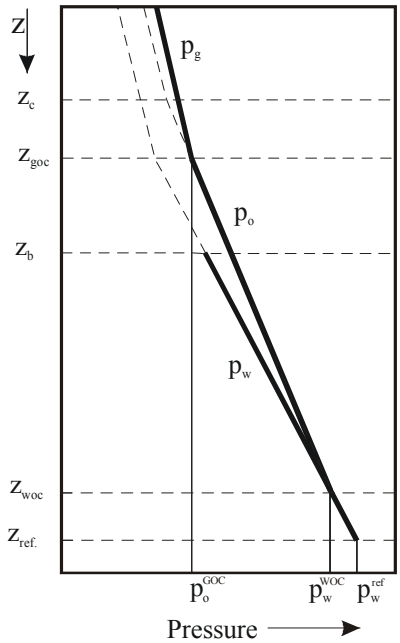

Figure 4.5: Initial pressure distribution in the reservoir

The vertical phase pressure distributions beyond the GOC are similar to those at the WOC:

$$p_g(z) = p_o^{GOC} + \int_{z_{GO}}^{z} \rho_g(z)dz \tag{4.10}$$

Due to the threshold pressure the gas saturation becomes greater than zero at the level $z_C < z_{GOC}$.

Equation 4.8 - Equation 4.10 are recursive for the pressures, which does not make any difficulties in the practical application.The following numerical solution can be applied for phase p:

$$p_p(z_{i+1}) = p_p(z_i) + g\rho(z_i)\Delta z; \qquad \Delta z = z_{j+1} - z_j \tag{4.11}$$

4.1.5 Initial Vertical Saturation Distribution

After defining the vertical distribution of the phase pressures it is simple to determine the saturation distribution:

$$
\begin{aligned}
&S_w = 1.; && \text{if} \quad z \geq z_{WOC} \\
&S_w = P_{cow}^{-1}(p_o - p_w); \quad S_o = 1. - S_w && \text{if} \quad z_{WOC} > z \geq z_{GOC} \\
&S_F = P_{cgo}^{-1}(p_g - p_o); \quad S_o = S_F - S_{wc} && \text{if} \quad z < z_{GOC}
\end{aligned}
\tag{4.12}
$$

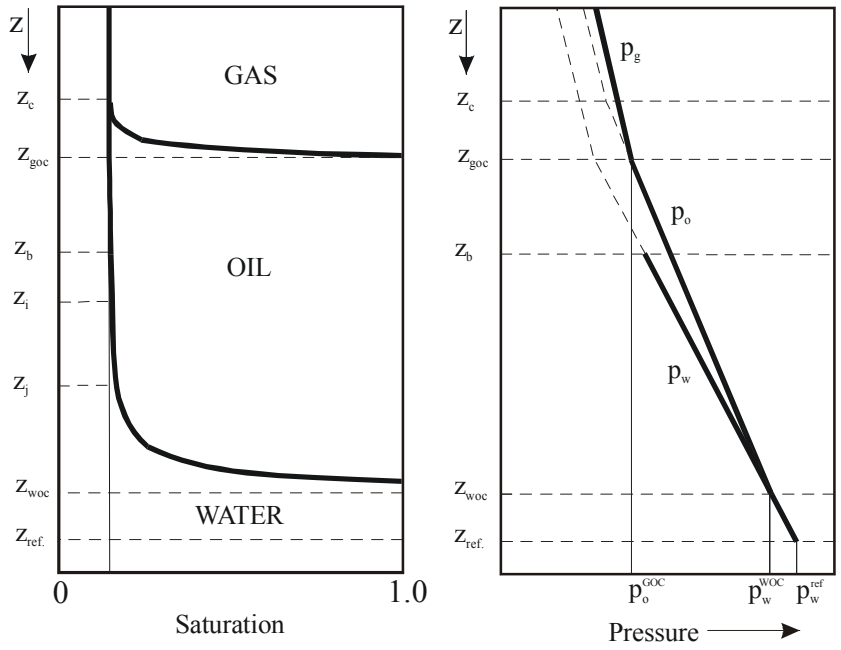

Figure 4.6: Initial saturation distribution in the reservoir

Figure 4.6 shows the vertical phase pressure and the corresponding vertical saturation distributions for a given set of capillary pressure and PVT functions. Taking two arbitrary depths z_I and z_J on this curves, then the following relation must be valid:

$$
\begin{aligned}
&\Phi_{oj} - \Phi_{oi} = p_j - p_i - g(\rho_{oj} z_j - \rho_{oi} z_i) \approx 0 \\
&\Phi_{wj} - \Phi_{wi} = p_j - P_{cow}(S_{wj}) - p_i + P_{cow}(S_{wi}) - g(\rho_{oj} z_j - \rho_{oi} z_i) \approx 0
\end{aligned}
\tag{4.13}
$$

Equation 4.13 becomes rigorous if $\rho_j = \rho_i$, which is practically true if the distance between the two points is not very large. If the reservoir is described using more rock and PVT regions then the vertical pressure and saturation distributions must be calculated for all combinations of the rock and PVT regions.

4.2. Assigning Pressure and Saturation Values to the Blocks

4.2.1 Equilibrium Based Initialization

The reservoir model is built - as result of the discretization of the flow equations - as a three dimensional system of blocks. Each block is representing one part of the reservoir rock and is characterized by the top depth, thickness, porosity and permeability. Initialization means to assign a pressure and the saturation value to each block. The initialization is correct if the following two requirements are satisfied:

1. No fluid movement takes place if the model is operated without production/injection.
2. The fluid content of every block is practically identical with those of the corresponding part of the reservoir.

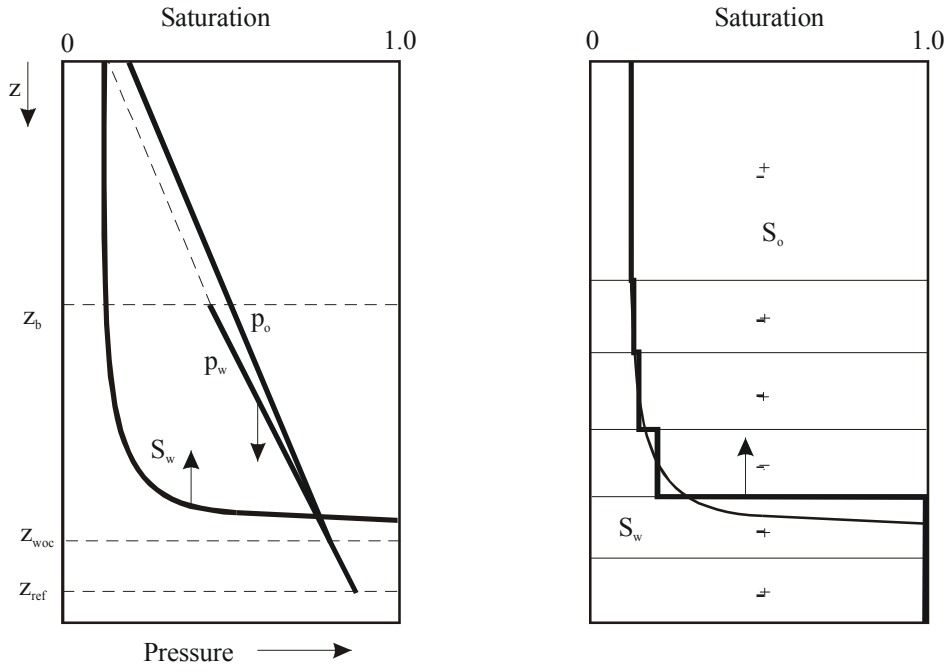

Figure 4.7: Initial saturation of the blocks using `INITM` option

Figure 4.7 shows a vertical column of blocks together with the vertical distribution of the pressure and the saturations. Two possibilities of initialization will be discussed:

`INITM`: Initialization at the middle-point,
`INITD`: Initialization based on fluid content.

`INITM` and `INITD` are not standardized abbreviations, they are used exclusively in this text for sake of brevity only! Use the full expressions “Block middle-point initialization” and

"Initialization by vertical integration of the fluid content" in daily communication.

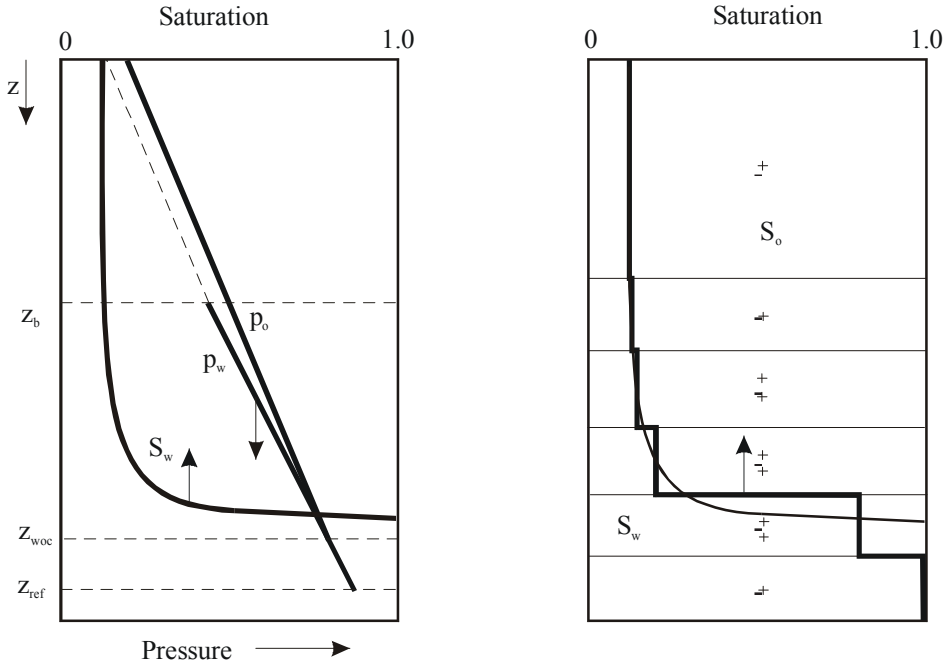

Figure 4.8: Initial saturation of the blocks using `INITD` option

`INITM` is the most simple initialization method and is used by most of the commercial simulators. The block pressure and saturations are taken from the vertical distributions at the grid point depths. Based on Equation 4.13, `INITM` satisfies the first requirement but fails regarding the second one. For blocks near to the phase contacts, the block saturation can be quite different to the real one. It may happen, that the middle-point of the block is situated just below of the WOC and the water saturation becomes 1.0. Contrary, point could be just slightly above of the WOC resulting in a considerable amount of oil in the block.

Using `INITD`, the saturation function will be vertically integrated between the top and the bottom of the block, determining the average water and oil or gas saturations. It's easy to solve this integration by calculating the integral of the saturations over the height at first. For water this means:

$$\Gamma(z) = \int_{z_{min}}^{z_{max}} S_w dz \tag{4.14}$$

where $\Gamma(z)$ is a function of the rock and PVT properties.The average initial water saturation in a given block can be easily calculated by:

$$\overline{S_{wi}} = \frac{\Gamma(z_b) - \Gamma(z_t)}{z_b - z_t} \tag{4.15}$$

Based on this average saturation, the position of the grid point z_i will be chosen on the vertical saturation distribution function and the block pressure will be interpolated to this depth. This method satisfies the first requirement as good as `INITM` but gives the right fluid in place, too. Figure 4.8 demonstrates the result of the `INITD` method. The distance of two neighboring blocks will be determined for this new grid point location.

Aziz[13] uses a correction term to the capillary pressure for each block instead of vertical shifting of the grid points. The correction term is calculated based on the correct capillary pressure (which maintain the initial equilibrium) and those saturation which results in the correct fluid in place:

$$P_{cow}^{corr} = P_{cow}^{ini} - P_{cow}(S_w) \tag{4.16}$$

This correction term must be added to the capillary pressures calculated in each time step, resulting in greater storage and CPU time and can therefore not be recommended.

The depth of the grid point determined by `INITD` will not be very different from the middle point. Therefore, it is normally not necessary to recalculate the block-pair transmissibilities if they are already available. The difference between the midpoint transmissibility and the corrected one is negligible compared to the usual uncertainties of the reservoir parameters. Nevertheless the recalculation is an easy issue.

4.2.2 Non Equilibrium Initialization

For non equilibrium initialization pressure and saturation values are assigned for each grid block from maps. To achieve no fluid movement at initial conditions, this means before production startup, certain measures (e.g. a pseudo capillary pressure) have to be taken.

Such kind of initialization is required in certain circumstances only, such as a tilted phase contact at initial time. Especially in the Persian gulf, such reservoirs can be frequently found.

4.2.3 Stability Condition

To have a stable initialization means, that the velocities (or rates) of all phases are zero at each communication surface of neighboring grid blocks. It means, that the phases do not move and the reservoir is in equilibrium.

The rate of the phases *p* through connection *ij* is:

$$q_p = \tau_{ij}\left(\frac{k_{rp}}{\mu_p}\right)_{ij}(\Phi_{p,j} - \Phi_{p,i}) = \tau_{ij}\lambda_{pij}(\Phi_{p,j} - \Phi_{p,i}) \tag{4.17}$$

where τ_{ij} is the constant transmissibility between block i and j, k_{rp} is the relative permeability, μ_p is the viscosity and Φ_p is the potential of the phase p. The mobility λ_{pij} will be calculated by one point upstream weighting:

$$\lambda_{pij} = \begin{cases} \lambda_{pj} \; if \; (\Phi_{p,j} - \Phi_{p,i}) \geq 0 \\ \lambda_{pi} \; if \; (\Phi_{p,j} - \Phi_{p,i}) < 0 \end{cases} \tag{4.18}$$

The rate between the two blocks is zero if (1) the phase potentials of the two blocks are equal or (2) λ_{pij} is zero. Based on Equation 4.13 the first condition must be satisfied if the saturation of the phase p is greater then the immobile saturation in both blocks. Consequently λ_{pij} is greater than zero, independent which of the blocks is the upstream one. If the mobility in the block j is zero but not in the block i, than the block j is already in the interval in which the (wetting) phase pressure gradient is parallel to the non-wetting ones (above the level z_b in Figure 4.7) and therefore for the wetting phase the block j becomes the "upstream" block and

$$\lambda_{pij} = \lambda_{pj} = 0\,. \tag{4.19}$$

It is easy to approve if the initialization is stable or not by calculating the model without production/injection. Some simulators provide so called uniforming options (see Aziz[13]) to counterbalance the instable initialization. This is not necessary if the method `INITD` will be used.

4.2.4 Segregated Flow

In important cases, especially for gas reservoirs, it is possible to use a simpler concept assuming a complete separation of the phases neglecting the capillary pressures. Figure 4.9 shows such a model.

Above the WOC or WGC the water saturation is immobile (S_{wc}) and above the GOC the oil saturation is zero.The average block saturations can be calculated easily based on the position of the blocks and the phase contacts. This results in two classes of blocks: (1) The blocks which are not cut by phase contacts. They contain one mobile phase only. The block pressure can be assigned to the midpoints in the same manner as it is done with `INITM`. (2) The phase contact is cutting the block. In this case the grid point depth must be equal with the depth of the phase contact, otherwise the potential difference between two neighboring blocks will not be zero and will induce an uncontrolled fluid movement.

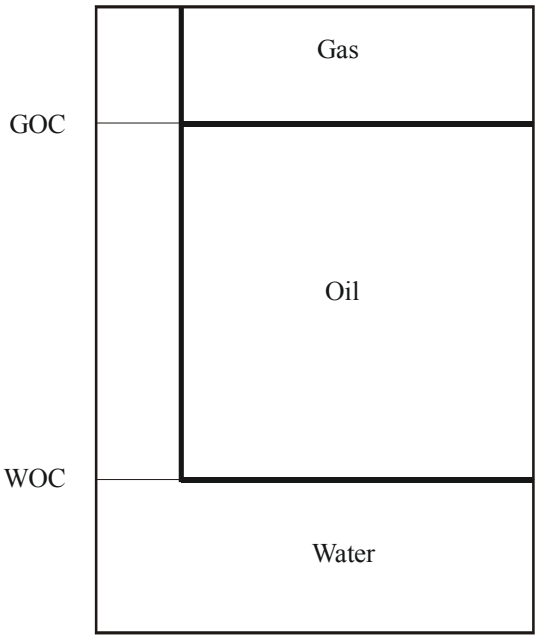

Figure 4.9: Segregated flow initialization (INITSF option)

4.3. Practical Remarks

1. The measured pressure p at a given depth will be equivalent with the pressure of those phase which is in contact with the pressure gauge. For the initial state we can assume that

$$\begin{cases} p = p_w \ \ldots & z \geq z_{WOC} \\ p = p_o \ ; p_w = p - P_{cow}(S_w) & z_{WOC} > z \geq z_{GOC} \\ p = p_g \ ; p_o = p - P_{cgo}(S_w + S_o) & z \geq z_{WOC} \end{cases} \tag{4.20}$$

Regarding the Equation 4.3 the phase densities are functions of their own phase pressure. This leads to the complication that they will not be a function of the measured pressure p only but based on the Equation 4.1 of the capillary pressures and the saturations, too. This does not effect the initialization but induces a more complicated and time consuming calculation of the coefficients of the flow equations which are required for all blocks and time steps. For the practical point of view it is enough to assume that the densities are functions of the measured pressure p (defined by Equation 4.20) only:

$$\rho_w = \rho_w(p) \quad \rho_o = \rho_o(p, R_s) \quad \rho_g = \rho_g(p) \tag{4.21}$$

2. For initialization the drainage type capillary pressure functions (see Figure 4.3), for calculating the displacement (simulation run) those for the imbibition types should be used. Although the drainage and imbibition curves are different in shape, they end up with equal values at the initial saturation for each individual block. Capillary pressure functions are not only a function of the saturation, they depend on the direction on saturation change, too. This phenomenon is called hysteresis. In many cases the hysteresis data are not available, therefore, one set of capillary (and relative permeability) functions will be used only. There is no doubt which type of relative permeabilities should be used during the simulation run because they are required for the dynamic calculation only. For an oil reservoir there will be the imbibition curve for k_{ro} and k_{rw} and the drainage curve for k_{rg}.

   If using one set of the capillary pressure curves an error will be introduced either in the initialization (in case of imbibition functions) or in the calculation of displacement (in case of drainage functions). Which error is more serious depends on the actual project. E.g. imbibition functions should be used for modeling a single well conning problem while drainage curves in most of the full-field cases.

   The drainage type capillary functions shows a jump at S_w=1, called threshold pressure. This cannot be handled mathematically, therefore, it is necessary to smear out the curve. The imbibition type capillary function has no values at S_w>(1.-S_{or}), still this interval must be defined when using the function for initialization, too. Therefore, the capillary functions must be given in a form when using for numerical calculation, that both

$$P_{cow} = P_{cow}(S_w) \quad and \quad S_w = S_w^{-1}(P_{cow}) \tag{4.22}$$

   become unambiguous. This numerical ‘corrections‘ are shown in Figure 4.10

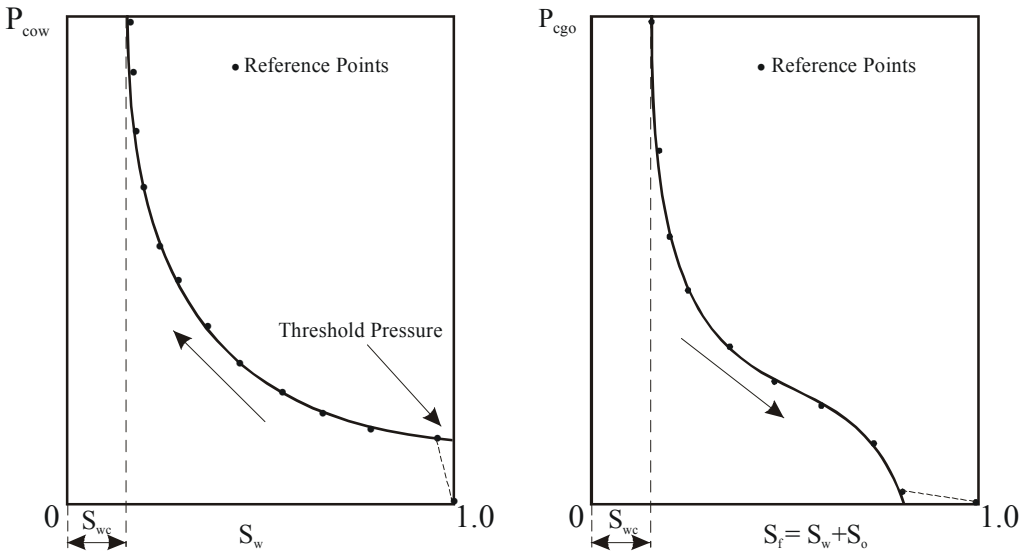

Figure 4.10: Numerical representation of drainage and imbibition type capillary pressure curves

5 Wells in Reservoir Simulation

5.1. The Well Models

To consider the wells in a numerical reservoir model to fundamental different approaches exist:

1. Using specialized grids (radial, unstructured, windows) that represent the well at its true scale.
2. Applying so called well models which relate the bottom hole flowing pressure to the pressure of the perforated grid cell.

The first approach is beyond the scope of this textbook. Therefore only the second one will be followed, which is the standard approach in commercial reservoir simulators.

In reservoir simulation models wells are usually defined as a "source" (or "sink"), located in a grid block with dimensions considerably larger than the wellbore. No special gridding technique is used around the well. Because of this dimension difference between the well and its grid block, the numerically calculated block pressure is different from the well bottom hole flowing pressure. A well model is therefore needed to translate the block pressure into wellbore pressure. It is a relationship between wellbore pressure p_{wf}, block pressure p_0, and well production rate q. The model describing this relationship may be called well index, numerical productivity index, or simply well model.

Peaceman[105] introduced the basis for the most common well model. The Peaceman-type well model calculates an equivalent well block radius r_0 which is defined as the radial distance from the well at which the numerically calculated block pressure equals the reservoir steady state pressure, hence

$$p_{wf} = p_0 - \frac{\mu q}{2\pi k h} \ln \frac{r_0}{r_w} \tag{5.1}$$

where

p_{wf} is the wellbore pressure,
p_0 is the block pressure,
q is the well production rate,
k is the well block permeability,
h is the well block effective thickness,
r_0 is the equivalent well block radius,

r_w is the wellbore radius.

5.2. The Peaceman Well Model

Peaceman's approach is based on the comparison of the analytical solution with the result of the numerical solution of a selected problem. He considers one phase flow in a two dimensional domain with constant pressure at the boundary. The wells have an arbitrary position (x_k,y_k) and produce with constant rate q_k (positive for production and negative for injection). Muskat [97] gave the analytical solution of this problem using the principle of superposition such that the pressure $p(x,y)$ at any point (xy) is given by Equation 5.2:

$$p(x,y) = c + \frac{\mu}{2\pi kh}\sum_k q_k \ln(r_{xyk}), \tag{5.2}$$

where r_{xyk} is the distance of the well k to the point (x,y), and c is an arbitrary constant determined by the boundary condition. The boundary pressure $p_\Gamma(x,y)$ can be chosen in such a way that the constant c becomes equal to zero. In this case the following equation must be valid:

$$p_\Gamma(x,y) = \frac{\mu}{2\pi kh}\sum_k q_k \ln r_{xyk} \tag{5.3}$$

From Equation 5.2 and Equation 5.3 the bottom hole flowing pressure for a well m can be calculated as follows:

$$p_{wfm} = \frac{\mu}{2\pi kh}\left[q_m \ln r_{wm} + \sum_{k \Diamond m} q_k \ln r_{km}\right] \tag{5.4}$$

where

q_m is the well rate,
q_k is the rate of offset wells,
r_{wm} is the considered well radius,
r_{km} is the distance between the considered well m and offset well k.

The same problem can be solved numerically using the finite difference method. The region is overlain by a rectangular grid having a grid aspect ratio $\alpha = \Delta y/\Delta x$. The pressure at the boundary nodes is set equal to the values given by Equation 5.3.

Using five point difference scheme, the finite difference equation is written as:

$$\frac{kh}{\mu}\left[\frac{\Delta y}{\Delta x}\{p_{(i+1,j)} - 2p_{(i,j)} + p_{(i-1,j)}\}\right] + \frac{kh}{\mu}\left[\frac{\Delta x}{\Delta y}\{p_{(i,j+1)} - 2p_{(i,j)} + p_{(i,j-1)}\}\right] = q_{ij} \tag{5.5}$$

where q_{ij} is the sum of the production rates of all wells located within block (ij). The solution of the linear equation system Equation 5.5 gives the block pressure p_{ijm}. Inserting this pressure the well bottom hole flowing pressure p_{wfm} can be calculated as follows:

$$p_{wfm} = p_{ijm} - \frac{\mu q_m}{2\pi kh}\ln\left(\frac{r_{0m}}{r_{wm}}\right) \tag{5.6}$$

By combining Equation 5.4 and Equation 5.6, and solving for the equivalent wellblock radius (r_{0m})

$$\ln(r_{0m}) = \frac{1}{q_m}\left[\frac{2\pi kh}{\mu}p_{ijm} - \sum_{k \Diamond m} q_k \ln r_{km}\right] \tag{5.7}$$

where p_{ijm} is the wellblock pressure.

Equation 5.7 is a general equation for the equivalent wellblock radius for regular 2D grids.

When a single well lies on the boundary of two blocks, each block has a rate q_{ij} equals half the well rate. p_{ijm} will be the same for both blocks because of similarity, and q_k will be 0 for k not equal to m (as no other wells exist when the well is considered isolated).

It should be emphasized that Equation 5.7 is valid only if the basic assumptions of Peaceman are satisfied. They are the following:

- the flow is two dimensional,
- the well(s) is isolated,
- regular grids (rectangular or square) are used, and
- the blocks are uniform (i.e. Δy and Δx are constants and no grid refinement is used).

A well is regarded as isolated, if it is far enough from any reservoir boundary and other wells, such that it may not be influenced by them. A conservative rule that the well is isolated if $r_{AB} >$ 10 max (Δy,Δx) where r_{AB} is the distance to the nearest well and

$$u > 5\Delta x + \frac{\alpha}{2} \text{ and } v > 5\Delta y + \frac{\alpha}{2} \tag{5.8}$$

where

u is the distance to the nearest boundary parallel to y direction.

v is the distance to the nearest boundary parallel to x direction.
α is the grid aspect ratio ($\Delta y/\Delta x$).

The most important results from Peaceman are presented in the following.

5.3. Peaceman Results for Different Well Geometries

Peaceman[106] made calculations for a square domain using the solution given by Equation 5.7 with the boundary condition defined by Equation 5.3. He found that the equivalent wellblock radius (r_0) is a function of the block diagonal

$$L_d = ((\Delta x)^2+(\Delta y)^2)^{0.5}. \tag{5.9}$$

For a well at the center of a rectangular block he found that

$$\frac{r_0}{L_d} = 0.14 \tag{5.10}$$

This ratio is constant regardless the grid aspect ratio $\alpha = \Delta y/\Delta x$. Peaceman[106] called the constant (0.14) as G. If the well is located within its block but off the center, the ratio (r_0/L_d) is still constant. The conclusion that the equivalent wellblock radius is constant regardless the position of the well in its block is somehow surprising.

In an anisotropic case L_d has to be calculated in the equivalent isotropic uv plane such that:

$$L_d = \sqrt{(\Delta u)^2 + (\Delta v)^2} = \sqrt{(\Delta x)^2\left(\frac{k_y}{k_x}\right)^{0,5} + (\Delta y)^2\left(\frac{k_x}{k_y}\right)^{0,5}} \tag{5.11}$$

$$\alpha = \frac{\Delta v}{\Delta u} = \frac{\Delta y}{\Delta x}\left(\frac{k_x}{k_y}\right)^{0,5} \tag{5.12}$$

For example in the case of a single well centered in its block in an anisotropic reservoir the equivalent well block radius is:

$$r_0 = \frac{0.14 \cdot \sqrt{(\Delta x)^2\left(\frac{k_y}{k_x}\right)^{0,5} + (\Delta y)^2\left(\frac{k_x}{k_y}\right)^{0,5}}}{\frac{1}{2} \cdot \left(\left(\frac{k_y}{k_x}\right)^{0,25} + \left(\frac{k_x}{k_y}\right)^{0,25}\right)} \tag{5.13}$$

For an isotropic reservoir, modelled with squared blocks of side length Δx Equation 5.13 simplifies to:

$$r_0 = 0.14\sqrt{2\Delta x^2} \approx 0,2\Delta x \tag{5.14}$$

5.4. Well Model for Horizontal Wells

For the simulation of a horizontal well parallel to *y* axis, Peaceman's [108] Equation 5.13 can be used by replacing the *y* axis by *z* axis thus

$$r_0 = \frac{0.14 \cdot \sqrt{(\Delta x)^2\left(\frac{k_z}{k_x}\right)^{0,5} + (\Delta z)^2\left(\frac{k_x}{k_z}\right)^{0,5}}}{\frac{1}{2} \cdot \left(\left(\frac{k_z}{k_x}\right)^{0,25} + \left(\frac{k_x}{k_z}\right)^{0,25}\right)} \tag{5.15}$$

such that the well model is written as:

$$p_{wf} = p_0 - \frac{\mu q}{2\pi\Delta y\sqrt{(k_z k_x)}}\ln\frac{r_0}{r_w} \tag{5.16}$$

Peaceman[108] emphasized that Equation 5.15 should be used only if the assumptions of uniform grid and isolated well are satisfied. He explained that the horizontal well can be considered isolated if the following condition is true:

$$\frac{\Delta x}{\Delta z} \cdot \left(\frac{k_z}{k_x}\right)^{0.5} < \frac{0.9 \cdot min(z_w, h - z_w)}{\Delta z} \tag{5.17}$$

where z_w represents the vertical distance between the lower boundary of the reservoir and the well

Δz is the vertical grid dimension
h is the reservoir thickness

This means that the scaled grid aspect ratio should be less than the number of blocks between the well and the nearest boundary.

If these conditions are satisfied then Equation 5.15 can be used with error less than 10%. If the condition in Equation 5.17 is not satisfied then Babu *et al.* [14] model should be used. However this well model is beyond the scope of the "Introduction to Reservoir Simulation" volume.

6 References

1 Aavatsmark, I., Barkve, T., Boe, O. and Mannseth, T.: "Discretisation on Unstructured Grid for Inhomogeneous, Anisotropic Media, Part I: Derivation of the Methods," SIAM J.Sci. Comput. **19** (1998), 1700-1716.

2 Aavatsmark, I., Barkve, T., Boe, O. and Mannseth, T.: "Discretisation on Unstructured Grid for Inhomogeneous, Anisotropic Media, Part II: Discussion and Numerical Results," SIAM J.Sci. Comput. **19** (1998), 1717-1736.

3 Aavatsmark, I., Barkve, T., Boe, O. and Mannseth, T.: "A Class of Discretisation Methods for Structured and Unstructured Grids for Anisotropic, Inhomogeneous Media," Proc. 5th European Conference on the Mathematics of Oil Recovery, Leoben/Austria, Sept. 3-6, 1996.

4 Aavatsmark, I., Reiso, E. and Teigland, R.: "MPFA for Faults and Local Refinements in 3D Quadrilatereal Grids With Application to Field Simulation," paper SPE 66356, presented at the SPE 16th Reservoir Simulation Symposium held in Houston,TX, 11-14 February 2001.

5 Abbas, H. and Neda, J: "Rock Mechanics in Wellbore Construction," Chap. **6** in Economides,M.J. at al. "Petroleum Well Construction," J.Wiley & Sons, Chichester (1998).

6 Abdelmawla A.M.: "Numerical Well Test Modeling in a Full-Field Simulator Offers New Opportunities for Reservoir Characterization", paper presented at the 6th European Conference on Mathematics of Oil Recovery (ECMOR VI), Peebles, Scotland, September 7-11, 1998.

7 Abdou,M.K., Pham,H.D. and Al-Aqueeli,A.S.:"Impact of Grid Selection on Reservoir Simulation,"JPT(July 1993) 664-69.

8 Abou-Kassem J.H., Aziz K.: "Analytical Well Models for Reservoir Simulation", paper SPE 11719, presented at 1985 SPE California Regional Meeting held in Ventura.

9 Afilaka, J. and Deimbacher, F.: ”Numerical Well Testing in Complex Reservoirs,” Petroleum Engineer International, June 1997, 21-28.

10 Agarwal, R.G.:”A New Method to Account for Producing Time Effect when Drawdown Type Curves are Used to Analyze Pressure Buildup and Other Test Data,” SPE 9289, paper presented at the 1980 Annual Technical Conference and Exhibition, Dallas, September 21-24.

11 Akbar, A.M., Arnold, M.D. and Harvey, A.H.:”Numerical Simulation of Individual Wells in a Field Simulation Model,” Paper presented at the 1972 SPE Annual meeting, San Antonio, October 8-11.

12 Amado, L.C.N, Ganzer, L. and Heinemann, Z.E.: "Finite Volume Discretization of the Fluid Flow Equations on General Perpendicular Bisection Grids", paper presented at the 1994 Fifth Intl. Forum on Reservoir Simulation, Muscat, Oman, Dec. 10-14.

13 Aziz, K. and Settari, A.: Petroleum Reservoir Simulation, Applied Science Publishers, 1979.

14 Babu, D.K., Odeh, A.S., Al-Khalifa, A.J.A. and McCann, R.C.:"The Relation between Wellblock and Wellbore Pressures in Numerical Simulation of Horizontal Wells," SPERE, August 1991, 324-328.

15 Babu, D.K. and Odeh, A.S.:"Productivity of a Horizontal Well," SPERE, November 1989, 417-421.

16 Beckner, B.L., Mutfilz, J.M., Ray, M.B. and Tomich, J.F.: "EM^{power}: New Reservoir Simulation System," paper SPE 68116 presented at 2001 SPE Middle East Oil Show held in Bahrain, 17-20 March 2001.

17 Bourdet, D., Ayoub, J. and Pirard, Y.:"Use of Pressure Derivative in Well Test Interpretation," SPE Formation Evaluation, June 1989, 293-302.

18 Brand, C.W. and Heinemann, Z.E.: "A New Iterative Solution Technique for Reservoir Simulation Equations on Locally refined Grids," SPE Reservoir Engineering, Nov.1990, p.555-560.

19 Brand, C.W. and Heinemann, Z.E.: "Fundamentals of Gridding Techniques in Reservoir Simulation," paper presented at the Forth Intl. Forum on Reservoir Simulation, Salzburg/Austria, Aug. 31-Sept. 4, 1992.

20 Bremeier, M., Fink, G., and Heinmann, Z.E.: Simulation of Dual Porous and Permeable Hydrocarbon Reservoirs. Erdoel-Erdgas-Kohle, March, 110-117, 1991.

21 Bremeier, M. (1991): *Numerical Simulation of Fractured Petroleum Reservoirs with Interchangeable Matrix-Fracture Transfer Terms and Optional Subdivision of the Matrix Grid Cells*. Ph.D. Dissertation, Mining University, Leoben.

22 Buckley, S.E. and Leverett, M.C.: "Mechanism of Fluid Displacement in Sands," Trans.AIME **146** (1942), p.107-116.

23 Chikhliwala, E.D. and Huang, A.B.: "Investigation on Viscous Fingering by Linear and Weakly Nonlinear Stability Analysis," SPERE (Nov.1988) p.1268-1278.

24 Chouke, R.L., van Meurs, P. and van der Poel, C.: "The Instability of Slow, Immiscible, Viscous Liquid-Liquid Displacements in Permeable Media," *Trans*.AIME **216**, (1959) p.188-194.

25 Coats, K.H. and Modine, A.D.: "A Consistent Method for Calculating Transmissibilities in Nine-Point Difference Equations," paper SPE 12248 presented at the 1983 SPE Symposium on Reservoir Simulation, San Francisco.

26 Coats, K.H.: "Implicit Compositional Simulation of Single-Porosity and Dual-Porosity Reservoirs". Presented at the First International Forum on Reservoir Simulation, Alpbach, September 12-16, 1988 and SPE 18427.

27 Coats, K.H., Nielsen, R.L., Terhune, M.H., and Weber, A.G.: "Simulation of Three-Dimensional, Two-Phase Flow in Oil and Gas Reservoirs". SPEJ, December, 377-88, 1967.

28 Collins D.A., Mourits F.M.: "Multigrid Methods Applied to Near-Wellbore Modeling in Reservoir Simulation", unconsolitied paper, SPE 23607, 1991.

29 Craft, B.C. and Hawkins, M.F.:"Applied Petroleum Reservoir Engineering," Prentice Hall, November 1964, 314.

30 Da Silva, F.V., and Belery, P.: "Molecular Diffusion in Naturally Fractured Reservoirs: A Decisive Recovery Mechanism". SPE 19672, presented at the 64th Annual Technical Conference and Exhibition, San Antonio, Texas, October 8-11, 1989.

31 Dean, R.H., and Lo, L.L.: "Simulations of Naturally Fractured Reservoirs". SPERE, May, 638-648, 1988.

32 Deimbacher, F.,X. and Heinemann, Z.E.: ”Time Dependent Incorporation of Locally Irregular Grids in Large Reservoir Simulation Models,” Paper presented at the 12th SPE Symposium on Reservoir Simulation, New Orleans, February 28 - March 3, 1993.

33 Deimbacher F.X., Komlosi F. and Heinemann Z.E.: “Fundamental Concepts and Potential Applications of the Windowing Technique in Reservoir Simulation”, SPE 29851, presented at 1995 SPE Middle East Oil Show held in Bahrain, 17-20 March 1995.

34 Ding Y., (1996): “Well Modeling in Reservoir Simulation,” paper presented at the 5th European Conference on the Mathematics of Oil Recovery, Leoben.

35 Ding., Y.:”A Generalized 3D Well Model for Reservoir Simulation” Paper presented at SPE Annual Technical Conference, Dallas, October 1995, 227-242.

36 Douglas, J., Peaceman, D. W. and Rachford, H. H.: "A Method for Calculating Multi-Dimensional Immiscible Displacement," Society of Petroleum Engineers, 1959.

37 Durlofsky, J.L.: “Numerical calculation of Equivalent Grid Block Permeability Tensor for Heterogeneous Media,” Water Resources Research, Vol.27, No.5, (May 1991) 699-708.

38 Earlougher, R.:”Advances in Well Test Analysis,” SPE Monograph Series No. 5, 1977, 22-23,42-45.

39 El-Mandouh, M.S., Betté, S., Heinemann, R.F., Ogiamien, E.B., Bhatia, S.K.: “An Integrated, Full-Field Compositional Simulation of the OSO Reservoir, Nigeria”, paper presented at the Forth Intl. Forum on Reservoir Simulation, Salzburg/Austria, Aug. 31-Sept. 4, 1992.

40 Ewing, R.E., Lazarov, R.D. and Vassilevski, P.S.: “Finite Difference Schemes on Grids with Local Refinement in Time and Space for Parabolic Problems I.Derivation, Stability, and Error Analysis,” *Computing* **45**, 193-215.

41 Fleming,G.C.:"Modeling the Performance of Fractured Wells in Pattern Floods Using Orthogonal Curvilinear Grids", paper SPE 20744 presented at the 1990 Annual Technical Conference and Exhibition, New Orleans, Sept. 23-26.

42 Forsyth P.A. and Sammon P.H.: “Local Mesh Refinement and Modeling of Faults and Pinchouts”, SPE 13524, SPEFE (June 1986) 275-85.

43 Forsyth, P.A.: “A Control Volume Finite Element Method for Local Mesh Refinement,” paper SPE 18415 presented at 1989 SPE Symposium on Reservoir Simulation, Houston, TX, Feb. 6-8.

44 Fung, L.S.K., Hiebert, A.D. and Nghiem, L.: “Reservoir Simulation with a Control-Volume Finite-Element Method,” paper SPE 21224 presented at 1991 SPE Symposium on Reservoir Simulation, Anaheim, CA, Feb 17-20.

45 Fung, L.S.K.: "Simulation of Block-to-Block Processes in Naturally Fractured Reservoirs". SPE 20019, presented at the 60th California Regional Meeting, Ventura, California, April 4-6., 1990.

46 Ganzer, L.:"A Novel Approach for Multi-Purpose Reservoir Simulators Using Mixed Models," Paper presented at the 6th European Conference on Mathematics of Oil Recovery (ECMOR VI), Peebles, Scotland, September 7-11, 1998.

47 Ganzer, L.:"Petroleum Reservoir Simulation Using Mixed Models," PhD. Dissertation at Mining University Leoben, September 1997.

48 Geoquest: "FlowGrid User Manual, Geoquest", Abingdon U.K. (1998).

49 Geoquest: "Welltest 200 User Manual", Geoquest, Abingdon U.K. (1997).

50 Gilman, G.R., and Kazemi, H.: "Improved Calculation for Viscous Gravity Displacement in Matrix Blocks in Dual-Porosity Simulators". SPE JPT, January, 60-70, 1988 and SPE16010.

51 Gunasekera, D., Cox, J and Lindsey, P.: "The Generation and Application of K-Orhogonal Grid Systems," paper SPE 37998, presented at the SPE 14th Reservoir Simulation Symposium held in Dallas,TX,, Jun. 8-11, 1997.

52 Gosselin, O. and Thomas, J.H.: "Domain Decomposition Methods in Reservoir Simulation Coupling Well and Full-Field Models," paper presented at the 1990 Second European Conference on the Mathematics of Oil Recovery, Arles, France, Sept. 11-14.

53 Gunasekara,D., Herring,J. and Cox,J.: "Segmented Coordinate Line Based Unstructured Grids", 6th European Conference on the Mathematics of Oil Recovery, Peebles, 8-11 Sept.1998.

54 Gunasekera, D., Childs, P., Herring, J. and Cox, J.: "A Multi-Point Flux Discretization Scheme for General Polyhedral Grids," paper SPE 48855, presented at the SPE 6th International Oil&Gas Conference and Exhibition held in China, Beijing, Nov. 2-6, 1998.

55 Hall, K.R. and Yarborough, L.: "New, Simple Correlation for Predicting Critical Volume," Chem. Eng. (Nov. 1971) 76-77.

56 Hegre, T.M., Dalen, V. and Henriquez, A.: "Generalized Transmissibilities for Distored Grids in Reservoir Simulation",paper SPE 15622 presented at 1986 SPE 61st Annual Technical Conference and Exhibition held in New Orleans, LA October 5-8.

57 Heinemann Z.E., Gerken G., and Meister, S.: "Anwendung der lokalen Netzverfeinerung bei Lagerstättensimulation" paper presented at the 1982 27th DGMK Annual Meeting held 8. Oct.1982 in Achen, Erdöl-Erdgas 6. (Jun.1983), 199-204.

58 Heinemann Z.E., Gerken G. and vonHantelmann G.: "Using Grid Refinement in a Multiple-Application Reservoir Simulator", SPE 12255, presented at the 1983 SPE Symposium on Reservoir Simulation, San Francisco, Nov. 15-18.

59 Heinemann, Z. E., Brand, C. W.: "Gridding techniques in reservoir simulation, Proc. First Intl. Forum on Reservoir Simulation, Alpbach 1988, pp. 339-425.

60 Z.E.Heinemann et *al.*:"Modeling Reservoir Geometry with Irregular Grids," Paper presented at the SPE Symposium on Reservoir Simulation, Houston, TX, February 6-8, 1989, 37-54.

61 Heinemann, Z.E. and Brand, C.W.: "Gridding Techniques in Reservoir Simulation," paper presented at the Second Intl. Forum on Reservoir Simulation, Alpbach/Austria, Sept. 4-8, 1989.

62 Heinemann, Z.E. and Deimbacher, F.X.: "Advances in Reservoir Simulation Gridding," paper presented at the Forth Intl. Forum on Reservoir Simulation, Salzburg/Austria, Aug. 31-Sept. 4, 1992.

63 Heinemann, Z.E.: “Interactive Generation of Irregular Simulation Grids and its Practical Applications” paper SPE paper SPE 27998 presented at the University of Tulsa Centennial Petroleum Engineering Symposium, Tulsa, OK, Aug. 29-31,1994.

64 Heinemann,Z.E.: “Advances in Gridding Techniques,” paper presented at the Fifth Intl. Forum on Reservoir Simulation, Muscat/Oman, Dec. 10-14, 1994.

65 Heinemann, Z.E., Heinemann, G.F. and Tranta B.M: “Modeling Heavily Faulted Reservoirs,” paper SPE 48998, presented at the SPE Annual Technical Conference and Exhibition held in New Orleans, Louisiana.,Dallas,TX, Sept. 27-30, 1998.

66 Heinemann G.F., Brockhauser S.: ”Implementation of Three-Dimensional KPEBI Grids for Slanted Wells in a Field-scale Reservoir Model,” Paper presented at the 6th European Conference on Mathematics of Oil Recovery (ECMOR VI), Peebles, Scotland, September 7-11, 1998.

67 Heinemann, G. and Abdelmawla, A.:”Comparison of ***SURE*** Simulator 3D Window Horizontal Well to Horizontal Well Analytical Solutions,” Internal report, HOT Engineering, April 1998.

68 Heinemann, G.F., Ahmed Abdelmawla and Brockhauser, S.: “Modeling of Fluid Flow around and within Highly Deviated Horizontal Wells,” Proc. 7th European Conference on the Mathematics of Oil Recovery, Baveno/Italy, Sept. 5-8, 2000.

69 Heinrich, B.: "Finite Difference Methods on Irregular Networks," Verlag Birkhäuser, Basel, Boston, Stuttgart. 1987, p.206.

70 Herweijer, J.C. and Durbule, O.R.F.: ”Screening of Geostatistical Reservoir Models with Pressure Transients,” JPT, November 1995, 973-979.

71 Hickernell, F.J. and Yortsos, Y.C.: "Linear Stability of Miscible Process in Porous Media in Absence of Dispersion," Stud.Appl.Math.. **74**, (1986) p.93-115.

72 Higgins, R.V. and Leighton, A,J.: " Computer prediction of Water Drive of Oil and Gas Mixtures Trough Irregulary Bounded Porous Media - Three phase Flow," JPT Sept. 1962, p.1048-54., Trans. ***AIME*** **255**.

73 Hirasaki, G.J. and O’Dell, P.M.: “Representation of Reservoir Geometry for Numerical Simulation,” Trans.AIME, 249,(1970), 393-404.

74 Homsy, G.M.: "Viscous Fingering in Porous Media," Ann.Rev.Fluid Mech.. **19** (1987), p.271-311.

75 Horner, D.R.:” Pressure Buildup in Wells,” Proceedings of Third World Petroleum Congress, The Hague, 1951, 503-523.

76 http://www.posc.org/rescue/Rescue980615_doc/WhatsInRescue.htm, August 16, 2001.

77 Jahveri, B.S. and Youngren, G.K.: “Three-Parameter Modification of the Peng-Robinson Equation of State to Improve Volumetric Predictions,” paper SPE 13118 presented at the 1984 Annual Meeting, Houston, Sept. 16-19.

78 Kamal, M., Freyder, D.G. and Murray, M.A.: ”Use of Transient Testing in Reservoir Management,” JPT, November 1995, 992-999.

79 Kazemi, H., Merril, L.S., Porterfield, K.L., and Zeman, P.R.: "Numerical Simulation of Water-Oil Flow in Naturally Fractured Reservoirs". SPEJ December, 317-326 and SPE Paper

5719, 1976.

80 Kesler, M.G. and Lee, B.I.: “Improve Predictions of Enthalpy of Fractions,” Hydro. Proc. (March 1976) 55, 153-158.

81 Kocberber, Sait.: “An Automatic, Unstructured Control Volume Generation System for Geologically Complex Reservoirs”, paper presented at the 1997 Reservoir Symposium held in Dallas, Texas, 8-11 June 1997.

82 Komlosi, F.:”Use of the Windowing Technique and a New Radial Grid for the Accurate Simulation of Transient Well Tests in a Field Scale Reservoir Model,” Master Thesis, Mining University Leoben, June 1994.

83 Krysl, P. and Oritz, M.: “Variational Delaunay Approach to the Generation of Tetrahedral Finite Element Meshes”. submitted on January 21, 1999 to the International Journal for Numerical Methods in Engineering.

84 Kunianski, J. and Hillestad, J.G.:”Reservoir Simulation using Bottomhole Pressure Boundary Conditions,” SPEJ, December 1980, 473-486.

85 Lee, J.:”Well Testing,” SPE Textbook Series, Vol. 1, 1982, 44.

86 Lee, S.H. and Milliken, W.J.:”The Productivity Index of an Inclined Well in Finite-Difference Reservoir Simulation,” Paper presented at the 12th SPE Symposium on Reservoir Simulation, New Orleans, February 28 - March 3, 1993.

87 Litvak, B.L.: "Simulation and Characterization of Naturally Fractured Reservoirs". Reservoir Characterization Conference, Dallas, Academic Press, New York City, 561-583, 1985

88 Lohrenz, J., Bray, B.G. and Clark, C.R.: “Calculating Viscosities of Reservoir Fluids From Their Compositions,” JPT (Oct. 1964) 1171-1176.

89 Manzocchi, T., Walsh, J.J., Nell, P. and Yielding, G.: “Fault Transmissibility Multiplier for Flow Simulation Models,” Petroleum Geoscience, Vol.5 1999, pp.53-63.

90 Martin, R.E. and Wegner, R.E.: "Two-Dimensional Incompressible Flow Using Stream-Tube Relationship," SPEJ Oct.1979, p.313-323.

91 Matijevic, P. and Deimbacher, F.X.: “Modeling Faults in Reservoir Simulation”, Proc. 4th European Conference on the Mathematics of Oil Recovery, Rørøs, Norway, June 7-10. 1994.

92 Matthews, C.S., Brons, F. and Hazebroek, P.:”A Method for Determination of Average Pressure in Bounded Reservoir,” Trans. AIME, 1954, 182-191.

93 Miller, C.C., Dyes, A.B. and Hutchinson, C.A., Jr.:”The Estimation of Permeability and Reservoir Pressure from Bottom Hole Pressure Build-up Characteristics,” Trans. AIME, 1950, 189, 91-104.

94 Mlacnik M.J. and Heinemann Z.E. (2001): “Using Well Windows in Full Field Reservoir Simulation”. SPE 66371, paper presented at the SPE Reservoir Simulation Symposium held in Houston, Texas, 11-14 February 2001.

95 Mlacnik M.J., Harrer A. and Heinemann G.F. (2001): “State-of-the-Art in the Windowing Technique”. PAPER 2001-03, paper presented at the Petroleum Society’s Canadian International Petroleum Conference 2001, Calgary, Alberta, June 12 - 14, 2001.

96 Mrosovsky, I. and Ridings, R.L.:"Two-Dimensional Radial Treatment of Wells within a Three-Dimensional Reservoir Model," SPEJ, April 1974, 127-131.

97 Muskat, M.:"The Flow of Homogeneous Fluids through Porous Media," McGraw-Hill Book Co., New York City (1937); reprint edition, International Human Resources Development Corp., Boston (1982).

98 Nacul E.C., Lepretre C. et al., (1990): "Efficient Use of Domain Decomposition and Local Grid Refinement in Reservoir Simulation", SPE 20740, 65th Annual Conference and Exhibition of the Society of Petroleum Engineers, New Orleans.

99 Nghiem, L.X.: "An Integral Approach for Discretizing the Reservoir Fluid Equations," SPERE (May 1988) 685-690.

100 Odeh,A. and Babu,D.:"Transient Flow Behavior of Horizontal Wells: Pressure Drawdown and Buildup Analysis," SPE Formation Evaluation, March 1990, pp. 7-15.

101 Palagi, C. and Aziz, K.:"A Dual Timestepping Technique for Simulating Tracer Flow," Unsolicited Paper, SPE 24220, September 1991.

102 Palagi, C.L., Aziz, K.:"The Modelling of Vertical and Horizontal Wells with Voronoi Grid," Paper presented at Western Regional Meeting, California, March 1992, 435-452.

103 Patgawkar, A., Shinkhare, D., Mahapatra, S., Gopalsamy, S. and Mudur, S.P.: "Tetrahedral Discretization of Complex Volumetric Spaces". National Center for Software Technology, India.

104 Peaceman, D.W.: Fundamentals of Numerical Reservoir Simulation, Elsevier Scientific Publishing Company, 1977.

105 Peaceman, D.W.:"Interpretation of Well-block Pressures in Numerical Reservoir Simulation," SPEJ, June 1978, 183-194.

106 Peaceman, D.W.: "Interpretation of Well-Block Pressures in Numerical Reservoir Simulation. Part 3: Some Additional Well Geometries" paper SPE 16976 presented at SPE Annual Technical Conference, Dallas, TX.,27-30 Sept. 1987.

107 Peaceman, D.W.:"Interpretation of Well-block Pressures in Numerical Reservoir Simulation with Nonsquare Grid Blocks and Anisotropic Permeability," SPEJ, June 1983, 531-543.

108 Peaceman, D.W.:"Representation of a Horizontal Well in Numerical Reservoir Simulation," Paper presented at 11th. SPE Symposium on Reservoir Simulation, California, February 1991, 153-162.

109 Pedrosa, Jr., O.A. and Aziz, K. "Use of Hybrid Grid in Reservoir Simulation," SPERE (Nov. 1986) 611-621.

110 Peery, J.H. and Herron, E.H.: "Three-Phase Reservoir Simulation," JPT **21** (1969), p.211-220., Trans AIME **246**, p.211-220.

111 Peneloux, A., Rauzy, E. and Freze R.: "A Consistent Correction for Redlich-Kwong-Soave Volumes," Fluid Phase Equilibria (1982) 7-23.

112 Peng, D.Y. and Robinson, D.B.: "A New Two-Constant Equation of State," Ind. Eng. Chem. Fund. (1976) 59-64.

113 Perrine, R.L.: "The Development of Stability Theory for Miscible Liquid-Liquid Displacement," SPEJ, March 1961, p.17-25.

114 Petterson, O.: “Building, Mapping, and History Matching very large and Complex Grids - with examples from the Gullfaks Field”, paper presented at the 1994 Fourth European Conference on the Mathematics of Oil Recovery, Rørøs, Norway, June 7-10.

115 Pointing, D.K.: "Corner Point Geometry in Reservoir Simulation," Mathematics of Oil Recovery, King, P.R.(ed) Oxford, 1992.

116 Puchyr, P.J.:”A Numerical Well Test Model,” Paper presented at the SPE Rocky Mountain Regional Meeting held in Denver, Colorado, April 1991, 125-139.

117 Quandalle P., Besset P.: “The Use of Flexible Gridding for Improved Reservoir Modeling”, SPE 12238, presented at the 1983 SPE Symposium on Reservoir Simulation, San Francisco, Nov. 15-18.

118 Reid, R.C., Prausnitz, J.M. and Poling, B.E.: The Properties of Gases and Liquids, 4th Edition, McGraw-Hill Inc., New York (1987).

119 Rozon, B.J.:"A Generalized Finite Volume Discretization Method for Reservoir Simulation", paper SPE 20744 presented 1989 at the 10th SPE Symposium on Reservoir Simulation, Huston, Feb.6-8.

120 Rossen, R.H., and Shen, E.I.: "Simulation of Gas/Oil and Water/Oil Imbibition in Naturally Fractured Reservoirs". SPE 16892, presented at the 62nd Annual Fall Meeting, Dallas, Texas, September 27-30, 1987.

121 Schwarz, H.A.: “Über einige Abbildungsaufgaben,” Gesammelte Mathematische Abhandlungen (Nov. 1889) 65-83.

122 Sharpe, H.N. and Ramesh, B.A.:”Development and Validation of a Modified Well Model Equation for Nonuniform Grids with Application to Horizontal Well and Coning Problems,” Paper presented at the 67th Annual Technical Conference and Exhibition of SPE held in Washington, DC, October 4-7, 1992.

123 Shiralkar, G.S.:”Calculating of Flowing Well Pressures in Reservoir Simulation Using Nine-point Differencing,” Journal of Canadian Petroleum Technology, November-December 1989, 73-82.

124 Snyder, L.J.: "two-Phase Reservoir Flow Calculation," SPEJ 9. (1969) p.170-182.

125 Soave, G.: “Equilibrium Constants from a Modified Redlich-Kwong Equation of State,” Chem. Eng. Sci. (1972) 1197-1203.

126 Søreide,I.: “Improved Phase Behavior Prediction of Petroleum Reservoir Fluids From a Cubic Equation of State,” Dr.Ing. thesis, IPT Report 1989:4, Norwegian Institute of Technology, Department of Petroleum Engineering and Applied Geophysics (1989).

127 Sonier, F., Souillard, P., and Blaskovich, F.T.: "Numerical Simulation of Naturally Fractured Reservoirs". SPERE 1988, November, 1114-1122.

128 Stiel, L.I. and Thodos G.: “The Viscosity of Polar Substances in the Dense Gaseous and Liquid Regions,” AIChE J. (Mar. 1964) 275-277.

129 Thomas, L.K., Dixon, T.N., and Pierson, A.G.: "Fractured Reservoir Simulation". SPEJ,

February, 638-648, 1983.

130 Van Golf-Racht, T.D. (1982): *Fundamentals of Fractured Reservoir Engineering*. Developments in Petroleum Science 12, Elsevier Scientific Publishing Company.

131 Van Poolen, H.K., Breitenbach, E.A. and Thurnau, D.H.:"Treatment of Individual Wells and Grids in Reservoir Modelling," SPEJ, December 1968, 341-346.

132 Verma, S.: "Flexible Grids for Reservoir Simulation," Ph.D. Dissertation, Departement of petroleum Engineering,Stanford University, Palo Alto, California, USA, June 1996.

133 Verma, S. and Aziz, K.: "A Control Volume Schema for Flexible Grids is Reservoir Simulation," paper SPE 37999 presented at 1997 SPE Symposium on Reservoir Simulation, Dallas, TX, June 6-8.

134 von Rosenberg D.W.: "Local Grid Refinement for Finite Difference Networks", SPE 10974, presented at the 1982 SPE Technical Conference and Exhibition, New Orleans, Sept. 26-29.

135 Warren, J.E., and Root P.J.: "The Behavior of Naturally Fractured Reservoirs". SPEJ, September, 245-255, 1963 and Transformations of the American Institute of Mining, Metallurgical, and Petroleum Engineers (AIME), 228.

136 Wadsley, W.A.:"Modelling Reservoir Geometry With Non-Rectangular Coordinate Grids," Society of Petroleum Engineers, 1980.

137 Watson, D.F.: "Computing the N-dimensional Delaunay Tesselation with Application to Voronoi Polytopes", Computer Journal, **24**, 167-172,1981.

138 Williamson, A.S. and Chappelear, J.E.:"Representing Wells in Numerical Reservoir Simulation: Part 1- Theory, Part 2- Implementation," SPEJ, June 1981.

139 Whitson, C.H., and Michelsen, M.L.: "The Negative Flash," Fluid Phase Equilibria, 53 (1989) 51-71.

140 Yanosik, L.J. and McCracken, T.A.: "A Nine-Point, Finite Difference Reservoir Simulator for Realistic Prediction of Adverse Mobility Ratio Displacements," SPEJ (Aug.1979) 253-62; Trans., AIME, **267**.

141 Yielding,G., Freeman, B. and Needham, D.T.: "Quantitative Fault Seal Prediction," American Association of Petroleum Geologists Bulletin, **81**, 897-917 (1997).

142 Yortsos, Y.C. and Huang, A.B.. Linear Stability Analysis of Immiscible Displacement," SPERE, (July 1986), p.378-390.

143 Young, L.C.: " Rigorous Treatment of Distorted Grids in 3D", paper SPE 51899 presented at 1999 SPE Symposium on Reservoir Simulation, Huston, TX, Febr. 14-17.